Metal Ion Distribution in Blood Plasma: Towards Metallo-Proteomics

by

Chantal A. Levesque

B.Sc., University of Saskatchewan, 2002

A THESIS SUBMITTED IN PARTIAL FULFILLMENT OF THE REQUIREMENTS FOR THE DEGREE OF

MASTER OF SCIENCE

in

THE FACULTY OF GRADUATE STUDIES

Biochemistry and Molecular Biology

THE UNIVERSITY OF BRITISH COLUMBIA
May 2005

© Chantal A. Levesque, 2005

Abstract

Considering the immense involvement of metal ions in metabolism, protein structure, electron transfer, and their relation to health and disease, deciphering the mechanisms by which metals are stored, transported, sensed and incorporated within the human biosystem is imperative to further understand metal homeostasis and metal-related diseases. In this "omics" age, the emerging field of metallomics sets out to do just that. The metallome of a tissue, fluid, or cell includes aquated trace elements and their complexes with endogenous and induced biomolecules, including organic acids, sugars, proteins, and oligonucleotides. Metallomic studies seek to determine the distribution of elements in a sample, the coordination environments of that element, and the concentrations of each metal-containing species present. The technology involved combines protemics methods with elemental analysis techniques. The most promising approach to studying the blood plasma metallome involves coupling size-exclusion chromatography (SEC) to inductively coupled plasma mass spectrometry (ICP-MS). This platform technology produces a two-dimensional metal distribution plot of the plasma proteome. The first phase separates the plasma's components based on size, and the resulting fractions are analyzed for metal content in the second phase. Combining two well-characterized and widely used analytical techniques, SEC and ICP-MS, effectively maps out where and how the transition elements distribute themselves in plasma. However, while few plasma metallomic studies have been reported to date, the involvement of the protein separation step (SEC) and its impact on the sample integrity prior to metal analysis has not been investigated, bringing into question the potential for processing artifacts.

In this work, I have shown that SEC fractionation of aqueous solutions containing simple and complex metal-ion equilibria can distort that equilibria such that metal-ion speciation patterns detected by ICP-MS do not reflect speciation in the parent sample. Some general guidelines for assessing the extent of perturbation away from the desired state are provided by the chromatographic behaviour of simple 1:1 chelate:metal complexes. In light of these limitations, I then assess the potential of SEC/ICP-MS to be a useful platform for analyzing the quality of plasma and sera samples, including the influence of sample processing and storage conditions. I report preliminary data that identifies significant differences in the metals content and distributions in plasma samples treated in four different ways: fresh plasma collected in sodium citrate; plasma collected in sodium citrate which has been frozen and thawed once; fresh plasma collected in lithium heparin; and plasma collected in lithium heparin which has been frozen and thawed once. In addition to supporting the development of SEC/ICP-MS for quality control of plasma samples, my results suggest that human plasma metallomic studies are best performed on fresh plasma drawn into lithium heparin.

Table of Contents

Abstract.....ii

Table of Contents.....iv

List of Tables.....vi

List of Figures.....vii

List of Abbreviations.....ix

Chapter 1 Thesis Overview and Objectives.....1

1.1 The Role of Metals in the Human Biosystem.....1

1.2 Blood Plasma Metallo-Proteomics.....8

1.3 Potential Technologies for Studying Metals in Plasma.....12

1.4 Thesis Objectives.....16

1.5 SEC/ICP-MS Technology Platform for Metallo-Proteomics.....18

Chapter 2 Effects of Chromatographic Processing on Sample Integrity.....22

2.1 Introduction.....22

2.2 Materials and Methods.....25
- 2.2.1 Reagents.....25
- 2.2.2 Isothermal Titration Calorimetry.....26
- 2.2.3 Chromatography.....27
- 2.2.4 Colorimetric Assays.....28
- 2.2.5 Monitoring of Copper by ICP-MS.....28

2.3 Results and Discussion.....30
- 2.3.1 Evidence of Perturbed Chemical Equilibria in the Cu(II) – Citrate System.....30
- 2.3.2 Stepwise Formation Constants for $H_x(Citrate)_yCu_z$ Complexes and the tendency for On-Column Complex Dissociation.....38
- 2.3.3 Binding Stoichiometry and Thermodynamics for Cu(II) – Peptide Complexes.....41
- 2.3.4 Elution Profiles for Cu(II) – Peptide Complexes.....44
- 2.3.5 Classification of Metallo-Complex Stabilities During SEC Processing.....49

2.4 Conclusions.....51

Chapter 3 Application of LC/ICP-MS to Determine the Effects of Blood Processing on Plasma Metal-Ion Content.....53
3.1 Introduction.....53
3.2 Materials and Methods.....58
3.2.1 Fresh and Thawed Plasma Sample Preparation for SEC.....58
3.2.2 Protein Concentration Assays.....59
3.2.3 Sample Preparation and ICP-MS Analysis.....60
3.2.4 Data Analysis.....61
3.2.5 Binding of Metals by Heparin.....62
3.2.6 Protein and Metal-ion Assignments in SEC Chromatograms.....62
3.3 Results and Discussion.....64
3.3.1 SEC Chromatograms for Plasma Samples.....65
3.3.2 Protein Concentration Comparison.....67
3.3.3 The Effect of Citrate on Metal-Ion Distribution in Fresh Plasma.....69
3.3.4 The Effect of Heparin on Metal-Ion Distribution in Fresh Plasma.....72
3.3.5 The Effects of Freezing and Thawing on the Distribution of Metal Ions in Plasma.....76
3.4 Conclusions.....79

Chapter 4 Concluding Remarks.....80

Appendix A: Metal ion Profiles in Blood Plasma Samples Achieved with SEC/ICP-MS.....82

Appendix B: Smoothed Metal ion Profiles in Blood Plasma Samples Achieved with SEC/ICP-MS.....95

Bibliography.....109

List of Tables

Table 1.1 Biological functions of selected metal ions.....2

Table 1.2 Common oxidation states of important trace elements in bioinorganic chemistry.....4

Table 1.3 A list of human diseases and their respective protein biomarkers in plasma.....9

Table 1.4 Metallo-proteins present in blood plasma and their respective bound metals.....12

Table 1.5 Mean concentrations of trace elements in serum or plasma of a population of Belgian subjects.....14

Table 2.1 Speciation, protonation constants, and overall stoichiometric formation constants for aqueous solutions at 20°C containing $CuCl_2$ (Cu), citric acid (L), and 0.1 M NaCl.....33

Table 2.2 Stepwise formation constants for citrate-containing $H_xL_yCu_z$ complexes.....40

Table 2.3 pH-Specific stepwise formation constants determined by ITC for 1:1 complexes formed between the model peptide indicated and the cupric ion.....42

Table 3.1 Anticoagulants used for venous blood collection.....54

Table 3.2 Properties of the Fractogel EMD Bio-SEC column and standard analytes used for column calibration.....63

Table 3.3 Total protein content of plasma samples studied.....68

Table 3.4 Total metal content of each plasma sample.....69

List of Figures

Figure 1.1 Schematic diagram of an inductively coupled plasma mass spectrometry.....19

Figure 2.1 SEC and ICP-MS chromatograms for a 1:1 48 mM Cu-citric acid solution.....31

Figure 2.2 SEC elution chromatogram (210 nm) for a 48 mM citric acid solution.....32

Figure 2.3 Citric acid structure.....35

Figure 2.4 Potentiometric profiles of aquated cupric ion and citric acid – copper complexes.....36

Figure 2.5 Normalized SEC and ICP-MS elution chromatograms for a 1:1 48 mM Cu-citric acid solution at two different volumetric flow rates.....37

Figure 2.6 Analysis of cupric-ion binding to the synthetic peptide GHG using isothermal titration calorimetry at 293 K.....43

Figure 2.7 Analysis of cupric-ion binding to the synthetic peptide HGGG using isothermal titration calorimetry at 293 K.....44

Figure 2.8 Elution chromatogram (210 nm) for 40 mM $CuCl_2$ and 40 mM GHG.....45

Figure 2.9 Elution chromatogram (210 nm) for 40 mM $CuCl_2$ and 40 mM Ac-HGGG.....46

Figure 2.10 Elution chromatogram (210 nm) for 40 mM $CuCl_2$ and 40 mM HGGG.....47

Figure 2.11 Elution chromatogram (210 nm) for 40 mM $CuCl_2$ and 40 mM Ac-GHH.....47

Figure 2.12 Elution chromatogram (210 nm) for 40 mM $CuCl_2$ and 40 mM GHH.....48

Figure 2.13 Elution chromatogram (210 nm) for 40 mM $CuCl_2$ and 40 mM HGHH.....49

Figure 3.1 Clotting cascade diagram identifying the importance of calcium.....55

Figure 3.2 Selectivity curve for the Merck Fractogel EMD Bio-SEC column.....64

Figure 3.3 SEC chromatogram for fresh blood plasma collected into 13 mM citrate.....65

Figure 3.4 SEC chromatogram for fresh blood plasma collected into lithium-heparin.....66

Figure 3.5 The effect of citrate on the (smoothed) distribution of Mn^{2+}, Co^{2+} and Sr^{2+} in fresh plasma.....71

Figure 3.6 The effect of citrate on the distribution of Cu^{2+} in fresh plasma.....71

Figure 3.7 The effect of heparin on the distribution of Cu^{2+} in fresh plasma.....72

Figure 3.8 The effect of heparin on the (smoothed) distribution of Mn^{2+} and Sr^{2+} in fresh plasma.....73

Figure 3.9 The effect of citrate on the (smoothed) distribution of Zn^{2+} in fresh plasma.....75

Figure 3.10 The effect of heparin on the distribution of Zn^{2+} in fresh plasma.....76

Figure 3.11 The effects of freezing on copper speciation in blood plasma collected in citrate.....77

Figure 3.12 The effects of freezing on copper speciation in blood plasma collected in lithium heparin.....78

List of Abbreviations

2-DE - two-dimensional gel electrophoresis

μ_f - rate constant for complex formation

μ_r - dissociation rate constant

AAS - atomic absorption spectroscopy

Ac – acyl group

ATP - adenosine tri-phosphate

BCA - bicinchoninic acid

CPDA-1 - citrate phosphate dextrose adenine

DNA - deoxyribonucleic acid

DRC - dynamic reaction cell

EDTA - ethylenediamine tetraacetic acid

FFT - fast Fourier transform

FPLC - fast protein liquid chromatography

FT-ICR - Fourier transform ion cyclotron resonance mass spectrometry

GFAAS - graphite furnace atomic absorption spectrometry

HPLC - high performance liquid chromatography

ICP-MS - inductively coupled plasma mass spectrometry

IgG - immunoglobulin G

IL-6 - interleukin 6

IL-2 - interleukin 2

ITC - Isothermal titration calorimetry

K_d - dissociation constant

L – ligand

LMWH - low molecular weight heparin

M - metal

ML_n - complex

MALDI-MS - matrix assisted laser desorption ionization mass spectrometry

MS/MS - tandem mass spectrometry

MTs - metallothioneins

Chapter 1

Thesis Overview and Objectives

1.1 The Role of Metals in the Human Biosystem:

The importance of metals to life is demonstrated by their roles in critical bioprocesses, including cellular respiration, metabolism, development, osteogenesis, protein structure/stability, nucleic acid stability, RNA and DNA synthesis, neural transmission, muscle contraction, signal transduction, and protection against toxic and mutagenic agents [1-4]. Metal ions are also key players in osmotic regulation (Na and K [1, 5]) and energy production (Mg [6]) within cells and biological fluids. The binding of oxygen to iron in hemoglobin of red blood cells demonstrates how iron is essential to that protein's structure and primary function of oxygen transport to the vascularized parts of our bodies [1, 6, 7]. In addition, the reactivity of amino acids and other small organic molecules is often modified when they are coordinated to metal ions. Nature exploits this effect through the construction of metal-ion binding cavities within the active sites of many enzymes (*e.g.*, pyruvate kinase, superoxide dismutase) that serve to accelerate reactions that would otherwise proceed too slowly to be useful in a living system. For example, the extraordinarily high rates of cleavage observed for the enzymatic hydrolysis of carboxylic esters and amides can often be accounted for by the effect of a bound metal ion acting either as a Lewis acid catalyst, by coordinating to a carbonyl oxygen atom and thereby polarizing the carbonyl group, or as an electrophile through coordination to a hydroxyl group [8]. Table 1.1 displays some of the biologically relevant metals and a few of their known functions in the human body.

Table 1.1 Biological functions of selected metal ions

Metal	Functions
Sodium	Charge carrier, action potential propagation, osmotic balance, blood pressure [1]
Potassium	Charge carrier, osmotic balance, blood pressure [1]
Magnesium	ATP stability, hydrolase, isomerase, DNA stability, alkaline phosphatase structure, bone formation, thiamine pyrophosphate cofactor activity [1, 3]
Calcium	Charge carrier, muscle contraction, cell signaling, heart function, blood clotting [2, 4]
Chromium	Glucose tolerance [4]
Manganese	Phosphoenolpyruvate carboxykinase (TCA cycle), bone structure, glycosyltransferases [4]
Iron	Oxygen transport, electron transfer, oxidase [1]
Cobalt	Structure of vitamin B_{12} [2]
Copper	Oxidase, electron transfer, cellular respiration, anti-oxidant (superoxide dismutase) [1]
Zinc	Protein structure, gene regulation, RNA and DNA polymerases, transcription factors, alkaline phosphatase, CO_2 hydrolysis (carbonic anhydrase), anti-oxidant (superoxide dismutase), growth and development, wound healing, insulin [1, 2, 4]
Selenium	Anti-oxidant (glutathione peroxidase), thyroid deiodination [4]

While the essential metal ions (Fe, Cu, Zn, Se) are important co-factors for a diverse array of catalytic functions, they can also be toxic when present at non-physiological levels. Too much zinc ingestion can cause vomiting and diarrhea, may interfere with copper metabolism, and can result in neutropenia (low white blood cell count) or red blood cell

microcytosis (small cell volume) [4]. At the other end of the spectrum, too little zinc can retard growth and sexual maturation, can lead to immune disorders and night blindness, and maternal zinc deficiency may cause fetal anencephaly [4, 9]. *In vitro* and *in vivo* studies of acute and chronic exposures to metals have established their potential toxicity. The presence of certain heavy elements such as mercury (Hg), lead (Pb), cadmium (Cd), and arsenic (As) in the environment, food sources, and water has been linked to a number of illnesses and life-threatening diseases [6, 10-12]. Consequently, regulatory guidelines for tolerable exposure levels for both essential as well as non-essential (Hg, Cd, Ni, Pb, As) metals have been established [13]. The logical ensuing question becomes, 'How does the human body deal with the many differing and changing loads of various metals?'

The presence of inorganic and often insoluble metals in the human body frequently requires the interaction of the metals with water-soluble ligands. Nucleic acids, small cytoplasmic constituents, organic cofactors, and water provide ligands that bind and solubilize metal ions. However, proteins provide the largest and most diverse array of metal-binding ligands. Binding of a transition metal to a given ligand depends on the valence/oxidation state of the metal. Table 1.2 reports the biologically relevant metals and their most common oxidation states [1]. However, the solution environment surrounding the ion can alter configurations of the outer electrons in its d-orbitals, enabling the metal to adopt other valence states [14, 15].

Table 1.2 Common oxidation states of important trace elements in bioinorganic chemistry [1]

Element	Redox State	Number of d electrons
Na	(I)	
K	(I)	
Mg	(II)	
Ca	(II)	
V	(III)	2
	(V)	0
Cr	(III)	3
Mn	(II)	5
	(III)	4
	(IV)	3
Fe	(II)	6
	(III)	5
Co	(I)	8
	(II)	7
	(III)	6
Ni	(II)	8
Cu	(II)	9
	(I)	10
Zn	(II)	10

Metal ions are generally chelated according to the hard-soft acid-base principle of Pearson [16], who was the first to explain the differential complexation behavior of cations and ligands in terms of electron-pair donating Lewis bases and electron-pair accepting Lewis acids. Pearson classified Lewis acids and bases as *hard* or *soft* in an effort to formalize the

observation that hard Lewis acids prefer to bind to hard Lewis bases, while soft Lewis acids prefer to bind to soft Lewis basis. Certain cations fall into neither category and are generally classified as *borderline* in the Pearson hierarchy. Examples of hard Lewis acids (also known as type A acids) of physiological importance include H^+, Na^+, K^+, Mg^{2+}, Ca^{2+}, Mn^{2+}, and Fe^{3+}. The most important soft Lewis acid (type B acids) in humans is Cu^+. Nonessential soft acids include Hg^{2+} and Cd^{2+}. Borderline ions include the essential metal ions Cu^{2+}, Fe^{2+}, and Zn^{2+}, as well as the nonessential ions Ni^{2+} and Pb^{2+}. From these classifications, it is clear that type A cations have high charge densities and do not contain electron pairs in their valence shells. Type B cations have larger radii and have electron pairs in their valence shells, making them much easier to polarize and oxidize.

Hard Lewis bases are small, highly-solvated electronegative atomic centers that are weakly polarizable and therefore difficult to oxidize. They include water, the hydroxide ion, the carboxylate group ($R\text{-}COO^-$), primary amines ($R\text{-}NH_2$), hydroxyl (R-OH) and ether (R-O-R') groups, and the soluble anions Cl^-, CO_3^{2-}, PO_4^{3-}, and SO_4^{2-}. Soft Lewis bases are large atoms of intermediate electronegativity, making them easy to polarize and oxidize. They include thiols (R-SH), thioethers (R-S-R'), and phenyl rings. Borderline Lewis bases include amino-benzyl and pyridine chemistry.

As an example, consider the selective coordination of the borderline Lewis acid Cu^{2+} to metallothioneins (MTs). MTs are a superfamily of low molecular weight cysteine-rich metallo-proteins and metallo-peptides responsible for regulating the intracellular supply of zinc and copper ions and for protecting cells from the harmful effects of exposure to elevated

levels of these and non-essential metal ions such as Cd^{2+} and Hg^{2+} [13]. Metallothioneins possess clusters of cysteine residues, the sulfhydryl groups of which are soft Lewis bases and therefore bind soft and borderline metal ions such as Cu^{2+}, Cd^{2+}, Hg^{2+}, and Pb^{2+} [17]. Upon binding to protein side-chains, the positive charge on these metals stabilizes the acid anion(s) by lowering the pKa values of the ligand(s). A shift in pKa associated with metal binding is common with thiols, imidazole, phenols, alcohols, phosphoric and carboxylic acids, and their derivatives [1]. This phenomena allows uptake and transport of sparingly soluble metals such as iron (III), which cannot exist in the blood at physiological pH without supporting ligands [1]. Consequently, a complex transport and delivery system carefully monitors and chaperones metal ions within the body from their point of entry in the small intestine, through the circulatory system, to their ultimate destination in organs, cells, and functional proteins [18]. Metal-ion homeostasis is maintained through highly regulated and coordinated processes of uptake, storage, and secretion utilizing low and high affinity ligands to achieve the proper distribution of metals throughout the various tissues and cells [19].

While transferrin is perhaps the best-known metal transport protein present in blood plasma, a number of other plasma proteins (i.e., albumin, ceruloplasmin) bind a wide range of metal ions with differing affinities. Transferrin is also able to bind metal ions other than iron if iron is present in sub-stoichiometric concentrations [18, 20, 21]. Indeed, metals commonly compete for the same ligands on proteins. Albumin, for example, has a number of metal-binding sites, including a high affinity N-terminal binding site for copper and a multi-metal binding site that enable the transport of copper, zinc and calcium in the blood [22, 23].

The potentially toxic metals, nickel and cadmium, compete readily with copper and zinc for these ligands, particularly those in the multi-metal binding site [20, 22, 24-26].

The ability of metals to compete for the same ligands indicates that metal-ion homeostasis can be disrupted by the presence of abnormal levels of a particular ion or by a change in the expression of a specific metallo-protein. This has been observed in the case of aceruloplasminemia, where the absence of ceruloplasmin, a copper binding protein, in plasma results in iron misdistribution leading to anemia [27]. In hepatocytes, ceruloplasmin's ferroxidase activity at one of its copper centers is required for ferric iron uptake by transferrin [7, 28]. As a result, a ceruloplasmin deficiency results in iron accumulation in the liver and insufficient iron delivery to the capillary system [29]. The anemic symptoms are alleviated with ceruloplasmin supplementation rather than iron supplementation [27, 29].

Increasing numbers of human diseases are now thought to be related to disturbances in metal-ion homeostasis. Al, Cu, Zn and Fe have been detected at increased levels in Alzheimer's disease post-mortem brains [17, 30-33]. Other neuro-degenerative diseases like Friedreich's ataxia and Parkinson's, as well as metal-ion overload and deficiency disorders like anemia, hemochromatosis, Menke's and Wilson's diseases are known to perturb metal-ion homeostasis, though the effects of these conditions on the distribution of metal ions between the various proteins have not been fully characterized [10, 19, 33, 34]. Nevertheless, the involvement of metals in human function and their implication in many

human diseases emphasizes the need to understand metal-ion homeostasis and the mechanisms that underlie their distributions in various tissues.

1.2 Blood Plasma Metallo-Proteomics:

As metals are transported throughout the body via the circulatory system, blood plasma is potentially the most useful tissue or fluid for the study of metal-ion homeostasis in humans. In addition, the blood is thought to provide the largest representation of the human proteome, due in part to tissue leakage [35-37]. Most of the body's cells communicate with the plasma either directly or indirectly through the interstitial or cerebrospinal fluids, and many cellular components are released into the blood upon tissue degeneration and damage. These proteins, not native to plasma, provide a snapshot of total body health by their presence and concentrations in plasma.

The analysis of proteins present in blood plasma has been a developing area of research for decades, due in part to the potential medicinal outcomes of mapping and quantifying the human proteome [38]. In particular, defining the entire inventory of human proteins and establishing methods to accurately measure absolute or relative abundances of proteins in plasma is expected to result in the discovery of new and more informative biomarkers for disease diagnosis and overall human health. The intense focus on blood plasma proteomics is easily understood. It is a clinically accessible sample that for decades has been assayed for specific analytes to detect a variety of disease states. New and more powerful proteomics technology is expanding that diagnostics library by effectively measuring relevant and detectable changes in expression levels of proteins in plasma

associated with the onset of diseases like Alzheimer's, rheumatoid arthritis, and various forms of cancer [37]. Table 1.3 lists some of the current disease states with protein biomarkers detected in plasma.

Table 1.3 Representative diseases and their respective protein biomarkers in plasma.

Disease	Protein Biomarker	Method of Detection	Reference
Alzheimer's	Oxidized forms of fibrinogen gamma-chain precursor and of alpha-1-antitrypsin precursor	2-DE/MALDI-MS	[38]
Ovarian cancer	Apolipoprotein A1 (down-regulated in cancer), transthyretin (down-regulated), inter-α-trypsin inhibitor heavy chain H4 (up-regulated), Cancer antigen 125	Protein chip analysis and SELDI-TOF-MS	[39, 40]
Prostate cancer	3 protein markers of molecular masses 15.2, 15.9 and 17.5 KDa	SELDI-TOF-MS	[41]
Rheumatoid arthritis	5 proteins up-regulated, 7 proteins down-regulated	2-DE	[42]

2-DE - two-dimensional gel electrophoresis; MALDI-MS - matrix assisted laser desorption ionization mass spectrometry; SELDI-TOF-MS - surface enhanced laser desorption ionization time of flight mass spectrometry.

The identification and quantification of proteins within plasma is inextricably linked to technology development. Two-dimensional gel electrophoresis (2-DE) has been the most common means of resolving complex proteomes to visualize proteins and their relative abundances. However, a number of faster and more reproducible proteome separation

technologies have emerged over the past decade, including capillary electrophoresis, capillary electro-chromatography, and various forms of one-dimensional and multi-dimensional HPLC [36, 43-48]. Proteins partially or fully isolated by these techniques are usually then tryptic digested, the peptide fragments resolved by reverse-phase liquid chromatography (RPLC), and sequenced with tandem mass spectrometry (MS/MS), matrix assisted laser desorption ionization mass spectrometry (MALDI-MS) [36], ion trap mass spectrometry [49], or Fourier transform ion cyclotron resonance mass spectrometry (FT-ICR) [43]. While a number of different couplings of high-resolution separation technologies to MS have shown success in proteomics applications, the inherent complexity of the blood plasma proteome presents unique challenges to proteomics technology. The dynamic range of proteins thought or known to be present in plasma extends over at least nine orders of magnitude, making detection of lower abundance proteins extremely difficult [36]. Albumin and IgG are present in plasma at concentrations greater than 10 mg/mL, and these highly abundant proteins often mask the detection of the remaining proteins which represent less than 2% of the total peptide mass in plasma [38]. Nevertheless, a recent proteomics study completed through a global collaboration claims to have identified 1175 distinct gene products in human plasma [35, 36, 38, 49, 50], including several proteins present at sub pg/mL levels such as the cytokines IL-6, IL-2, and TNF α [51]. This large number of peptides illustrates both the complexity of the plasma proteome and the potential for advances in analytical technology to provide detailed information on plasma proteins and the overall composition of plasma.

My interests are in the development of analytical technology for plasma metallo-proteomics, a subset of blood proteomics focusing on metal-binding proteins, their concentrations, and their chemical equilibria in blood. While the major metallo-proteins in plasma are known and their metal-binding specificities are reasonably well characterized, considering the recent report of over a thousand gene products in plasma [35, 36, 49, 50], it is likely that additional metal-binding proteins are present. Moreover, the distribution of metals among the various proteins and other ligand-bearing analytes within blood plasma has not been fully elucidated; nor has the impact of a perturbation in individual ion or protein abundance on the composition of the plasma metallo-proteome. Thus, there is much to be discovered in the area of metallo-proteomics, including the potential use of metallo-proteome analysis in the screening of blood disorders, and in quality control of transfused blood and blood products. Table 1.4 reports the plasma proteins known to bind metal ions under physiologically relevant conditions. The goal of metallo-proteomics is to complete that list and to establish uses for metallo-proteome analysis in human biology and human health.

Table 1.4 Metallo-proteins present in blood plasma and their respective bound metals.

Plasma Protein	MW (Da)	Mg	Al	Ca	Cr	Fe	Co	Ni	Cu	Zn	Se
α-fetoglobulin	64 000									✓	
α-2-macroglobulin	725000									✓	
α-2-glycoprotein	41000									✓	
γ2- globulins	9000-14000									✓	
β- globulins	14 000									✓	
β- thromboglobulin	35404									✓	
Albumin	66 458	✓		✓				✓	✓	✓	
Ceruloplasmin	134 000								✓	✓	
Factor II (prothrombin)	72000			✓							
Factor I (fibrinogen)	340000									✓	
Hemopexin						✓					
Immunoglobulin A	160000									✓	
Insulin	5700									✓	
Lipoproteins (α1α2)	45300-175000									✓	
Pseudo/serum cholinesterase	348000									✓	
Selenoprotein P (SePP)	41677										✓
Thymulin										✓	
Transcobalamin I	12000						✓				
Transcobalamin II	53900						✓				
Transcobalamin III	100000						✓				
Transferrin	79 570		✓		✓	✓			✓	✓	

Molecular weight (MW) values: [52-55]; Bound metals: [21, 23, 52-62].

1.3 Potential Technologies for Studying Metals in Plasma:

Based on current literature, metallo-proteomics can be partitioned into three general levels of study. The first, and by far the simplest, involves measuring the total abundance of each metal in a tissue or fluid sample collected from a subject. The second level qualitatively connects metals with their associated ligands by partitioning/separating the components of the tissue or fluid sample based on a specific physico-chemical property, and then assessing the metal content within each of the resulting fractions. This level of study may be useful for metallo-protein discovery, but is likely to have more use as a tool for detection of blood disorders and for screening of blood products. The final level involves fully describing the

chemical equilibria of all metals in blood by identifying the abundances of all metallo-proteins and other metal-binding ligands in plasma, and the distribution of metals among them. At present, no analytical technology is capable of probing the blood plasma proteome at this level of detail. I therefore focus on progress made in the first two levels of analysis and the impact these approaches have had on science and medicine.

Both traditional atomic absorption spectroscopy (AAS) and inductively coupled plasma mass spectrometry (ICP-MS) provide accurate, highly sensitive measurement of metal concentrations in complex aqueous media. As a result, AAS and ICP-MS, as well as several other analytical methods, have been applied to the determination of total metal composition of various human tissues, including plasma [26, 33, 63-67]. For example, Table 1.5 summarizes the average total metal concentrations found in blood plasma samples from a population of Belgian subjects [64].

Studying variations in total metal levels can help with the detection and possible diagnosis of various disease states. For example, Muniz et al. [67] used double-focusing ICP-MS to detect significant differences between the total content of metals in hemodialysis patients and that of normal subjects from the same region. Similarly, changes reported in the levels of individual metal ions in plasma from patients with cutaneous Leishmaniasis have been used to address how activation of the immune system affects metal-ion homeostasis in the blood [68]. In principle, the effects of the treatment therapies employed can also be assessed through their influence on the overall metal content of the appropriate tissues.

Table 1.5 **Mean concentrations of trace elements in serum or plasma of a population of Belgian subjects [64]**

Element	Analytical technique	Mean concentration	
		µg/L	nmol/L
Aluminum	GFAAS	2.86	106.05
Antimony	RNAA	0.014	0.11
Arsenic	RNAA	0.705	9.411
Barium	ICP-MS	1.02	7.425
Bismuth	ICP-MS	0.063	0.3
Boron	ICP-MS	17.25	1.6 µmol/L
Bromine	PIXE	5.565 mg/L	69.65 µmol/L
Cadmium	RNAA	0.168	1.49
Cesium	ICP-MS	0.7	5.27
Chromium	RNAA	0.16	3.08
Cobalt	AAS	0.327	5.55
Copper	AAS	1.09 mg/L	17.14 µmol/L
Gold	RNAA	6.6 ng/L	33.5 pmol/L
Lead	ICP-MS	4.21	20.32
Lithium	ICP-MS	0.982	85
Manganese	RNAA	0.635	11.55
Mercury	RNAA	1.156	5.76
Molybdenum	RNAA	0.63	6.57
Nickel	GFAAS	0.23	3.92
Rubidium	AAS	0.168 mg/L	1.97 µmol/L
Scandium	RNAA	1.73 ng/L	38.5 µmol/L
Selenium	AAS	0.095 mg/L	1.20 µmol/L
Silver	RNAA	0.084	0.78
Strontium	ICP-MS	26	0.3
Tin	ICP-MS	0.96	8.085
Vanadium	RNAA	31 ng/L	0.61
Zinc	RNAA	0.94 mg/L	14.38 µmol/L

GFAAS - graphite furnace atomic absorption spectrometry

RNAA - radiochemical neutron activation analysis

ICP-MS - inductively coupled plasma mass spectrometry

PIXE - particle-induced X-ray emission

AAS - atomic absorption spectrometry

It is well-established that metal ions are predominantly transported through the vasculature by metal-binding plasma proteins. By fractionating the plasma proteome according to specified protein characteristics (molecular weight, charge, hydrophobicity, or a combination) and then identifying the metals associated with the various fractions, one can fingerprint the distribution of metal ions in plasma. The separation method must first be calibrated with protein standards to allow inferences to be made about which proteins are associated with which metal peaks. Recently, several chromatographic and gel-based separation methods have been joined with elemental analysis techniques to assess the distribution of metal ions among protein fractions [69-80]. Size exclusion chromatography (SEC) is generally the preferred method for plasma fractionation due to its ability to separate proteins in their native state with minimal influence on the composition of the sample material, as chemical interactions between the sample and the stationary-phase resin used in SEC are generally weak [77]. My work follows this strategy by establishing a platform that combines SEC with ICP-MS to identify the distribution of the metal ions in blood plasma. Assessing plasma components, keeping them as close as possible to their *in vivo* state, will contribute to the expanding field of native proteomics. Precise identification of the proteins associated with the metal profiles is not generally possible with this approach, but the fingerprint can still prove useful in comparing profiles from disease samples with those from healthy controls. Modest variations in metal homeostasis can be readily observed. Moreover, unexpected metal-ion elution peaks can serve as a reference point for more careful separation and sequencing analysis of the proteins within the associated fraction to permit discovery of new metal-binding proteins.

1.4 Thesis Objectives:

The focus of this work is to advance metallo-proteomics analysis platforms that combine size exclusion chromatography (SEC) with inductively coupled plasma mass spectrometry (ICP-MS) to map out metal-ion profiles in biological samples. There are two main objectives to this thesis: (1) to determine the effects of the SEC column on the sample prior to metal analysis, and (2) to apply the technology to determine the effects of anticoagulants on the content of metal ions and distributions in plasma preparations for clinical use.

Size exclusion chromatography separates sample components largely on the basis of size and shape, with enthalpic interactions between the solute and stationary phase providing only a small contribution to the partition coefficient. The mechanism of separation and the classic mode of operation of SEC are well understood and comprehensive treatments of the subject can be found elsewhere [81]. Here I simply note that the SEC separation, by its nature, processes the sample at conditions away from chemical equilibria. Thus, when a complex mixture of metallo-protein complexes are fractionated by SEC, the equilibrium constants for ion binding, the dissociation rate constants of the complexes, and the time required for elution from the column, will determine the integrity of the sample prior to mass spectrometry analysis. Trace element complexes have a limited lifetime when equilibria are perturbed and will dissociate at a defined rate. Any free metal that may have transiently dissociated from its protein complex has the potential to interact with the separation resin and move away from the vicinity of its transporter protein due to differences in size, and associated migration rates. The remaining metallo-protein complexes are then

thermodynamically driven to further dissociate in an attempt to reestablish equilibrium. Sample manipulations before and during fractionation by SEC, therefore, have the potential to disturb the existing chemical equilibria such that the concentrations of trace-element complexes determined by AAS or ICP-MS do not reflect those present in the original sample [82]. However, the effects of the SEC step on metallo-proteome equilibria have not been investigated. Initial efforts toward understanding these effects are made in this work as part of a collaboration with Dr. Peter Pang, a postdoctoral fellow in the laboratory of Dr. Charles Haynes. Only those components of the collaboration that relate to this thesis will be presented. The complete, more comprehensive study can be found in a follow-up publication currently in preparation.

After studying the impact of SEC on sample integrity, I then assess the effects of common plasma anticoagulation and storage strategies by applying SEC/ICP-MS technology to the analysis of plasma samples treated in four different ways: (1) fresh plasma collected in sodium citrate, (2) plasma collected in sodium citrate, flash-frozen, then thawed, (3) fresh plasma collected in lithium heparin, and (4) plasma collected in lithium heparin, flash-frozen, then thawed. Considering the different modes of action of citrate and heparin as anti-coagulating agents, differences between the two sets of metal profiles produced may be observed. Likewise, upon freezing plasma samples, the stabilities of some plasma proteins may be affected [83, 84] and potentially lead to other distortions in the metal-ion profiles. I have, therefore, determined the ability of the SEC/ICP-MS technology to detect changes in metal distribution profiles according to changes in plasma sample handling.

1.5 SEC/ICP-MS Technology Platform for Metallo-Proteomics:

The pairing of size-exclusion chromatography (SEC) with inductively coupled plasma mass spectrometry (ICP-MS) is intended to provide a two-dimensional analysis of the plasma proteome. The first dimension categorizes plasma components on the basis of size, with UV absorbance at 280 nm serving as the detector. The second dimension utilizes ICP-MS to report the abundance of each detectable metal ion within each fraction created in the first dimension. As a result, the technology can provide a quantitative readout of how essential and nonessential transition elements distribute themselves within the plasma proteome. In this work, plasma metallo-proteome samples will be studied by fractionating the proteins on a Merck Bio-SEC™ column, and by analyzing the protein chromatogram with UV absorbance and the distribution of key metal ions (Ti, Cr, Mn, Co, Cu, Zn, Se, Sr) using a prototype ICP-MS instrument donated by Perkin-Elmer Sciex. As the mode of operation of an ICP-MS may not be known to all readers of this thesis, I provide below a brief description of the technology.

The trace element analysis of blood plasma demands an instrument sensitive enough to detect metals bound to proteins present in lower abundances. ICP-MS allows absolute determination of the concentrations of metals in the ng/L (ppt) to μg/L (ppb) range. It uses a high speed, high temperature flow of electrons to excite, atomize and ionize elemental species [77]. Figure 1.1 schematically illustrates the internal architecture of an ICP mass spectrometer.

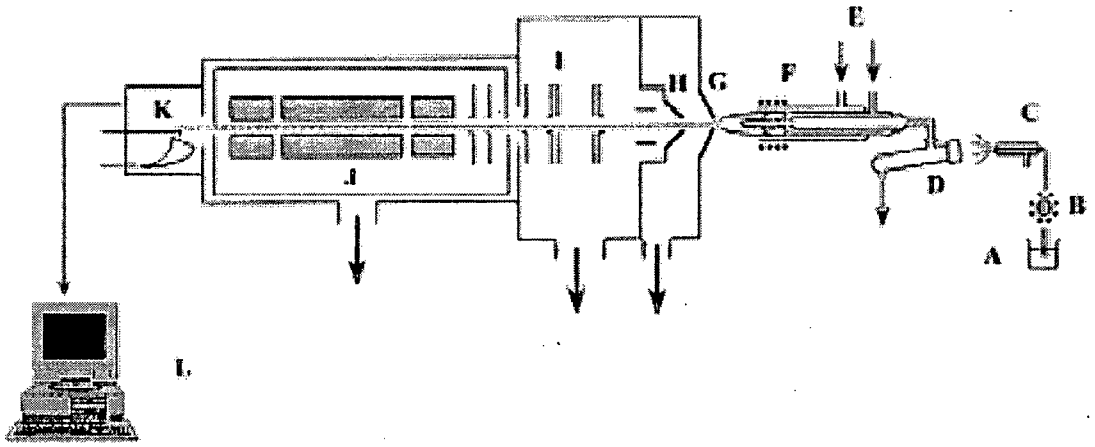

Figure 1.1 Schematic diagram of an inductively coupled plasma mass spectrometer [77]. (A) liquid sample, (B) pump, (C) nebulizer, (D) spray chamber, (E) argon gas torch inlets, (F) torch, (G) sampler cone, (H) skimmer cone, (I) ion lenses, (J) quadrupole mass analyzer, (K) electron multiplier detector, (L) data collection.

Plasma is formed from an argon gas feed within a quartz torch operating between 6,000 and 10,000 K [76]. A spark created with a tungsten pin seeds electrons that are then accelerated by oscillating magnetic and electric field vectors produced by a radio-frequency generator attached to the torch by a load coil. The electrons accelerated to a threshold kinetic energy cause ionization of the argon feed, which is introduced tangentially into the torch to create a vortex flow that sustains the plasma by enabling further ionization through collisions between excited electrons and argon atoms [77].

The sample is introduced into the ICP-MS as a liquid and is subsequently aerosolized in the nebulizer spray chamber. The sample droplets are then transported by the nebulizer gas flow into the plasma where they are vaporized, atomized, and ionized into singly charged species. Plasma proteins and other organic material in the sample are combusted by this

process. The protein-free singly charged ion beam is then focused through a series of nickel-plated cones and electrode lenses of varying voltages to a quadrupole mass analyzer where the ions are separated according to their mass-to-charge ratio and the signal intensities detected.

While ICP-MS has several inherent advantages over other trace element analysis techniques, its application to the analysis of complex mixtures can be challenging [76, 77, 82, 85]. In particular, the ICP-MS detector is extraordinarily sensitive. Although appropriate controls can eliminate background and matrix effects, improper sample preparation and handling prior to ICP-MS analysis can lead to contamination artifacts in the resulting data. The preparation of blood plasma samples for ICP-MS analysis necessarily requires a number of steps, beginning with blood collection, that may introduce trace elements into the sample. Contamination with non-physiological metals may also occur upon sample contact with air, with glassware, and with the components of the front-end HPLC system. Although not much can be done to address these sources of contamination, reducing the amount of handling significantly improves the sample purity. In addition, control experiments involving water samples from three sources (tap, distilled, and nanopure) were performed to assess the magnitude of the contamination effect. The variance between sample readings was significantly reduced with technique improvements.

The ICP-MS used in this study is a research-grade Elan-DRC 6000 ICP-MS prototype donated by Perkin-Elmer Sciex. This particular instrument is not equipped with a functioning dynamic reaction cell (DRC), and higher background noise and atomic

interaction effects are, therefore, expected in the spectra from this instrument as compared with those from a state-of-the-art ICP-MS [86]. Nevertheless, spectra from the prototype instrument are of sufficient quality to allow the objectives of this thesis to be met.

Chapter 2

Effects of Chromatographic Processing on Sample Integrity

2.1 Introduction

Plasma facilitates the transport of metal ions from one body organ to another through a series of complexation reactions involving the blood proteome and low-molecular weight ligands of blood plasma [6, 19, 38, 53, 60, 87]. It is, therefore, generally acknowledged that determination of chemical speciation data, rather than total element content, is necessary to establish a meaningful understanding of the biochemistry of trace elements in nutrition and in disease states. Methods for determining chemical speciation in aqueous environments have been evolving for more than a century, and the interested reader is referred to several authoritative reviews on the subject [47, 76, 88-90]. Here, I focus on the determination of metal-ion speciation in blood plasma and the methods used to monitor those chemical equilibria.

The need for high-sensitivity instrumentation to characterize metal-ion equilibria within blood plasma was recognized more than two decades ago by Scott and Bradwell [91], who combined two-dimensional immunoelectrophoresis with autoradiography to probe the distribution of metal ions in the blood. Their work identified the main metallo-proteins binding Fe, Zn, Ca, Ni and Cd in plasma and in so doing demonstrated the potential value in fractionating and probing the plasma metallo-proteome. Current metallo-proteomics strategies tend to hyphenate separation schemes such as chromatography or electrophoresis with element-specific detection to identify and quantify species of interest [69, 70, 74-79, 92,

93]. Separation schemes that have been used to probe distributions of metals in blood plasma and human urine include one- and two-dimensional gel electrophoresis [69], affinity (competitive-chelation) chromatography [76], hydrophobic interaction chromatography [74], ion-exchange chromatography [78, 94], and various forms of reversed-phase chromatography [92]. However, the most common strategy has been to use size-exclusion (gel-permeation) chromatography to separate the plasma metallo-proteome prior to investigating ion abundances using an appropriate ion-specific detection method [70, 75, 77].

Speciation results to date have been qualitative in nature, due in part to uncertainties related to the effect of the separation strategy on chemical equilibria within the parent plasma sample. An objective of this work is to gain a better understanding of if and how fractionation of the plasma metallo-proteome by size exclusion chromatography (SEC) alters metal-ion speciation. The selection of the SEC column to be used in this analysis is important, as although interactions with the stationary phase are weak in SEC, the results will nevertheless be at least somewhat specific to the resin used. Care must be taken to ensure that the selected resin fractionates over a wide molecular mass range and does not interact chemically with plasma components. Surprisingly few commercially available supports meet these criteria. For example, SEC resins based on silica gel, while useful in most applications, are known to activate clotting factors, particularly factor VIII [95]. Others do not allow for column sanitation with sodium hydroxide or nitric acid, making results acquired from repeated column use unreliable [96]. Two SEC resins that have found widespread use in plasma fractionation are Superose 6 [GE Healthcare; Upsalla, Sweden] and Fractogel EMD Bio-SEC [E. Merck; Darmstadt, Germany]. Both resins offer outstanding chemical

resistivity and the ability to fractionate linearly up to protein molecular masses above one million Daltons. In addition, neither resin has been seen to activate clotting factors or to react with any plasma components [97]. Here, I investigate the effect of fractionation, using a Fractogel EMD Bio-SEC column, on the stability and abundance of metal-ion complexes within a plasma sample. I first investigate whether copper speciation is perturbed during SEC processing of copper-citrate samples. I then carry out experiments on a series of model metal-ion complexes with known speciation thermodynamics to establish guidelines for understanding the tendency of the abundance of a given metal-ion complex to be altered during an SEC separation, and to establish a useful database for validating a model proposed by a collaborating scientist (Dr. Peter Pang). Dr. Pang's model is intended to predict the changes to elution chromatograms resulting from the dissociation of a metal-ion complex during fractionation by SEC. I focus on Cu(II)-binding model systems to avoid aquated-ion solubility limitations that complicate the handling of other metals essential to the human biosystem.

Copper, a transition metal with three biologically relevant oxidation states (Cu^{1+}, Cu^{2+}, and Cu^{3+}), is most often found in the Cu(II) form in biological systems. It is an essential ion, due in part to the fact that a large number of human proteins displaying oxidoreductase activity are copper containing. Copper functions as an electron transfer intermediate in redox reactions and has been shown to be an essential cofactor for catalytic activity in both oxidative and reductase enzymes, including catechol oxidase [98], superoxide dismutase 1 [99], cytochrome c oxidase [100], ceruloplasmin [101], and lysyl 6-oxidase [102]. Finally, copper is an essential component in gene expression. For example, the

copper ion has a functional role in Ace1, Amt1, Mac1 and other regulatory proteins that act as components of metal-responsive genetic switches [103].

Based on published speciation data, [104], copper ions in plasma may be partitioned into four distinct classes: (1) those which are bound effectively irreversibly to associated proteins and are therefore non-exchangable, (2) those which are strongly but reversibly bound to other proteins and therefore able to exchange slowly with similar ions in solution, (3) those that are more weakly and reversibly complexed with proteins and the numerous low molecular weight ligands present in plasma (ascorbate, amino acids, carboxylates, carbonates, phosphates, etc.), and (4) those in their free (aquated) state. The intent of this work is to clarify the boundaries of these four classes by connecting them more closely with stoichiometric formation constants and complex stabilities within the SEC column.

2.2 Materials and Methods

2.2.1 Reagents

All aqueous copper-citrate solutions were prepared in the absence of background buffer from copper chloride ($CuCl_2$ - Baker Analyzed Reagent, 97%, F.W. 170.48 g/mol), citric acid monohydrate (Sigma, F.W. 210.1 g/mol), and sodium chloride (NaCl - Sigma, 99.9%, F.W. 58.44 g/mol). All solutions were adjusted to pH 4 with NaOH or HCl stock solutions as described below. In the preparation of all aqueous solutions, water was first distilled and then treated with a NANOpure® II ultrafiltration system (Barnstead; Dubuque, IW). Acid and base standards (1 M) were generally prepared by diluting KOH and HCl Titrisol ampoules (Merck) according to the manufacturer's instructions.

The short Cu-binding peptides GHG, Ac-HGGG (Ac – acyl group), HGGG, Ac-GHH, GHH, and HGHH were synthesized and HPLC purified by the Nucleic Acids and Protein Service (NAPS) unit of the Michael Smith Laboratories. Each peptide is fully soluble in aqueous solution and was used without further purification.

2.2.2 Isothermal Titration Calorimetry

Isothermal titration calorimetry (ITC) studies of model metal-binding peptides were carried out on a MicroCal MCS-ITC (MicroCal Inc., Northampton, MA) by my collaborator Dr. Peter Pang following consultation on experimental design. Data analysis was performed using software (Origin) supplied by MicroCal and the method of Sigurskjold et al. [105] to allow for determination of stepwise formation constants for tight-binding complexes though competitive titration experiments. All experiments were carried out in 20 mM Hepes, pH 7.2 ± 0.2 (the pH of each solution characterized by ITC was adjusted to within ± 0.05 pH units) through sequential additions of 5-μL aliquots of 0.1 M KOH or HCl standard.

Metal-ion binding titrations were performed by sequentially injecting 25 consecutive 5-μL aliquots of $CuCl_2$ solution (with titrant concentration set to reach a 2-fold molar excess of NTA) into the sample cell (volume = 1.3528 mL) containing 20 to 100 μM peptide. The time between each injection was 5 minutes to ensure system equilibration following each injection. Contamination by CO_2 was avoided by flushing the ITC sample cell and the injection syringe with pure nitrogen before filling.

Control experiments to determine the heat of dilution were performed by titrating $CuCl_2$ solution into ligand-free buffer. All samples were degassed before loading into the sample cell and injection syringe. Each ITC experiment was performed two to three times and the average binding parameters and associated error calculated.

2.2.3 Chromatography

Size-based separations of plasma and various Cu-containing model solutions were carried out on an AKTA Explorer 100 FPLC system [GE Healthcare, Upsalla, Sweden] equipped with a pre-packed Fractogel-EMD Bio-SEC (600 x 16 mm) column [E. Merck, Darmstadt, Germany]. Eluent was monitored on-line at both 210 nm and 280 nm. Copper does not absorb light at 280 nm whereas citrate does, allowing facile assignment of peptide and citrate peak locations. Column cycling during operation consisted of first washing with 0.1% research grade HNO_3 to provide stringent cleaning of the column, resin equilibration in 4 column volumes (500 mL) of the 100 mM NaCl running buffer, and pulse sample injection onto the column in the same running buffer. Running buffer was degassed and filtered with 0.22 μm GV durapore membrane filters [Millipore] before use.

All samples were prepared in 15 mL polystyrene falcon tubes with solution concentrations determined gravimetrically. Each sample was filtered through a 0.22 μm GHP membrane (HPLC certified, Gelman Laboratory) into 2 mL Eppendorf tubes. Filtered samples (1 to 3 mL) were then manually injected into the 500-μL sample loop of the AKTA system using a BD syringe with a 0.7 x 50 mm metal needle. Excess sample was applied into the sample loop to ensure complete filling of the loop and reproducibility of subsequent

experiments. The 500-μL sample was applied to the SEC column and separated at a fixed flow rate between 0.25 and 1.0 mL/min. The void volume of the column was determined by first moment analysis to be 38 ± 2 mL.

2.2.4 Colorimetric Assays

Colorimetric titrations specific for citrate and copper were performed to identify the components in the eluted peaks. The citrate specific colorimetric assay involved spiking elution fractions with a phenolphthalein (PHT) indicator in 70% ethanol and then titrating with 1 mM potassium hydroxide (KOH). Hereafter, this procedure is termed the PHT assay. The end-point of the titration and the presence of citrate are indicated by a change in the solution color from clear to pink. A 100 mM citrate solution and a 100 mM $CuCl_2$ solution acted as controls to negate false positive results.

The copper specific colorimetric assay was based on addition of 1-(2-Pyridylazo)-2-Naphthol indicator (PAN) to each eluted fraction and titration of the resulting mixture with 10 mM EDTA. A change in the solution color from red to yellow indicates the end-point of the titration from which a mass balance may be used to determine copper concentration. Hereafter this procedure is termed the PAN assay. Citrate (100 mM), $CuCl_2$ (10 mM), and Cu-citrate (10 mM) solutions were titrated as controls and calibration standards.

2.2.5 Monitoring of Copper by ICP-MS

The distribution of copper within an elution chromatogram was also determined by sequentially analyzing each 1 mL column elution fraction with a prototype Elan 6000 – DRC

[Perkin Elmer – Sciex] inductively coupled plasma mass spectrometer (ICP-MS). Following ignition of each new plasma flame, the mass spectrometer was calibrated with standard copper solutions (0.1 parts per billion - ppb, 10 ppb, 50 ppb, and 100 ppb) made from a commercially available 100 mg/L (100 ppm) calibrant (Instrument Calibration Standard, Fisher Scientific, ICP-MS grade, cat. # CL-CAL-2) containing 1% HNO_3 (Fisher Scientific, trace metal grade). Metal-ion contamination of samples was minimized by preparing all solutions in acid-treated plastic-ware. Acid treatment consisted of soaking the plastic containers in 3% HNO_3 + 3% HCl overnight, followed by rinsing three consecutive times with nanopure water. The plastic-ware included Nalgene containers (VWR catalogue # 16058-145), metal-free pipette tips (VWR cat. # 53508-991 and Sigma cat. # Z35, 155-5), 250-mL polymethyl pentene beakers (Fisher cat. # 02-591-15E), 1 L polymethyl pentene volumetric flasks (Fisher cat. # 10-198-52G), and 15 mL Sarstedt conical tubes. The argon gas used for plasma generation was welder's grade from Praxair.

Each fraction (1 mL) was gravimetrically diluted 1000-fold in 1% HNO_3 prior to ICP-MS analysis to supply sufficient sample volume for the measurement. A minimum of 2 mL of each sample was nebulized into the mass spectrometer to ensure uniform readings for the one- second analysis. Between the analysis of subsequent samples, the sample tubing was rinsed with 1% HNO_3 and soaked in HNO_3 for 3 minutes to eliminate copper contamination from the previous sample within the lines and the nebulizer. The signal intensity of the copper isotope (Cu 63 – 69%) was reported in counts and converted to ppb. Following completion of data collection, the sample transfer lines were rinsed with Nanopure water for five minutes, with the plasma ignited, to clean and to prevent corrosion of the

interior of the mass spectrometer. The signal intensity for each fraction was corrected for matrix background effects by subtracting the copper intensity of Cu-free buffer eluted from the SEC column.

2.3 Results and Discussion

2.3.1 Evidence of Perturbed Chemical Equilibria in the Cu(II) – Citrate System

Copper-citrate solutions were resolved into two connected peaks following size-exclusion chromatography performed at a volumetric flow rate of 1 mL min^{-1}. Figure 2.1 shows results for the SEC separation of a 48 mM solution that contains equimolar amounts of Cu(II) and citrate, buffered to pH 4 in a background of 0.1 M sodium chloride (NaCl). Detection by the PHT assay and by absorbance at 280 nm indicates that citrate, in both its complexed and free states, elutes within the single peak centered at an elution volume of 84 mL. This citrate peak assignment is supported by experimental elution volumes for citrate in the absence of added Cu(II) (Figure 2.2), which show that free citrate at pH 4 elutes as a near-gaussian peak with a center-point volume of 87 ± 1 mL. Cu(II) concentrations in eluent fractions were independently monitored by the PAN assay, ICP-MS analysis, and absorbance at 210 nm, which shows significant sensitivity to Cu(II) concentration. The co-localization of ICP-MS and absorbance data (Figure 2.1) indicates that Cu(II) is present both in the citrate containing peak eluting at 84 mL and in the citrate-free peak eluting at 108 mL. Eluent fractions from both peaks were also analyzed by matrix-assisted laser desorption/ionization time of flight mass spectrometry (MALDI-TOF-MS). The absence of citrate in the second peak was confirmed. The late eluting peak, therefore, provides a measure of the aquated Cu(II) concentration following SEC processing.

Calibration of absorbance data at 280 nm to molar citrate concentration and at 210 nm to molar $CuCl_2$ concentration resulted in linear relations (data not shown) that were used to establish a Cu(II) mass balance within the column. This analysis, when combined with the integrated area of the peak centered at 108 mL in Figure 2.2, indicates that 16.7 ± 3% of the total Cu(II) introduced into the column as a 1:1 Cu:citrate mixture elutes as aquated cupric ions.

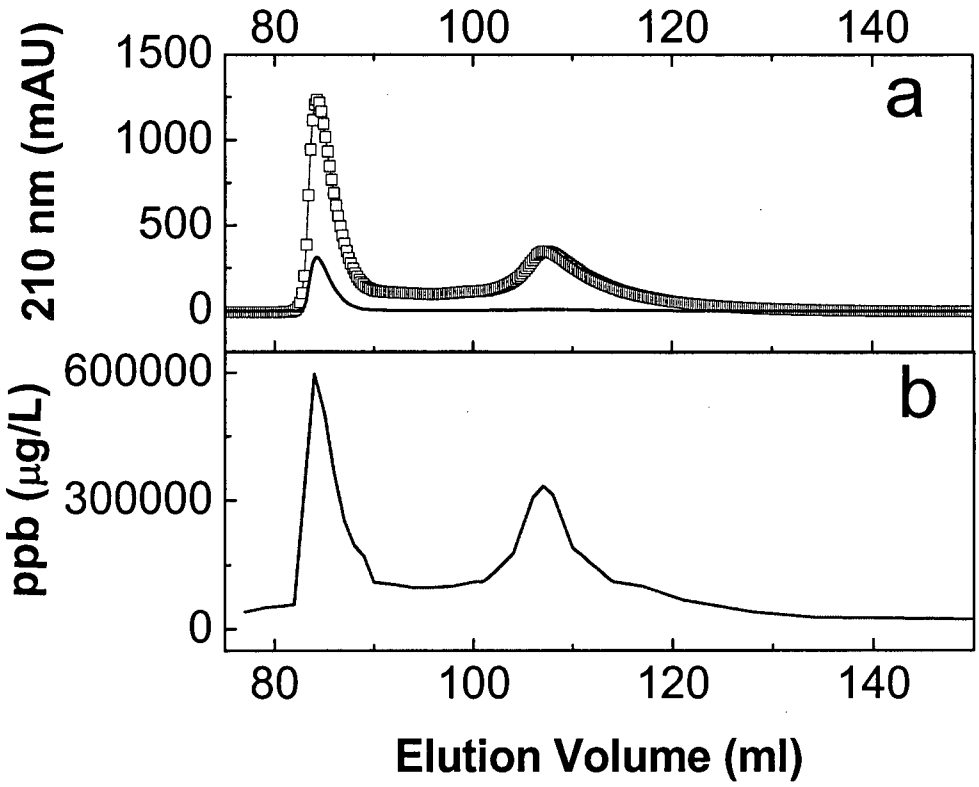

Figure 2.1 Elution chromatogram at room temperature (20°C) for 500 µL of an aqueous solution containing 48 mM $CuCl_2$, 48 mM citric acid, and 0.1 M NaCl onto the Bio-SEC column at a mobile-phase volumetric flow rate of 1 mL min^{-1}: (a) Eluent monitoring at 280 nm (line) and 210 nm (squares), (b) cupric ion concentrations (ppb) in eluent fractions determined by ICP-MS.

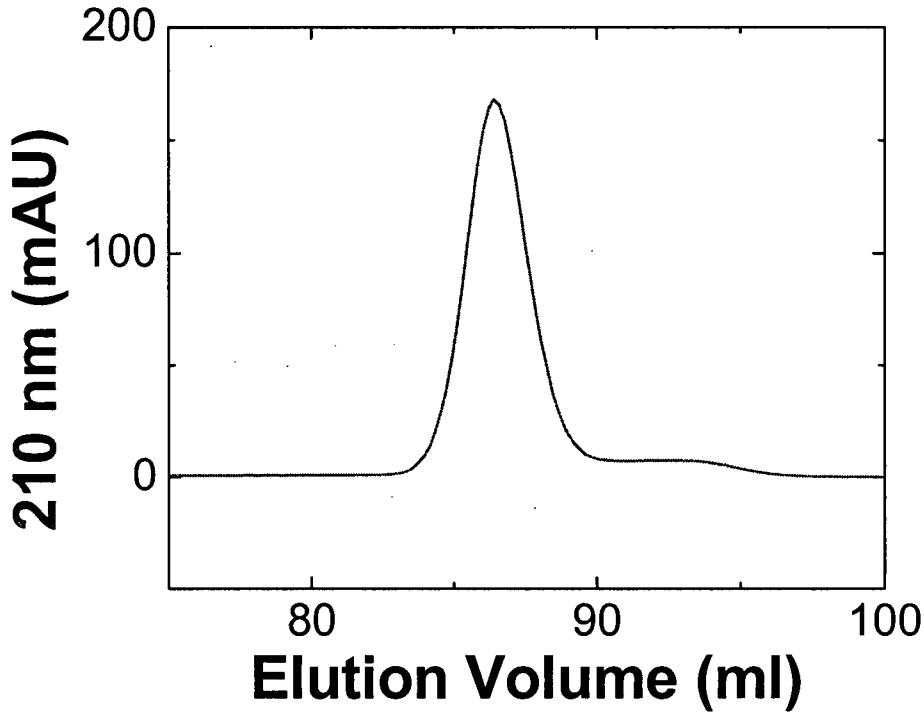

Figure 2.2 Elution chromatogram (210 nm) at room temperature (20°C) for 500 μL of an aqueous solution containing 48 mM citric acid and 0.1 M NaCl onto the Bio-SEC column at a mobile-phase volumetric flow rate of 1 mL min^{-1}.

Chemical equilibria within the aqueous $CuCl_2$ – citric acid system at 25°C are well defined [106-109]. Martell and Smith [104] have unified all reliable potentiometry results for this system to generate a complete picture of speciation thermodynamics. Species present between pH 2 and 6, the pH range of our chromatographic studies, are shown in Table 2.1 along with the corresponding overall stoichiometric formation constant values.

Table 2.1 **Speciation, protonation constants, and overall stoichiometric formation constants for aqueous solutions at 20°C containing $CuCl_2$ (Cu), citric acid (L), and 0.1 M NaCl. Data taken from Martell E, Smith RM, NIST Standard Reference Database version 6.0 (2000).**

Species	pK_a	$Log_{10}\ \beta_{xyz}$
HL	5.65	5.65
H_2L	4.35	9.99
H_3L	2.90	12.89
H_2LCu		11.93
HLCu		9.55
L_2Cu_2		14.77
$H_{-1}LCu$		2.16
$H_{-2}L_2Cu_2$		5.61

Both overall formation constants, also known as stability constants and denoted by the symbol β, and stepwise formation constants, denoted by the symbol *K*, are reported in this work. To understand the relation between these quantities, consider the binary metal (*M*) - ligand (*L*) complex ML_n. The reaction

$$M + nL \xleftrightarrow{\beta_{0n1}} ML_n \qquad \text{(Constant T and P)}$$

may be used to define for the complex the overall stoichiometric formation constant β

$$\beta_{0n1} = \frac{[ML_n]}{[M][L]^n} \qquad (1)$$

which is expressed in Equation (1) in terms of *equilibrium concentrations* of the reactants in their fully uncomplexed states. We therefore designate β_{0n1} and all others reported in this work as *stoichiometric* formation constants to clearly differentiate them from *absolute* formation constants based on the activities of the reactants. The subscript 0n1 on the β defined in Equation (1) indicates the molecules of protons (0), ligand (n), and Cu^{2+} (1), respectively, present in the complex. When citric acid serves as the ligand, a negative number in the first subscript register indicates deprotonation of the C3 hydroxyl group on the molecule (see Figure 2.3) which deprotonates at very high pH (pK_a = 12.4) in aqueous solution in the absence of a strongly coordinating metal ion such as Cu(II).

The stepwise stoichiometric equilibrium constant for the same binary ML_n complex may be defined from the reaction

$$ML_{n-1} + L \xleftrightarrow{K_{0n1}} ML_n \qquad \text{(Constant T and P)}$$

as

$$K_{0n1} = \frac{[ML_n]}{[ML_{n-1}][L]} \tag{2}$$

From the above definitions it is evident that

$$\beta_{0n1} = K_{011}K_{021}\ldots K_{0n1} = \prod_{i=1}^{n} K_{0i1} \tag{3}$$

The normalized equilibrium concentrations of species formed in the aqueous $CuCl_2$ – citric acid system at 25°C are shown in Figure 2.4 as a function of solution pH. The solution composition is the same as in the sample applied to the SEC column to generate the elution chromatogram shown in Figure 2.1. At pH 4, the pH used in the SEC studies, Cu(II) is distributed between five equilibrium complexes (HLCu, L_2Cu_2, $H_{-1}L_2Cu_2$, $H_{-1}LCu$, and $H_{-2}L_2Cu_2$), with the $H_{-1}L_2Cu_2$, L_2Cu_2, HLCu and $H_{-1}LCu$ complexes being the most abundant. The equilibrium concentration of the aquated cupric ion is very near zero at this pH and solution composition. As the initial sample was equilibrated prior to injection, it is evident that significant dissociation of the cupric ion from copper-citrate complexes occurs during sample transport through the SEC column, providing clear evidence that SEC processing can disturb equilibria. The analysis of metal-ion distribution in chromatographic fractions by ICP-MS therefore may not provide an accurate representation of how that metal ion is distributed in the parent sample.

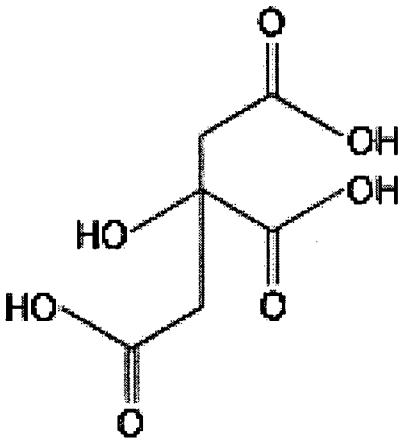

Figure 2.3 Citric acid structure. The C3 hydroxyl group deprotonates only at high pH (pK_a = 12.4) or through metal-ion complexation. The pK_a for the carboxylate protons are shown in Table 2.1.

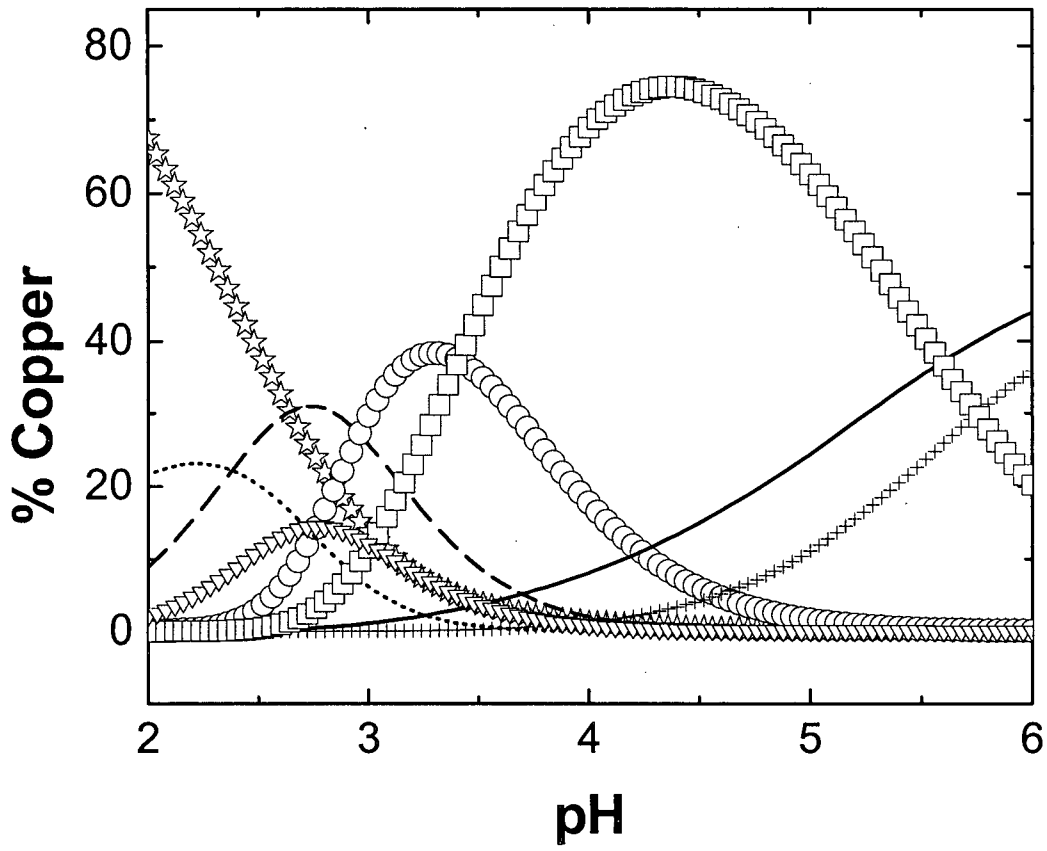

Figure 2.4 Speciation diagram of aquated cupric ion and citric acid – copper complexes for the condition where $[Cu^{2+}]$ = [Citrate] = 48 mM (0.1 NaCl, 20°C). L = citrate and H = hydrogen. Refer to table 2.1. The following species are minimally present at pH 4: aquated Cu^{2+} (stars), HLCu (dashed line), LCu_2 (triangles), H_2LCu (dotted line), $H_{-1}LCu$ (solid line), and $H_{-2}L_2\ Cu_2$ (+ line). The $H_{-1}L_2Cu_2$ (squares) and L_2Cu_2 (circles) complexes dominate the system at pH 4.

The monitoring of the elution chromatogram by ICP-MS and using the PAN assay shows nonzero Cu(II) concentrations in all elution fractions lying between the two major elution peaks. This is consistent with the dynamic dissociation of the cupric ion from various parent $H_xL_yCu_z$ complexes that results from the slow migration of the Cu(II) ion within the SEC column relative to that of the larger citrate ligand and complexes containing that ligand. As the kinetics of these dissociation processes are dictated by the Cu(II) dissociation rate constant μ_r (s^{-1}) for each complex present in the citrate-containing peak, one predicts from

the bimolecular-complex dissociation rate equation that the amount of free cupric ion [Cu^{2+}] present in the eluted fraction should increase with the amount of time each complex is held away from equilibrium in a cupric-ion poor environment. Thus, [Cu^{2+}] should increase either with increased column length at fixed mobile-phase flow rate or with decreased mobile-phase flow at fixed column length. Qualitative evidence of the latter effect is shown in Figure 2.5, where ICP-MS data show an increase in free copper when the mobile-phase flow rate is decreased four-fold under otherwise constant column operating conditions (pH 4, 1:1 Cu-citrate solution: 48 mM Cu^{2+}, 48 mM Citrate in 0.1 M NaCl).

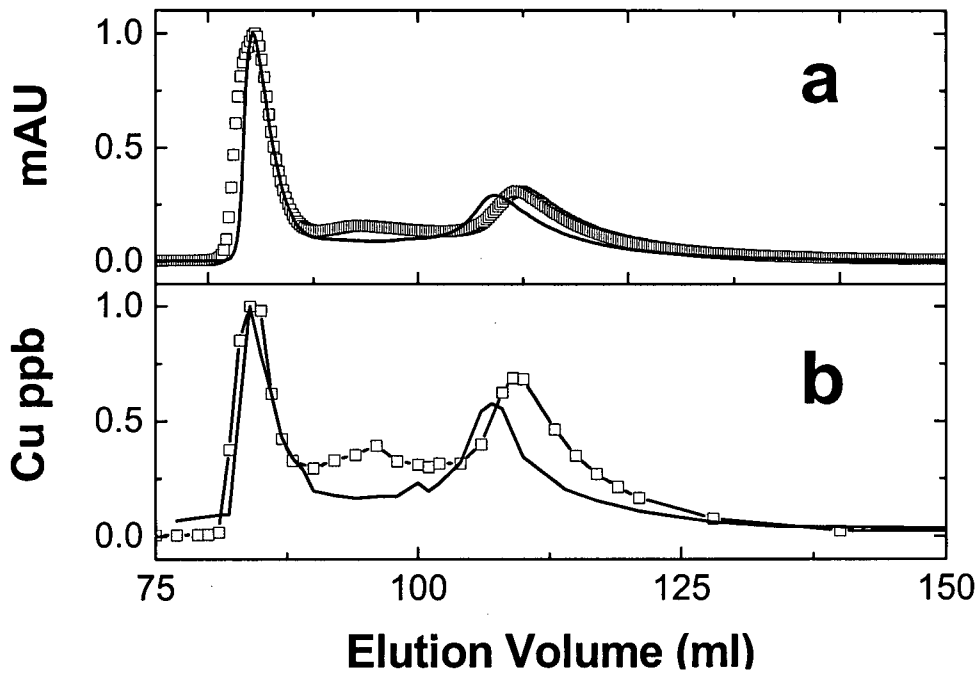

Figure 2.5 Normalized elution chromatograms for the system described in Figure 2.1 at two different volumetric flow rates: 0.25 mL min^{-1} (squares) and 1 mL min^{-1} (solid line). Chromatogram detection at 210 nm and by ICP-MS are shown in panels (a) and (b), respectively.

2.3.2 Stepwise Formation Constants for $H_x(Citrate)_yCu_z$ Complexes and the tendency for On-Column Complex Dissociation

While the dissociation rate constant provides an unambiguous measure of the lifetime of a complex, μ_r data are scarce, particularly for metallo-protein dissociation reactions. An alternative, more widely available metric is therefore required for my analysis. Stepwise formation constants (*i.e.*, stability constants) have been reported for metal-ion binding to a number of plasma proteins and low-molecular-weight ligands within plasma [21, 23, 87, 110, 111]. As they refer to the equilibrium state, formation constants provide no direct indication of the kinetics of complex dissociation (*i.e.*, the lifetime of a complex). However, the stepwise dissociation constant (K_d), which is given by the inverse of the corresponding stepwise formation constant,

$$K_d = \frac{1}{K_a} = \frac{\mu_r}{\mu_f} \qquad (4)$$

should in general be a rough qualitative predictor of the lifetimes of complexes. A simple analysis provides an understanding as to why this is the case. Known rates of molecular diffusion provide an upper limit for the frequency with which analytes can collide in solution to form a complex. For a bimolecular complexation process in aqueous solution, this diffusional limit sets the maximum value for μ_f, the rate constant for complex formation, to be about 10^9 M^{-1} s^{-1}. As not all collisions will result in complex formation, the actual μ_f will be less than 10^9 M^{-1} s^{-1}. Where they have been measured, μ_f values for protein-ligand complexation reactions generally lie between 10^5 and 10^7 M^{-1} s^{-1}, but a relatively small number of faster on-rates (*i.e.* 10^8) have been reported [112]. Forward rate constants near

10^7 M^{-1} s^{-1} have been reported for weak antibody-antigen complexes, which are characterized by K_d values of *ca.* 10^{-7} M. Similarly, a μ_f of 5.6 x 10^6 M^{-1} s^{-1} (i.e., close to 10^7) has been reported for biotin – avidin, despite the significantly higher stability of that complex (K_d = 10^{-15} M) [113, 114]. If we accept a three-order of magnitude uncertainty in the value of μ_f such that it lies somewhere between 10^5 and 10^8 M^{-1} s^{-1}, the value of μ_r for the biotin – avidin complex is predicted to be at least 1,000,000 fold less than that of the weak antibody - antigen complex. As a result, while the half-life ($t_{1/2}$) of the antibody – antigen complex is at most 10 seconds,

$$t_{1/2} = \frac{\ln 2}{\mu_r}, \tag{5}$$

that of the avidin – biotin complex is at least 100 days. We, therefore, might expect passage of a weak antibody – antigen complex through an SEC column to diminish the concentration of the complex in the eluent, but we would not expect the same process to alter the concentration of an avidin – biotin complex unless additional ion-transfer dynamics were introduced into the system through the addition of a competitive biotin-binding ligand. A key objective of this work is to show that this expectation is reflected in the K_d values (and thus the formation constants) for each complex.

As indicated by the protonation constants and overall formation constants reported in Table 2.1, citric acid is mainly present in its monoprotonated (HL) state with some diprotonated (H_2L) state present at pH 4. Understanding why Cu(II) dissociation is observed (Figure 2.1) during SEC processing of equimolar Cu(II):citric acid solutions at pH 4 is,

therefore, facilitated by determination of the stepwise formation constants for Cu(II) complexes formed with citric acid in either of these favored protonation states. Table 2.2 reports stepwise formation constants for the various $H_xL_yCu_z$ complexes formed between the cupric ion and citric acid in its HL state in aqueous solution at pH 4. I note here that protons are released during formation of these complexes, making the concentration of each complex relative to that of the aquated cupric ion a pH dependent quantity. As the data reported in Table 2.2 provide the value of $[H_xL_yCu_z]/[HL]^y[Cu^{2+}]^z$ for each complex formed at pH 4, the contribution of the concentration of free protons released as a reaction product is not included. As a result, unlike the corresponding β_{xyz} values, the reported $K_{xyz}/[H^+]^{y-x}$ are pH dependent quantities valid only at pH 4. The stepwise stabilities at pH 4 reveal why Cu(II) is predominantly found in $H_{-1}L_2Cu_2$ and L_2Cu_2 complexes at that pH. Furthermore, estimated minimum and maximum half-lives computed for these complexes are *ca.* 50 μs (HLCu) and 100 days ($H_{-1}L_2Cu_2$), respectively, which correlate well with the observed partial dissociation of bound Cu(II) during SEC column processing.

Table 2.2 **Stepwise formation constants for citrate-containing $H_xL_yCu_z$ complexes formed according to the reaction** $yHL + zCu^{2+} \xleftrightarrow{K_{xyz}} H_xL_yCu_z + (y-x)H^+$ **in aqueous 0.1 M NaCl solution at 20°C.**

Species	$\log_{10}\left(\frac{K_{xyz}}{[H^+]^{y-x}}\right)$
$H_{-1}L_2Cu_2$	12.16
L_2Cu_2	11.47
$H_{-1}LCu$	4.51
HLCu	3.90

What remains is to establish an understanding of the general boundaries separating those metal-ion complexes that fully dissociate during column processing from those that partially dissociate during this process, and in turn from those that do not dissociate to any significant extent. In the Cu(II) – citric acid system, this level of knowledge would require precise experimental determination of the half-lives of each complex formed and the development of a reaction-transport model for analyte migration in and elution from the SEC column. This model has been developed by my collaborator, Dr Peter Pang, and although data I acquired was used for model development, the derivation and validation of that model were not the focus of my thesis research. Instead, efforts where made to determine stabilities for model 1:1 Cu(II):peptide complexes and to then correlate those stabilities with the chromatographic behavior of each Cu(II):peptide complex within the SEC column.

2.3.3 Binding Stoichiometry and Thermodynamics for Cu(II) - Peptide Complexes

A number of short peptides is known to bind the cupric ion. Most have been extracted from Cu(II) binding sites within various metallo-proteins [115, 116], while others are based on the known divalent metal binding properties of the histidine ligand [117-119]. While formation constants have been reported for cupric-ion binding to some of these peptides, different solution conditions (temperature and ionic strength) were used in each measurement, making comparison of values difficult. A set of 1:1 Cu(II) binding peptides (Table 2.3) with anticipated complex stabilities covering nearly 10 orders of magnitude were therefore selected from those described in previous studies and then characterized by isothermal titration calorimetry (ITC) to determine stepwise formation constants under identical solution conditions (20°C, pH 5, 0.1 M NaCl).

Table 2.3 **pH-Specific stepwise formation constants determined by ITC for 1:1 complexes formed between the model peptide indicated and the cupric ion according to the reaction $yHL + zCu^{2+} \xleftrightarrow{K_{xyz}} H_xL_yCu_z + (y-x)H^+$ in aqueous 0.1 M NaCl solution at 20°C and pH 5. The regressed complex stoichiometry n (moles Cu^{2+} bound per mole peptide) is also provided.**

Peptide (L)[1]	n	$\log_{10}\left(\frac{K_{xyz}}{[H^+]^{y-x}}\right)$ *or* $\log_{10} K_{xyz}$
GHG	0.79	4.65(1)[4]
Ac-HGGG[2]	0.85	4.24(2)
HGGG	1.12	6.82(3)
Ac-GHH	0.96	9.44(3)
GHH[3]	1.09	11.9(2)
HGHH[3]	1.04	13.7(3)

1) ITC data acquired by Dr. P. Pang in consultation with C. Levesque
2) Ac – Acylated N-terminus
3) Stepwise formation constant measured by displacement ITC using HGGG as the displaced ligand as described in Sigurskjold et al. (1994).
4) Value in parenthesis represents standard error in last digit of reported formation constant.

Figure 2.6 shows ITC data for titration of the peptide GHG with $CuCl_2$ at pH 5 and 20°C. The relatively slow transition from unsaturated to saturated peptide is indicative of a weak binding complex. Slight under-estimation by ITC of reaction stoichiometry is frequently observed in weak binding systems [Creagh et al., 2005]. Equimolar stoichiometry has been confirmed for the Ac-HGGG:Cu complex [120] but not for the GHG:Cu complex. A mixture of 1:1 and 2:1 complex formation could therefore be responsible for the low

reaction stoichiometry observed for the GHG peptide. For comparison, ITC results for the tighter binding HGGG peptide are shown in Figure 2.7.

As noted in Table 2.3, the reported ITC results are based on experiments carried out by Dr. Peter Pang in consultation and as part of a collaboration with the author. This partitioning of experimental work was established to allow me to focus my second year of research on the ICP-MS studies of blood plasma reported in Chapter 3 of this thesis.

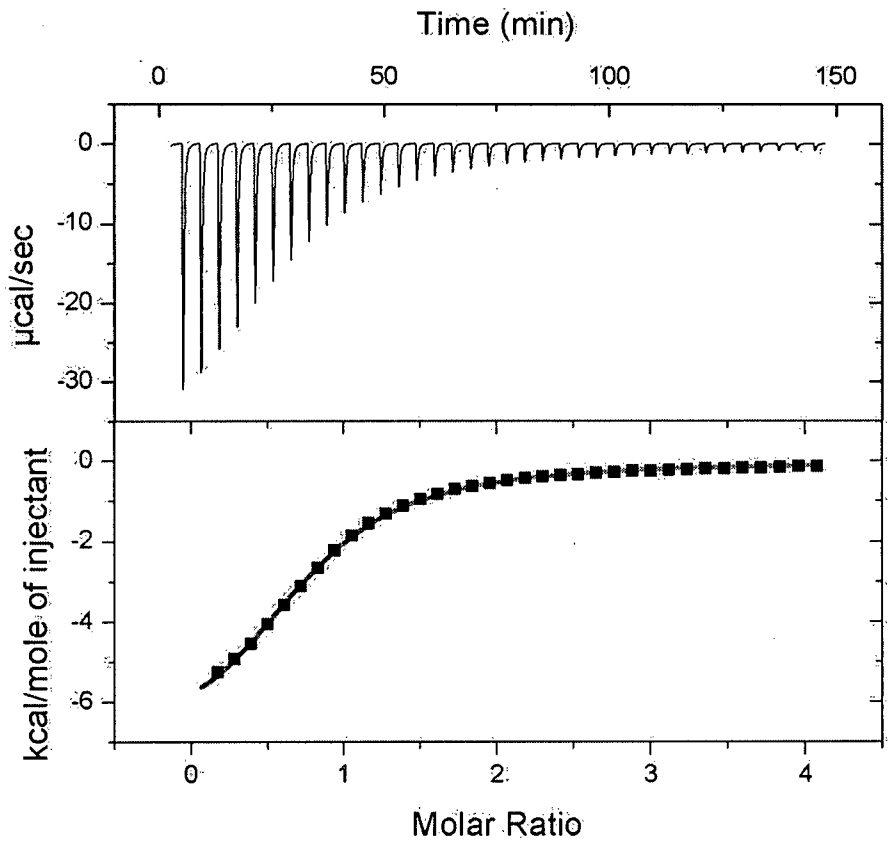

Figure 2.6 Analysis of cupric-ion binding to the synthetic peptide GHG using isothermal titration calorimetry at 293 K. (Top) Raw titration data showing the heat response resulting from each 10 µL injection of 0.24 mM $CuCl_2$ into an ITC cell containing 30 µM GHG in 0.1 M NaCl at pH 5. (Bottom) Peak area normalized to the moles of copper added and corrected for the heat of dilution (squares), and nonlinear least squares fit (line) to a single-site bimolecular interaction model.

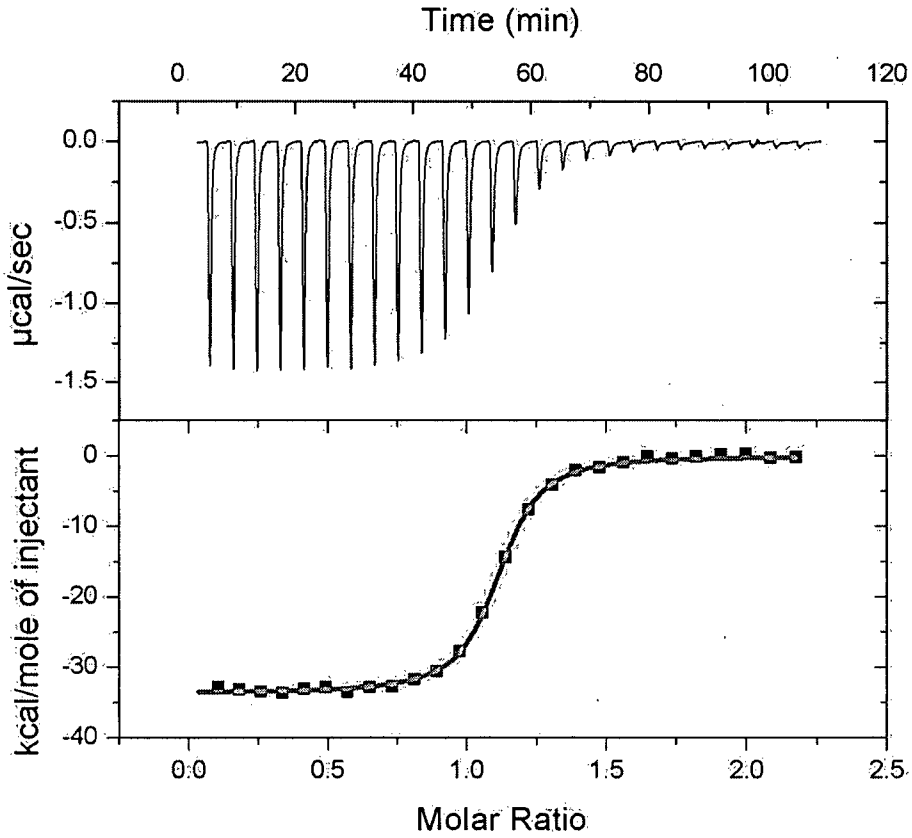

Figure 2.7 Analysis of cupric-ion binding to the synthetic peptide HGGG using isothermal titration calorimetry at 293 K. (Top) Raw titration data showing the heat response resulting from each 10 µL injection of 300 µM $CuCl_2$ into the ITC cell containing 20 µM HGGG in 0.1 M NaCl at pH 5. (Bottom) Peak area normalized to the moles of copper added and corrected for the heat of dilution (squares), and nonlinear least squares fit (line) to a single-site bimolecular interaction model.

2.3.4 Elution Profiles for Cu(II) – Peptide Complexes

Elution chromatograms for equimolar peptide:Cu^{2+} mixtures in 0.1 M NaCl (pH 5, 20°C) are shown in Figures 2.8 to 2.13. The simple 1:1 binding stoichiometry of each of these two-solute systems greatly simplifies data analysis relative to the more complex speciation dynamics observed in the Cu^{2+}:citric acid system. For the two peptides (GHG and Ac-HGGG) that bind Cu^{2+} weakly, sample migration through the Fractogel-EMD Bio-SEC column results in complete baseline separation of the peptide and Cu^{2+} elution peaks,

suggesting that both peptides elute in their *apo*-forms. Cu^{2+} mass balances based on the area of the metal-ion elution peak support this finding, as the Cu^{2+} within that peak closes the mass balance to within ± 15% in both cases.

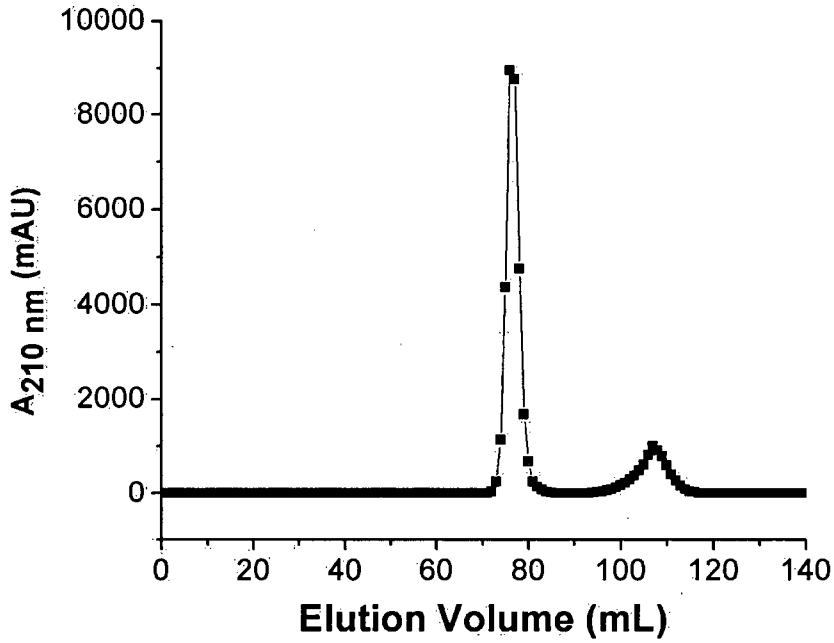

Figure 2.8 Elution chromatogram (210 nm) at room temperature (20°C) for 500 μL of an aqueous solution (pH 5) containing 40 mM $CuCl_2$, 40 mM GHG, and 0.1 M NaCl onto the Bio-SEC column at a mobile-phase volumetric flow rate of 1 mL min.

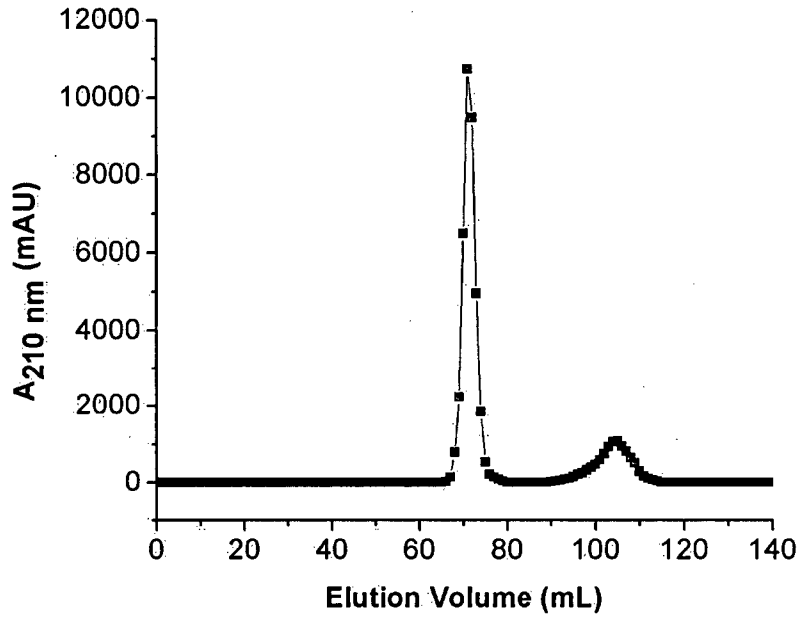

Figure 2.9 Elution (210 nm) chromatogram at room temperature (20°C) for 500 μL of an aqueous solution (pH 5) containing 40 mM $CuCl_2$, 40 mM Ac-HGGG, and 0.1 M NaCl onto the Bio-SEC column at a mobile-phase volumetric flow rate of 1 mL min^{-1}.

The tighter binding HGGG and Ac-GHH peptides exhibit elution profiles similar to those observed in the Cu^{2+}:citric acid system, suggesting that column-mediated Cu(II) dissociation from these complexes occurs on a time scale on the order of the peptide elution time. As predicted through arguments presented in section 2.3.2, the concentration of aquated Cu(II) in the column eluent decreases with increasing complex stability constant. Here it is important to note that even in the weak binding (GHG and Ac-HGGG) systems, the equilibrium concentration of Cu^{2+} in the parent sample is less than 1% of the total copper in the sample. Thus the size of the free copper peaks in the elution chromatograms reflects the extent of complex dissociation to within experimental error.

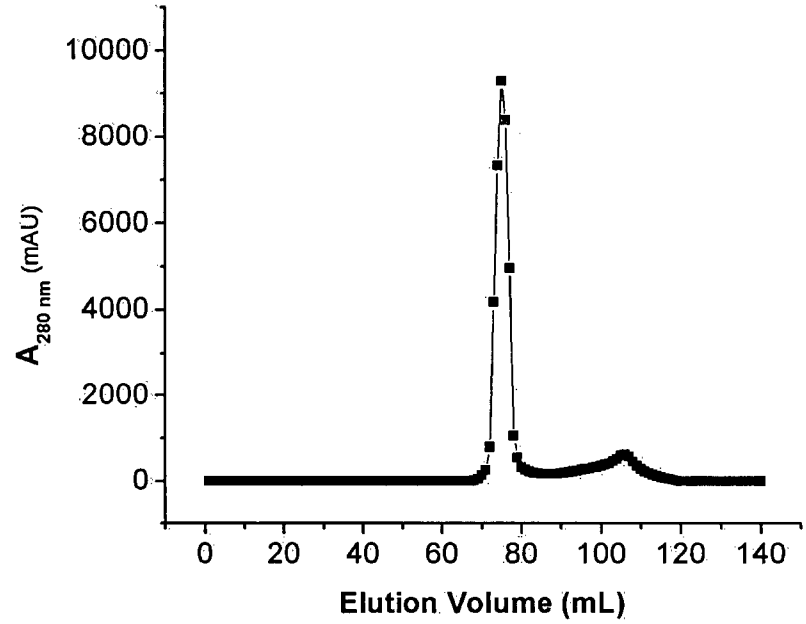

Figure 2.10 Elution (210 nm) chromatogram at room temperature (20°C) for 500 μL of an aqueous solution (pH 5) containing 40 mM $CuCl_2$, 40 mM HGGG, and 0.1 M NaCl onto the Bio-SEC column at a mobile-phase volumetric flow rate of 1 mL min^{-1}.

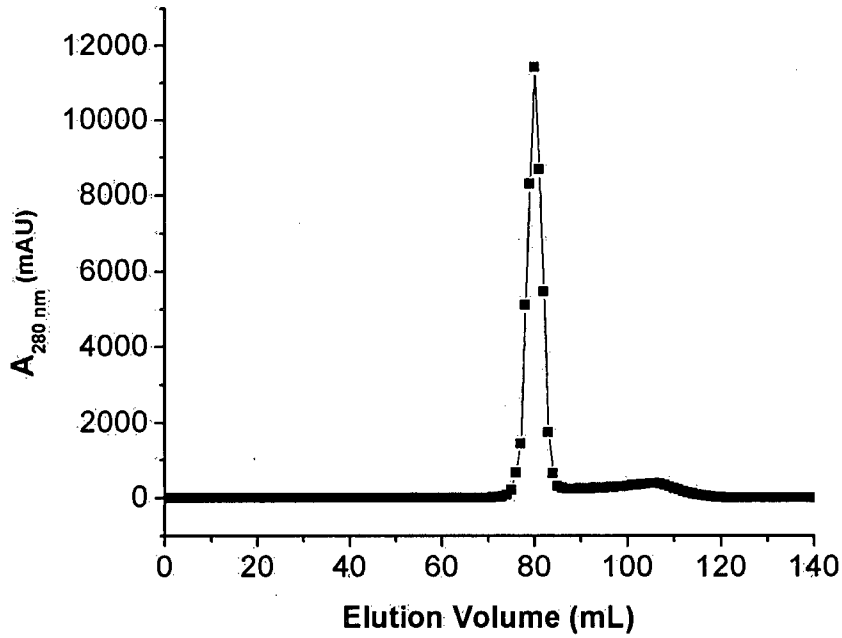

Figure 2.11 Elution (210 nm) chromatogram at room temperature (20°C) for 500 μL of an aqueous solution (pH 5) containing 40 mM $CuCl_2$, 40 mM Ac-GHH, and 0.1 M NaCl onto the Bio-SEC column at a mobile-phase volumetric flow rate of 1 mL min^{-1}.

A distinct free-Cu(II) elution peak is not observed in the chromatogram for the GHH peptide. However, the asymmetric tail on the trailing end of the peptide elution peak indicates that a minor amount of dissociation may have occurred during column processing. In contrast, no tailing effects are observed in the elution peak for the highly stable HGHH:Cu^{2+} complex.

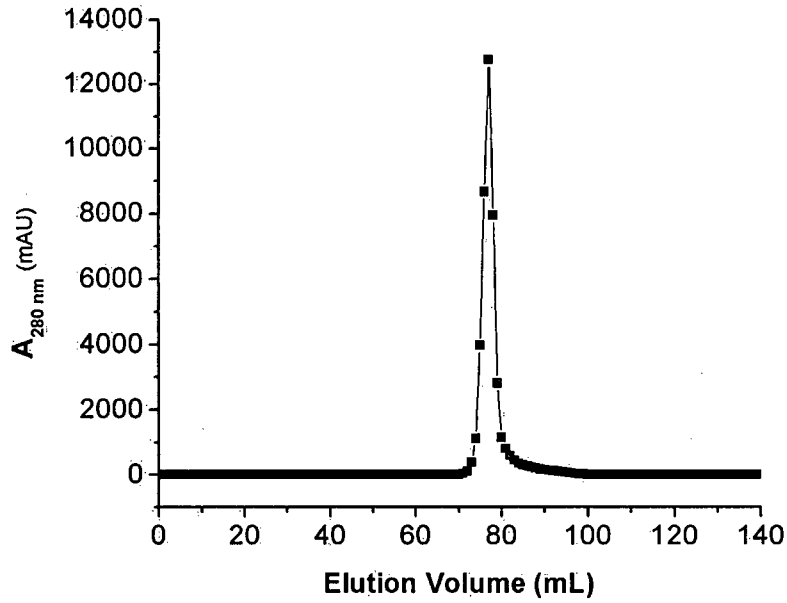

Figure 2.12 Elution (210 nm) chromatogram at room temperature (20°C) for 500 μL of an aqueous solution (pH 5) containing 40 mM $CuCl_2$, 40 mM GHH, and 0.1 M NaCl onto the Bio-SEC column at a mobile-phase volumetric flow rate of 1 mL min^{-1}.

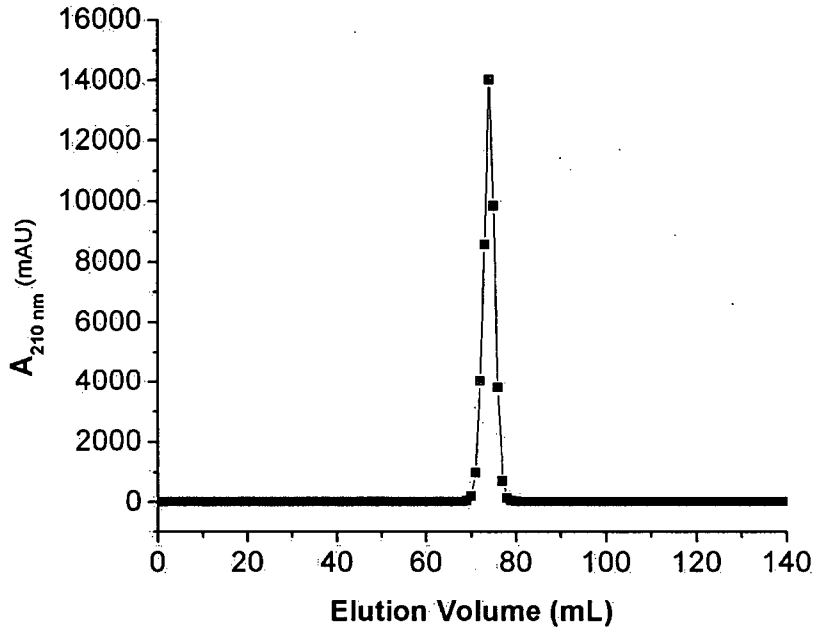

Figure 2.13 Elution (210 nm) chromatogram at room temperature (20°C) for 500 μL of an aqueous solution (pH 5) containing 40 mM $CuCl_2$, 40 mM HGHH, and 0.1 M NaCl onto the Bio-SEC column at a mobile-phase volumetric flow rate of 1 mL min^{-1}.

Although limited in number, the elution behavior and stepwise formation constants for the six model peptide:Cu^{2+} complexes (as well as for the citric acid:Cu^{2+} system) appear to provide a sound basis for qualitatively predicting the behaviours of metal-ion complexes during chromatographic processing on the Fractogel-EMD Bio-SEC column.

2.3.5 Classification of Metallo-Complex Stabilities During SEC Processing

For the six model peptide:Cu^{2+} complexes studied, the extent of Cu(II) dissociation during SEC processing is seen to correlate well with stepwise stability constants, suggesting that $\log_{10}$ ($K_{xyz}/[H^+]^{y-x}$) data can provide a useful metric to evaluate the reliability of SEC/ICP-MS in interrogating metal-ion content within an isolated 1:1 complex. When its $\log_{10}$ ($K_{xyz}/[H^+]^{y-x}$) is higher than *ca.* 11, the complex is unlikely to dissociate significantly during Bio-SEC processing, so that the resulting ICP-MS data should provide an

unambiguous measure of metal within the parent sample. While SEC/ICP-MS may be used to interrogate metal-ion complexes having stepwise stabilities less than 10^{11}, the ability to quantitatively determine the stoichiometry of such complexes will be compromised by metal-ion dissociation. Indeed, the two model complexes of lowest stability are seen to completely dissociate in the SEC column, effectively precluding the use of SEC/ICP-MS in identifying and analyzing metal-ion complexes with $\log_{10} (K_{xyz}/[H^+]^{y-x})$ values less than *ca.* 5.

The interpretation of SEC/ICP-MS data for more complex samples, such as blood plasma, using the simple classification scheme outlined above assumes that the lifetime of a more stable metal-ion complex is not influenced by the presence of ligands and complexes of lower stability competing for the same metal. My SEC/ICP-MS data for the Cu(II):citrate system indicates that this assumption is a poor one. Over 91% of the Cu(II) in the 48-mM 1:1 Cu(II):citric acid (pH 4, 20°C) sample loaded onto the Bio-SEC column is present within two complexes of stepwise stability greater than 10^{11} (see Figure 2.4 And Table 2.2). However, 17% of the total Cu(II) injected elutes as aquated Cu^{2+}, indicating appreciable loss of copper from the two most stable complexes, $H_{-1}L_2Cu_2$ and L_2Cu_2. The lifetime of a given complex within a multi-complex solution matrix is therefore not solely dependent on the reaction/stability constants for the isolated complex and the properties of the column itself but also depends on the concentrations and stabilities of all complexes within the sample competing for the metal.

2.4 Conclusions

Although a number of studies have shown that size-exclusion chromatography can be coupled to ICP-MS to interrogate metal-ion speciation in blood plasma [75, 76, 93], my work indicates that the value of the resulting data may be limited by ill-defined dissociation kinetics within the column that perturb the species distribution in the analyte away from that in the parent sample. Extreme care must therefore be taken in experimental design and in data interpretation to eliminate procedural artifacts. While it remains likely that metal ions bound within ultra-stable metallo-protein complexes, such as holo-transferrin, which at physiological conditions is characterized by two high-affinity iron binding sites ($\log_{10}(K_{xyz}/[H^+]^{y-x}) = 22.7$, $\log_{10}(K_{xyz}/[H^+]^{y-x}) = 22.1$) [21], do not dissociate during SEC-mediated fractionation, weaker binding metallo-proteins will almost certainly cloud interpretation of the resulting ICP-MS chromatograms. The presence of albumin in human plasma is particularly important in this context. Albumin has a binding constant for zinc somewhere between $\log_{10}(K_{xyz}/[H^+]^{y-x}) = 7.1$ [58] and $\log_{10}(K_{xyz}/[H^+]^{y-x}) = 7.53$ [23]. Albumin also weakly binds several other metals and, since it constitutes 60% of the total protein in plasma, has the potential to severely alter speciation during LC(SEC)/ICP-MS analysis of plasma samples. For example, albumin is the most abundant copper carrying protein in plasma with a reported Cu^{2+} stepwise binding constant of $\log_{10}(K_{xyz}/[H^+]^{y-x}) = 11.18$ [23]. Albumin may therefore serve as an effective but unwanted scavenger of Cu^{2+} from the many Cu(II)-binding proteins within plasma as SEC fractionation proceeds. This suggests that as a discovery tool, LC/ICP-MS may only be useful in identifying new metallo-proteins that bind Cu^{2+} (or by analogy other metals) with ultra-high affinity (*i.e.*, > *ca.* 10^{22}).

An alternative and likely more rewarding use of LC(SEC)/ICP-MS in plasma metallo-proteomics is its application to quality control of plasma samples. In this case, the intent is not to extend our understanding of ion homeostasis, but rather the more applied and straightforward task of determining the effects of plasma collection, processing and storage procedures on plasma properties.

Chapter 3

Application of LC(SEC)/ICP-MS to Determine the Effects of Blood Processing on Plasma Metal-Ion Content

3.1 Introduction

Plasma is obtained by collecting blood into an anticoagulant and then centrifuging the sample to remove cellular material. The anticoagulant prevents fibrin clot formation in response to tissue damage at the time of blood collection. The properties of the three most widely used anticoagulants are listed in Table 3.1 with the ultimate choice of anticoagulant largely depending on the final destination of the plasma or blood product. A brief description of the mode of action of the two most important anticoagulants, citrate and heparin, is provided below.

Citrate is a tri-protic acid with weak buffering capacity in the pH range of 2.5 to 7.0 (see Figure 2.3). Present in blood at concentrations near 0.1 mM [111], citrate binds calcium with $10^{3.5}$ M affinity [121]. The anticoagulant activity of citrate follows from this affinity for calcium, as clotting factors require calcium to bind to the membrane of activated platelets and thereby activate the clotting cascade [122] (Figure 3.1).

Table 3.1 Anticoagulants used for venous blood collection [121].

	Citrate (2-Hydroxy-1,2,3-propanetricarboxylic acid)	Heparin	EDTA (ethylenediamine tetraacetic acid)
Formulations used	Na-Citrate, Citrate phosphate dextrose adenine	Li-Heparin, Na-Heparin	K_2EDTA, K_3EDTA, Na_2EDTA
Mechanism of action	Binds calcium disabling the clotting cascade	Increases the activity of antithrombin	Binds calcium disabling the clotting cascade
Chemical Formula	$H_3C_6H_5O_7$	ill-defined	$C_{10}H_{14}N_2Na_2O_8 \cdot 2HO$
Molecular Weight	192.12 Da	5,000-30,000 Da	372.24 Da

Heparin is a polymer of glycosaminoglycans composed of alternating glucosamine and sulphated iduronic acid residues, making it negatively charged. Although it offers very little anticoagulant effect on its own, heparin acts on the coagulation factors in both the intrinsic and extrinsic coagulation pathways (see Figure 3.1) [123]. Low concentrations of heparin bind to endogenous antithrombin and the resulting complex inactivates factor Xa preventing the conversion of prothrombin to thrombin. In higher doses, heparin inactivates thrombin, blocks the conversion of fibrinogen to fibrin, and through its binding affinity for antithrombin inactivates factors IX, X, XI, XII. By inhibiting the activation of factor XIII (fibrin stabilizing factor), heparin also prevents the formation of stable fibrin clots.

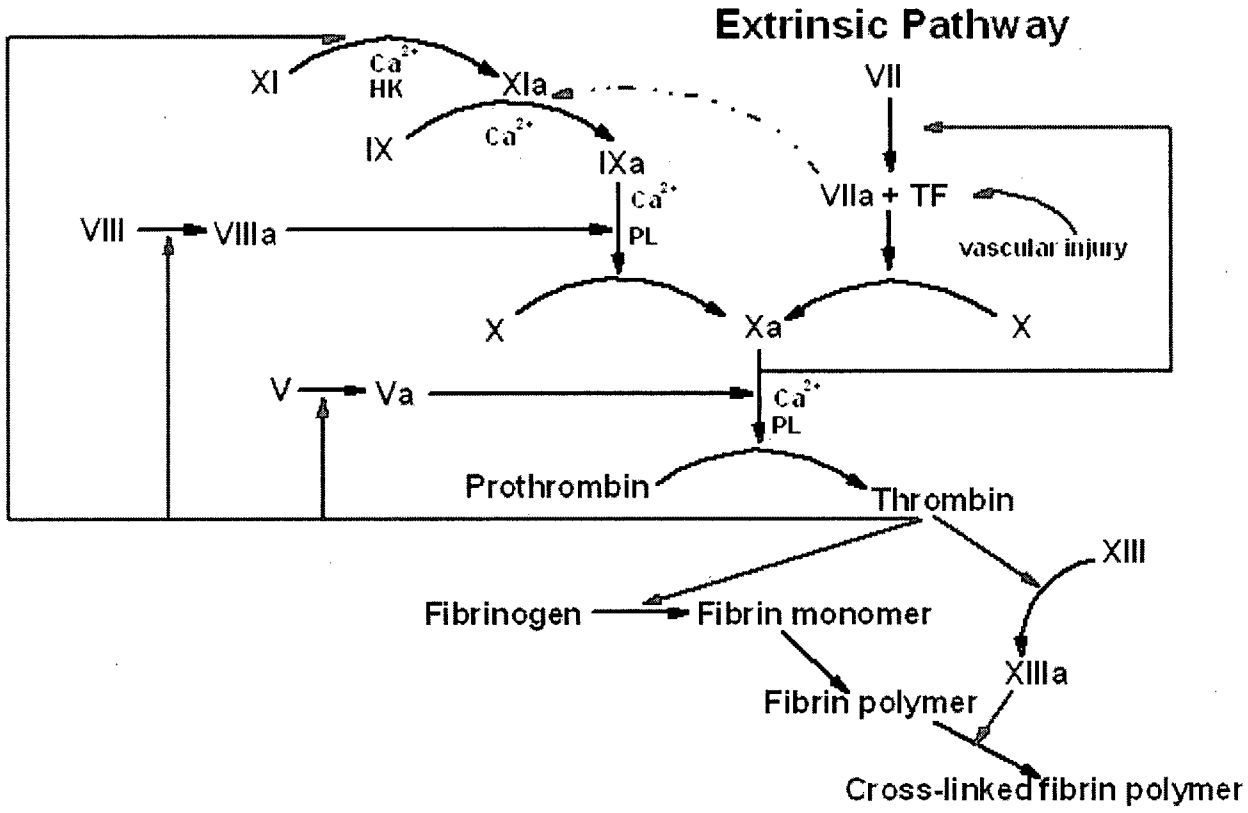

Figure 3.1 Clotting cascade diagram identifying the importance of calcium [124]. The clotting cascade has two pathways. The intrinsic pathway has all of its components within blood while the extrinsic pathway is triggered by extravascular tissue damage. Both pathways result in activation of prothrombin (factor II) and the conversion of fibrinogen to a fibrin monomer, which is then polymerized to form a fibrin clot.

As the primary anticoagulant activity of heparin is due to its binding to the serine protease inhibitor (serpin) antithrombin [123], a brief explanation of the function of antithrombin in the coagulation cascade is warranted. Antithrombin is central to the biochemical process that keeps the blood in a fluid state under physiological conditions. The

vascular endothelium protects blood from highly thrombogenic elements of the surrounding tissues and maintains blood fluidity by inhibiting blood coagulation and platelet aggregation while promoting fibrinolysis. When a blood vessel is injured, the blood exposed to the sub-endothelial matrix forms a haemostatic plug [125]. Synthesized in the liver and in endothelial cells, antithrombin prevents thrombosis by directly binding the serine protease factors Xa, IXa, XIa, XIIa, and thrombin, thereby inhibiting the cleavage of their respective substrates in the coagulation cascade [126-128] (see figure 3.1). Heparin increases the rate of proteinase inhibition by bridging the clotting cascade serine proteases to their inhibitors through the formation of intermediate proteinase-heparin-serpin complexes [123, 129].

Due to their different modes of action, citrate and heparin have different clinical applications. If the collected blood is to be used for transfusion therapy, the anticoagulant of choice is citrate, typically provided in commercial blood bags in the form of sodium citrate or citrate phosphate dextrose adenine (CPDA-1). Unfractionated heparin (UFH) is not generally used as an anticoagulant for stored blood for transfusion because it has a longer half-life in the recipient and can cause platelet activation. Moreover, UFH-stabilized blood cannot be stored for long periods, while blood collected in CPDA-1 may be safely stored at 4°C for up to 3 weeks. Heparin and EDTA (a non-therapeutic anticoagulant) are therefore more widely used as *in vitro* anticoagulants in the collection and preparation of blood or plasma samples intended for laboratory testing. Low molecular weight heparin (LMWH) with a mean molecular weight of about 5,000 is commercially prepared by enzymatic depolymerization of UFH. In medicine, LMWH is used as an intravenous anticoagulant in

diseases that feature thrombosis, as well as for prophylaxis in situations that lead to a high risk of thrombosis [130].

While it is clear that each of the anticoagulants listed in Table 3.1 offers a unique mode of action, the effect of the anticoagulant on the distribution of metal ions within the blood plasma proteome is not well understood. Similarly, the effect of routine plasma handling steps, such as freeze-thaw cycles, may also alter metal-ion speciation. In particular, during pathological and epidemiological studies blood sampling is done over a period of time. It is preferred that all analyses are done in one batch to minimize analytical variation since the same batch of reagents, controls, and calibration material can be used throughout. Plasma samples are, therefore, usually stored frozen at –70°C to –80°C for varying lengths of time, risking alterations in plasma protein concentration and activity through cryo-effects [84, 131]. As the variability of these cryo-effects is not well understood, samples that have been frozen for different lengths of time, as is the current situation in many laboratories, may not be comparable. Several studies have been done measuring the stability of coagulation proteins, as well as various hormones and nutrients, during frozen storage [132-134], but the effect of the freeze-thaw cycle on metal-ion distribution, and thus the state of the plasma metallo-proteome, has not been described.

The aim of this study is to evaluate the impact of anticoagulants and standard freeze-thaw procedures on the distribution of trace elements within plasma using LC(SEC)/ICP-MS. The investigation focuses on plasma samples treated in four different ways. Fresh samples of plasma collected in two different anti-coagulating agents (citrate and heparin) are examined

by SEC/ICP-MS and compared with each other, and with results for the same two samples subjected to a standard freeze-thaw cycle.

3.2 Materials and Methods

Detailed descriptions of many of the materials and methods used in this work are provided in Chapter 2 and will not be repeated here.

3.2.1 Fresh and Thawed Plasma Sample Preparation for SEC

Plasma samples were drawn from one healthy female donor (the author), following an overnight fast, into blood collection tubes (BD Bioscience vacutainers) containing the specified anticoagulant. The first 3 mL of collected blood were discarded. The citrate vacutainers contained 500 µl of 105 mM citrate sodium (9:1) without dextrose (BD Vacutainer #369714, 13 x 75 mm, glass). At a final volume of ~ 4 mL, the blood collected in each tube contained citrate at a concentration *ca.* 13 mM. The heparin tubes contained an inert gel, spray-coated with lithium heparin (BD Vacutainer # 367960, 13 x 75 mm, plastic with polymer separator gel, 45 USP of heparin, MW range 15 – 30 KDa). The heparin tubes have a capacity of 3 mL. Following collection, the blood-filled tubes were gently mixed end-to-end, and then centrifuged in a Beckman GS-6R centrifuge (rotor GH3.8) at 3000 rpm and 25°C for 15 minutes. The clarified plasma was removed from the vacutainers with plastic pipette tips, transferred to a 15 mL acid-treated conical tube and divided into fifteen 1-mL aliquots. Some were frozen in liquid nitrogen and stored in -80°C according to standard procedures. The remaining fresh plasma (~ 3-4 mL) was analyzed by LC(SEC)/ICP-MS within 20 minutes of collection. Prior to sample injection, the sample loop was flushed with

12 mL of elution buffer. Bio-SEC column eluent was collected into 1 mL fractions in acid-washed Eppendorf tubes (see section 2.2.5) for subsequent ICP-MS analysis.

Plasma samples frozen at -80°C were thawed in a 37°C water bath for five minutes. The thawed plasma was then centrifuged (ten minutes, 2000 rpm), and the clarified supernatant fluid was analyzed by SEC/ICP-MS. As before, Bio-SEC column eluent was collected into 1 mL fractions in acid-treated Eppendorf tubes for subsequent ICP-MS analysis.

3.2.2 Protein Concentration Assays

The total protein concentration in each plasma sample was determined using a Micro-BCA Protein Assay Kit from Pierce (product # 23235), which uses bicinchoninic acid (BCA) for the colorimetric detection and quantification. BCA allows total protein detection by producing a reaction product visible at 562 nm upon binding Cu^{+}, which is formed when Cu^{2+} is reduced by proteins in an alkaline environment [135]. Dilutions of a bovine serum albumin standard were used to construct a linear calibration curve between 0.5 and 40 μg/mL total protein. Sample dilution buffer was prepared using phosphate buffer tablets from Sigma (0.01 M phosphate buffer, 0.0027 M potassium chloride and 0.137 M sodium chloride, pH 7.4, at 25 °C; Sigma P-4417). Assuming normal plasma protein levels, (~100 g/L), serial dilutions were made to reduce the total protein concentration to within the linear region of the calibration curve (10 μg/mL).

3.2.3 Sample Preparation and ICP-MS Analysis

ICP-MS analysis was performed on both unfractionated and fractionated plasma using 1% nitric acid as the metals-free control. Unfractionated plasma samples were diluted 100-fold by mass in 1% nitric acid (trace metal grade HNO_3, Fisher cat. # A5095K-212). Bio-SEC column fractions (1 mL) were diluted 10-fold by mass in 1% nitric acid. The 20 mM Tris + 100 mM NaCl running buffer of the column was also diluted in 1% nitric acid to the same final concentration to allow for subtraction of the background content of metals within the solvent.

Operation of the prototype Elan 6000 – DRC was essentially as described in Chapter 2. The metal content of each fraction and control sample was determined by an inductively coupled plasma mass spectrometer (ICP-MS), the prototype Elan 6000 – DRC, donated by Perkin-Elmer Sciex. The ignited plasma was seeded with welder's grade argon gas from Praxair. Following ignition of each new plasma flame, the mass spectrometer was calibrated with multi-element standard solutions (0.1 parts per billion - ppb, 1 ppb, 10 ppb, and 50 ppb) made from a commercially available 100 mg/L (100 ppm) Instrument Calibration Standard (Fisher Scientific, ICP-MS grade, cat. # CL-CAL-2) with 1% HNO_3 (Fisher Scientific, trace metal grade). Contamination of samples was minimized by preparing all solutions in acid-treated plastic-ware. Between analysis of standards and samples, the sample tubing was rinsed with 1% HNO_3 and then soaked in HNO_3 for 3 minutes to ensure minimal metal contamination in the lines and in the nebulizer.

The ICP-MS was operated in quantitative mode to collect two 1-second readings with five sweeps per reading. The signal intensity from each isotope is reported either in counts or converted to ppb. Following completion of data collection, the sample transfer lines were rinsed with Nanopure water for five minutes with the plasma flame ignited to prevent corrosion of the interior of the mass spectrometer.

3.2.4 Data Analysis

Elemental analysis data were collected for both unfractionated and fractionated plasma samples by detecting the most abundant isotopes of titanium (Ti^{48} – 74%), manganese (Mn^{55} – 100%), chromium (Cr^{52} – 84%), cobalt (Co^{59} – 100%), copper (Cu^{63} – 69%), zinc (Zn^{64} – 49%), selenium (Se^{82} – 9%), and strontium (Sr^{88} – 83%). The signal intensity for each fraction was corrected for matrix background effects by subtracting the respective blank. Collected data were converted to parts per billion (ppb, μg/L) of the analyzed isotope in the original fraction by dividing the detected counts by the extinction coefficient regressed from linear signal calibration against standard solutions. The concentration of each metal ion (ppb) was plotted as a function of elution volume (mL).

In certain spectra, background noise was filtered to obtain smooth metal profiles using a three-point fast Fourier transform (FFT) filter which aided in the discrimination of statistically significant metal peaks.

3.2.5 Binding of Metals by Heparin

During blood collection, heparin is released from the inert gel of the lithium-heparin vacutainer into the collected blood. The metal-binding potential of the heparin, particularly to the sulfate groups contained within the heterogeneous polydisperse polymer, was investigated to determine the effects on the metal-ion profiles observed for plasma samples. Blank solutions mimicking the metal and salt composition of plasma were divided into two 4 mL aliquots, with the first aliquot being introduced into a heparin-coated vacutainer while the other was placed into a 15 mL conical tube without heparin as a control. The sample and control were treated in the same manner as all blood samples to reproduce any effects of the plasma handling techniques used. The heparin- equilibrated and heparin-free solutions were transferred to and processed in conical centrifugal filters with a 5 KDa cut off (Millipore Amicon Ultra centrifugal filter cat # UFC8 005 08) to obtain a heparin-free filtrate for ICP-MS analysis. A metal-ion mass balance was then used to determine the amount of each metal retained with the heparin.

For each metal ion analyzed by ICP-MS, the metal content of the filtered heparin-containing sample was equal to that in the corresponding heparin-free control, indicating that the heparin does not bind metals with an affinity that will influence metal-ion distributions in the reported LC(SEC)/ICP-MS for plasma samples.

3.2.6 Protein and Metal-ion Assignments in SEC Chromatograms

The selectivity curve for and the projected protein elution volumes from the Merck Fractogel EMD Bio-SEC column were established by eluting a series of protein standards.

The properties of the standard proteins used are provided in Table 3.2, and the resulting selectivity curve is shown in Figure 3.2.

Table 3.2 Properties of the Fractogel EMD Bio-SEC column and standard analytes used for column calibration.

Column Property	
Dimensions	16 x 600 mm
Total bed volume (V_{total})	120 mL
Stationary phase pore volume (V_p)	59.88 mL
Void volume (V_{void})	35 mL

Analyte	MW (Da)	Ve Run 1(mL)	Ve Run 2(mL)	Ve Avg (mL)
blue dextran	2000000	35.33	35.16	35.27
thyroglobulin	669000	42.04	42.16	42.10
apoferritin	443000	45.49	45.53	45.51
ferritin	440000	45.20	45.15	45.18
catalase	232000	50.31	49.86	50.09
β-amylase	200000	48.85	48.81	48.83
aldolase	158000	52.21	52.07	52.14
alcohol dehydrogenase	150000	51.58	51.45	51.52
conalbumin	77000	55.59	55.62	55.61
BSA	67000	54.67	54.49	54.58
ovalbumin	43000	58.13	58.15	58.14
β-lactoglobulin A	36600	62.69	62.96	62.82
carbonic anhydrase	29000	63.53		63.53
trypsin inhibitor	20100	64.70	64.66	64.68
myoglobin	17600	66.54	66.46	66.50
α-lactoalbumin	14400	67.13	67.15	67.14
insulin	5700	74.13	74.54	74.34
KNO_3	101	95.11	95.18	95.15

The linearity of column selectivity over *ca.* four molecular-weight decades allows plasma protein elution volumes to be predicted with reasonable accuracy. For example, human serum albumin (66 KDa) is predicted to elute at a volume V_e (peak center point) of 57 mL. Therefore, in the absence of significant metal-ion dissociation, we would expect a

portion of the calcium, magnesium, copper, and (ca. 80% of the) zinc [56] present in the sample to elute as peaks centered around this V_e (see Table 1.4 in Chapter 1). Ceruloplasmin (134 KDa) should elute near 53 mL, so that a co-localized copper peak and possibly a small zinc peak should be observed at this V_e. Finally, a large selenium peak should be observed around 60 mL since selenoprotein P (42 KDa) is predicted to elute at this V_e.

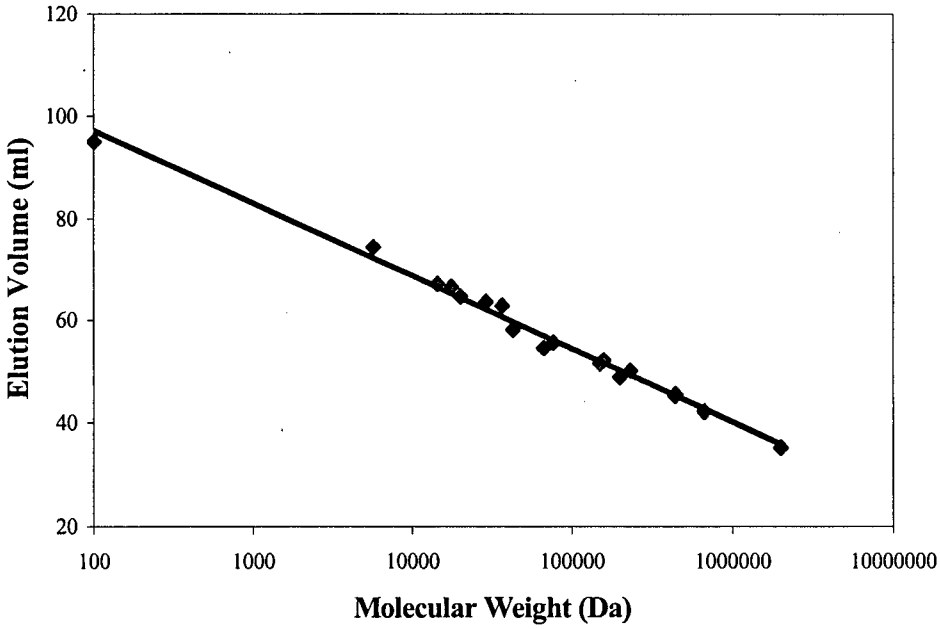

Figure 3.2 Selectivity curve for the Merck Fractogel EMD Bio-SEC column. 100 µL of each protein was loaded at a flow rate of 1 mL/min in a mobile phase of 20 mM Tris + 20 mM NaCl at pH 8.

3.3 Results and Discussion

All raw metal-ion distribution chromatograms are provided in *Appendix A*; the corresponding FFT filtered data are provided in *Appendix B*. The following discussion

focuses on a subset of metals analyzed by SEC/ICP-MS that provide the most reliable and significant insights into ion distributions within the four types of plasma investigated.

3.3.1 SEC Chromatograms for Plasma Samples

A typical SEC chromatogram for fresh plasma collected in citrate as monitored at 210 nm and 280 nm is shown in Figure 3.3.

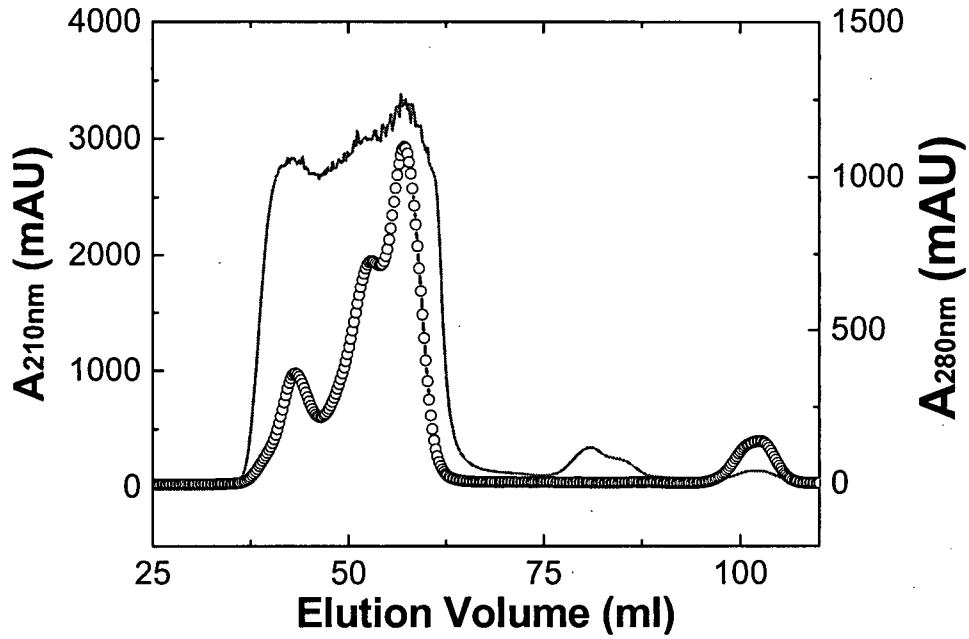

Figure 3.3 Chromatogram for fresh blood plasma collected into 13 mM citrate and processed on the Merck Fractogel EMD Bio-SEC column at 20°C and a mobile-phase flow rate of 1 mL min^{-1}: $A_{280\ nm}$ (circles), $A_{210\ nm}$ (solid line).

Proteins absorb light at 280 nm based on their content of the aromatic amino acids tryptophan, phenylalanine, and tyrosine [136-138]. The plasma proteome fractionates on the Bio-SEC column as three major overlapping peaks eluting between 35 and 65 mL. The large peak eluting at 40 mL contains the immunoglobulins, while the major peak eluting near 60 mL contains albumin and other high-abundance lower-molecular weight plasma proteins

(*e.g.*, transferrin). Free-metal ion control experiments indicate that the peak around 100 mL largely consists of unbound, spectroscopically active metals, most of which have dissociated from metallo-proteins within plasma during SEC processing. The peak at 80 mL, visible at 210 nm but not at 280 nm, contains the anticoagulant citrate, based on chromatograms for free citrate (see Chapter 2) where elution is observed as a peak centered around 80 mL. In addition, the total peak area corresponds closely with that predicted from a mass balance on total citrate added, suggesting that the peak primarily represents citrate, either in its free states or complexed with various metal ions. The elution peaks shown in Figure 3.3 can therefore be used to interpret the fates of various metals during SEC/ICP-MS processing of either fresh or freeze-thawed plasma that has been collected into citrate.

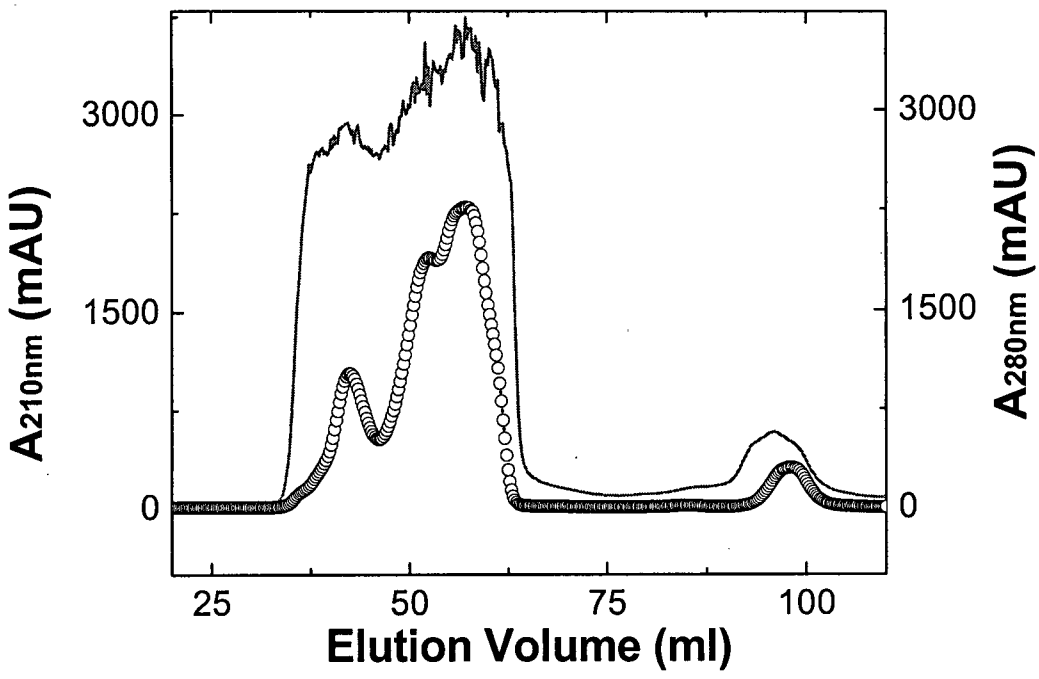

Figure 3.4 Chromatogram for fresh blood plasma collected into lithium-heparin BD Vacutainer tubes and processed on the Merck Fractogel EMD Bio-SEC column at 20°C and a mobile-phase flow rate of 1 mL min^{-1}: $A_{280\ nm}$ (circles), $A_{210\ nm}$ (solid line).

Figure 3.4 shows a typical SEC chromatogram for blood plasma collected in heparin-coated tubes. Peak assignments are as described above, with the exception that no anti-coagulant (citrate/heparin) associated peak is observed.

3.3.2 Protein Concentration Comparison

Natural variations in the protein content and overall composition of plasma are expected in samples collected at different times or from different subjects due to variations in dietary intake, lifestyle, etc. Thus, a comprehensive analysis of the utility of SEC/ICP-MS in quantitative analysis of plasma samples will require a careful study of natural variations in metal content and distribution. However, this study focuses on proof of concept: in particular, the basic question of whether the LC(SEC)/ICP-MS system constructed in this work can identify significant differences in metal-ion distribution due to plasma processing strategies.

The blood collected for the analysis of heparin as an anti-coagulating agent was drawn on a separate date from that of the citrate collections and due to unforeseen circumstances, the citrate samples were also collected on different dates. Table 3.3 compares the total protein content of each plasma sample prior to loading onto the SEC column. Natural variations in total protein (ca. ± 6 g/dL) are noted when comparing the fresh plasma samples stabilized by citrate and heparin, respectively. Freeze-thawing of the samples significantly reduced the total protein content, presumably due to cryo-precipitation of plasma proteins [132-134]. However, another possible explanation for this protein variation

may rest with the anticoagulants themselves. It would be of value to investigate in the future whether the anticoagulants themselves interfere with the BCA assay.

Table 3.3 Total protein content of anticoagulated plasma samples studied

	Citrate	Heparin
Fresh plasma	14.7 g/dL	8.3 g/dL
Freeze-thawed plasma	8.7 g/dL	4.4 g/dL

Comparing the metal ion profiles of fresh and frozen plasma samples stabilized in a particular anti-coagulant is therefore complicated by the loss of metal to the un-retained fraction of total protein during the freeze-thaw cycle. For lower abundance metals in plasma, the total concentration following the freeze-thaw cycle will fall below the level of detection by the ICP-MS. Table 3.4 compares between each plasma sample the total content (g/dL) of each detected metal ion as determined by ICP-MS. Some of the less abundant metals, Mn and Co, become undetectable by ICP-MS following the freeze-thaw process.

Table 3.4 Total metal ion content of each plasma sample as determined by ICP-MS

Metal	Fresh Citrate (g/dL)	Thawed Citrate (g/dL)	Fresh Heparin (g/dL)	Thawed Heparin (g/dL)
Ti	1.16E-06 ± 1.35E-08	7.66E-07 ± 5.68297E-09	1.34E-06 ± 8.76422E-09	1.21E-06 ± 2.69947E-08
Cr	3.44E-06 ± 3.48E-09	1.25E-06 ± 5.16331E-09	3.82E-06 ± 2.62297E-09	3.96E-06 ± 6.25013E-09
Mn	1.70E-07 ± 1.47E-10	Undetectable	1.96E-07 ± 2.94433E-10	2.16E-07 ± 4.25105E-10
Co	4.20E-08 ± 3.67762E-11	Undetectable	Undetectable	Undetectable
Cu	3.12E-05 ± 9.74497E-09	6.38E-06 ± 1.9208E-08	2.56E-05 ± 1.53244E-08	3.99E-05 ± 1.34298E-08
Zn	3.08E-05 ± 5.20361E-09	3.98E-06 ± 1.11076E-08	5.34E-05 ± 4.45745E-08	3.99E-05 ± 1.24358E-08
Se	9.24E-07 ± 3.70808E-09	4.22E-07 ± 1.21705E-09	1.54E-06 ± 1.27718E-08	1.18E-06 ± 2.82887E-09
Sr	2.42E-07 ± 3.69943E-10	1.50E-07 ± 6.18988E-11	1.34E-07 ± 1.94992E-10	1.00E-07 ± 4.02875E-10

3.3.3 The Effect of Citrate on Metal-Ion Distribution in Fresh Plasma

In addition to its affinity for the cupric ion, citrate is known to bind a large number of physiological bivalent and trivalent metal ions, including Fe^{3+}, Al^{3+}, Zn^{2+}, Ni^{2+}, Co^{2+}, Mn^{2+}, Cd^{2+}, Mg^{2+}, and Ba^{2+}. Binding of Fe^{3+} and Al^{3+} is relatively strong, while citrate binds the remaining ions with an affinity similar to or slightly less than that for Cu^{2+} [93]. Thus, at a solution concentration of 13 mM following blood collection, citrate has the potential to successfully compete with plasma metallo-proteins and thereby alter metal-ion speciation in collected blood and plasma prepared from it.

Chromatograms measured by SEC/ICP-MS defining the distribution of Mn^{2+}, Co^{2+}, and Sr^{2+} in fresh plasma prepared from blood drawn into citrate are shown in Figure 3.5. All three metals are shown to strongly associate with the citrate-rich peak centered near V_e = 80 mL. Variations in V_e for each metal likely reflect differences in the stoichiometries of the complexes each metal preferentially forms with citrate. In the case of Co^{2+}, essentially all of the metal present in the plasma sample is complexed with citrate. It is important to recognize that manganese, cobalt, and strontium are present in extremely low amounts in plasma due to their limited involvement in biological pathways and their potential toxicity at increased levels. In contrast, strong metal-ion stripping behavior is not observed for the higher abundance cupric ion (Figure 3.6), indicating that citrate alters metal-ion speciation in plasma in an ion-specific manner, effectively stripping select soluble and essential metal-ions from their metallo-protein hosts in blood. As the binding strength of Mn^{2+}, Co^{2+} and Sr^{2+} to citrate is similar to that for the cupric ion, the ability of citrate to effectively extract these metals suggests that they are not strongly associated to any plasma protein [104].

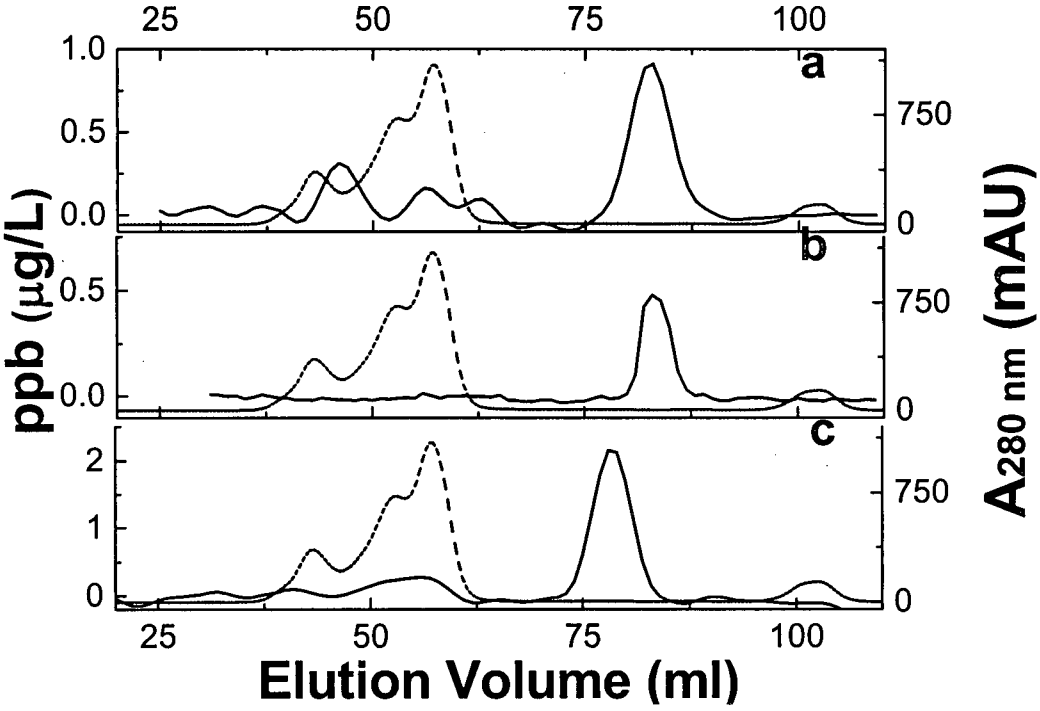

Figure 3.5 The effect of citrate on the (smoothed) distribution of (a) Mn^{2+}, (b) Co^{2+}, and (c) Sr^{2+} in fresh plasma: plasma protein absorbance at 280 nm (dashed line), metal-ion concentrations (ppb) as measured by ICP-MS (solid line).

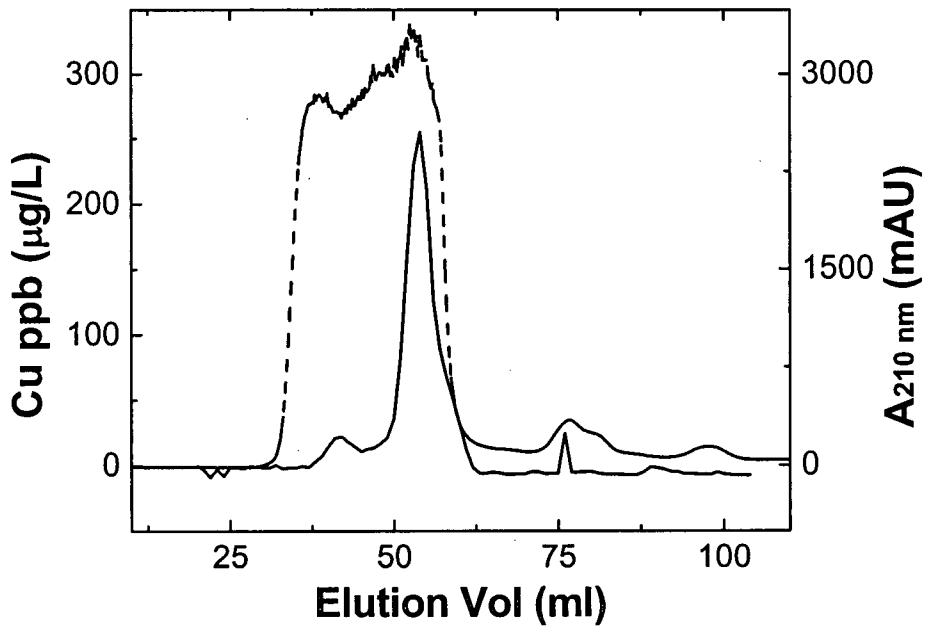

Figure 3.6 The effect of citrate on the distribution of Cu^{2+} in fresh plasma: plasma protein absorbance at 210 nm (dashed line), copper concentrations (ppb) as measured by ICP-MS (solid line).

3.3.4 The Effect of Heparin on Metal-Ion Distribution in Fresh Plasma

Although the lower total protein content of the blood sample collected into heparin resulted in weak ICP-MS signals for several metals, the data suggest that trace elements largely remain associated with the metallo-protein containing fractions of the SEC/ICP-MS chromatogram. This is clearly the case for Cu^{2+} (Figure 3.7), and appears to be true for Sr^{2+}, and to a lesser extent Mn^{2+} (Figure 3.8). However, replicate data sets on blood samples containing a higher total protein concentration are required to verify this. Note that Co^{2+} is present at undetectable levels in the sample drawn into heparin.

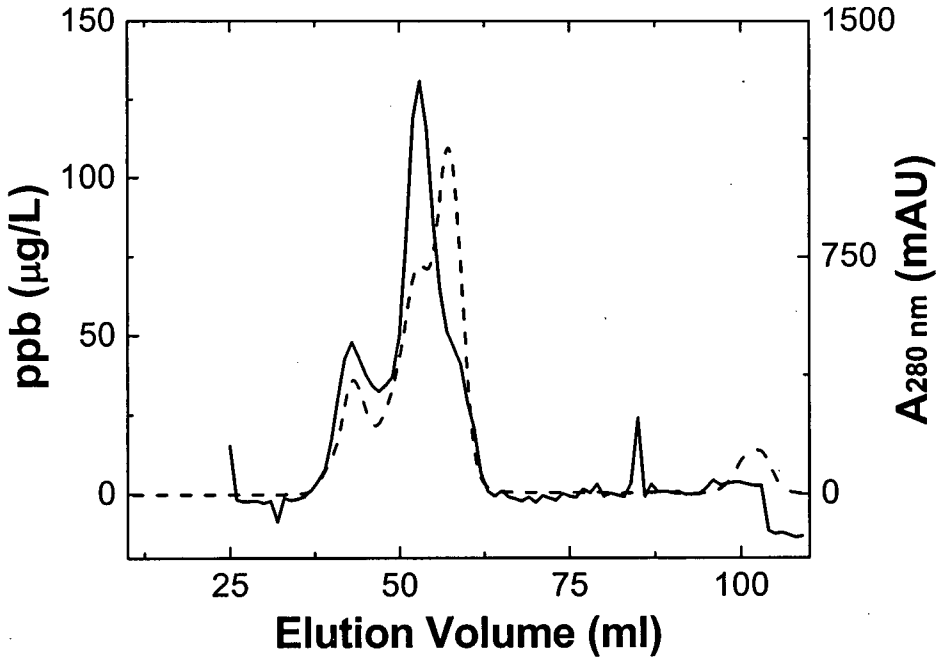

Figure 3.7 The effect of heparin on the distribution of Cu^{2+} in fresh plasma: plasma protein absorbance at 280 nm (dashed line), copper concentrations (ppb) as measured by ICP-MS (solid line).

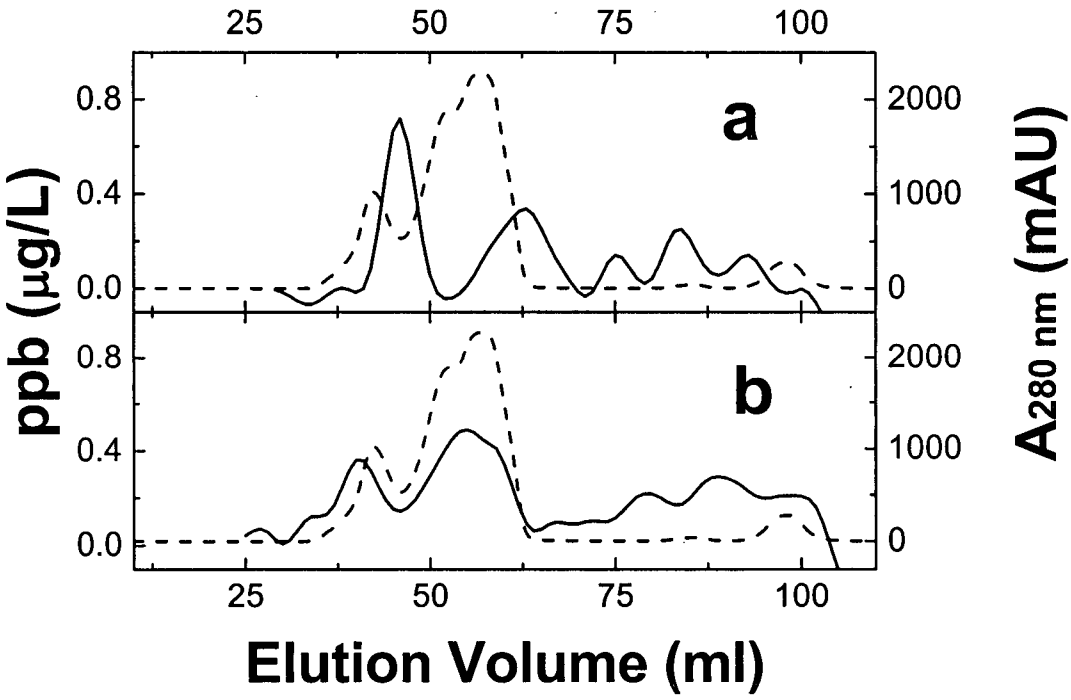

Figure 3.8 The effect of heparin on the (smoothed) distribution of (a) Mn^{2+} and (b) Sr^{2+} in fresh plasma: plasma protein absorbance at 280 nm (dashed line), metal-ion concentrations (ppb) as measured by ICP-MS (solid line).

Despite their preliminary nature, my results may help to explain recent results from a number of groups who have studied the effect of anticoagulants on the stability of biomarkers in clinical plasma and serum samples [139-143]. For example, Chan et al. [141] observed that the choice of anticoagulant has a dramatic effect on the stability of the receptor activator for nuclear factor-κB ligand (RANKL) and osteoprotegerin (OPG) in plasma and serum samples.

RANKL and OPG expression levels are perturbed in a number of osteoclastogenesis and bone-remodeling disorders; therefore, the quantification of each protein in either serum or plasma samples collected from patients has been used to diagnose bone-related diseases and to monitor treatment efficacy [141, 144]. However, measurement of the RANKL/OPG

ratio to detect Paget disease and to determine the effect of bisphosphonate treatment for that bone-remodeling disorder has shown inconsistent results [145]. Chan et al. [2003] found that these inconsistencies were largely due to inaccuracies resulting from the sampling process; in particular, the variability of results depended strongly on the choice of anticoagulant. Significantly higher and more reproducible concentrations of RANKL and OPG were detected when blood samples were collected into EDTA (an anticoagulant whose mode of action is similar to that of citrate) compared with lithium heparin. Chan et al. [2003] suggest that the ELISAs used in the RANKL/OPG-based bone disease assay may be selective for uncomplexed forms of RANKL and OPG. Alternatively, my results may help further explain these findings by demonstrating the connection between plasma sample stability with respect to a particular protein assay (*e.g.*, RANKL or OPG) and the effectiveness of the anticoagulant at partitioning metals away from their metallo-protein hosts in blood.

Metallo-proteases, also known as metallo-proteinases, use a bound zinc atom in their catalytic center to degrade a wide variety of proteins in the extracellular matrix [146, 147]. Present in blood in low dosages, metallo-proteases, including collagenases, stromelysins and gelatinases [148], have the potential to degrade the plasma proteome during sample processing and storage. Both RANKL and OPG are known to be susceptible to metallo-proteinase-catalyzed cleavage [149, 150]. Thus, the use of an anticoagulant that scavenges free Zn^{2+} ions has the potential to alter metallo-proteinase activity and thereby increase RANKL and OPG stability. The anticoagulant-induced partitioning of zinc and other metals away from their host metallo-proteins could improve the sensitivity and reliability of the RANKL/OPG concentration ratio assay. My results show that chelate-type anticoagulants

such as citrate (and EDTA) are able to bind a wide range of the metals in blood, including a significant fraction (but not all) of the zinc in plasma (Figure 3.9). In contrast, Zn^{2+} remains associated with the plasma proteome during SEC/ICP-MS analysis of fresh plasma drawn into lithium heparin (Figure 3.10).

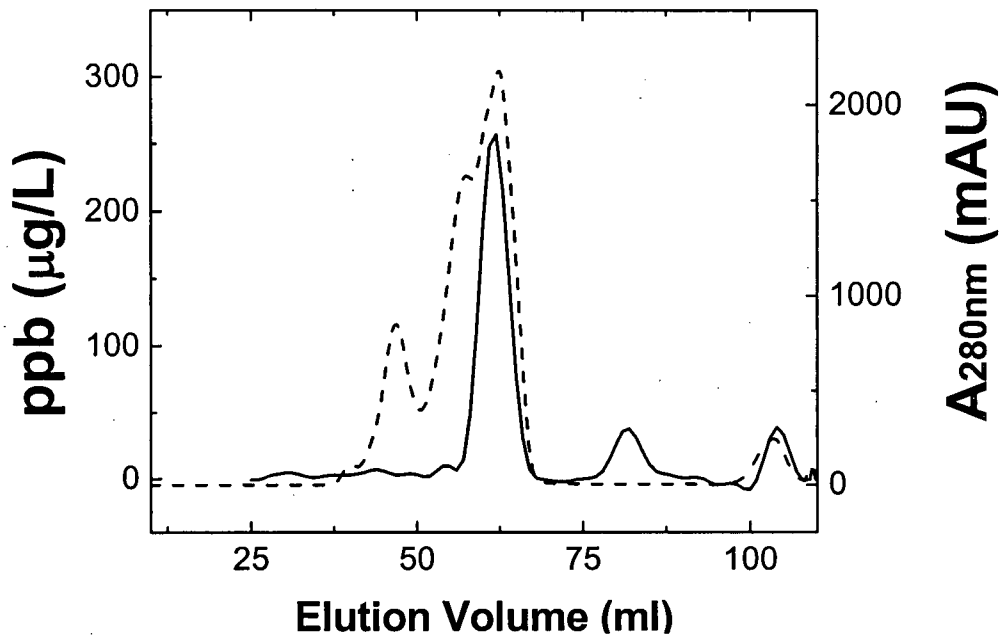

Figure 3.9 The effect of citrate on the (smoothed) distribution of Zn^{2+} in fresh plasma: plasma protein absorbance at 280 nm (dashed line), zinc concentrations (ppb) as measured by ICP-MS (solid line).

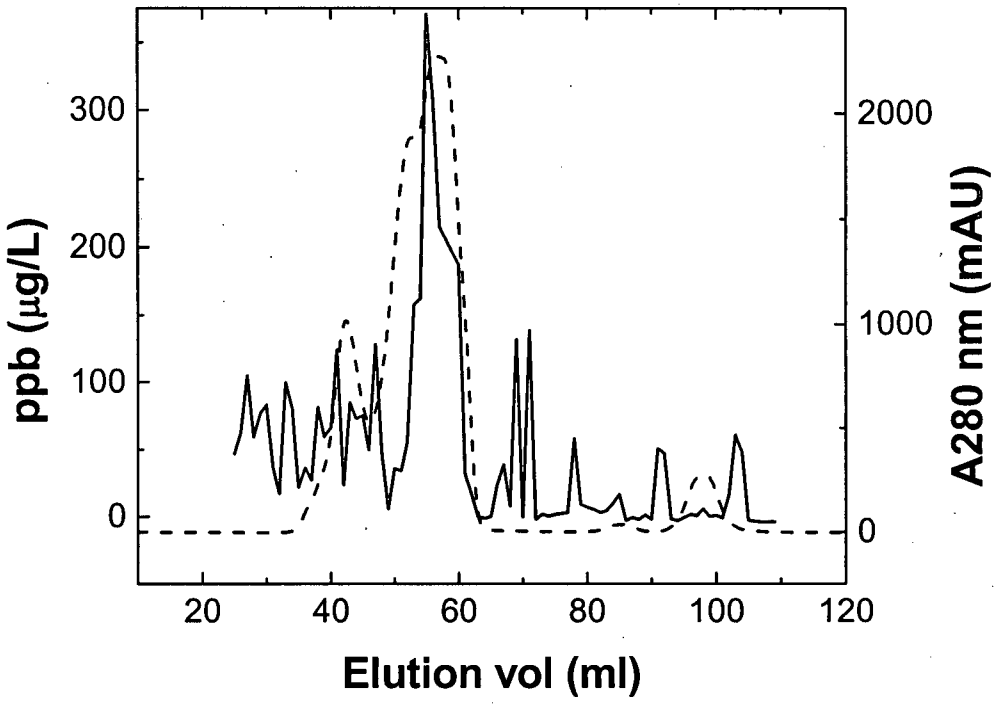

Figure 3.10 The effect of heparin on the distribution of Zn^{2+} in fresh plasma: plasma protein absorbance at 280 nm (dashed line), zinc concentrations (ppb) as measured by ICP-MS (solid line).

3.3.5 The Effects of Freezing and Thawing on the Distribution of Metal Ions in Plasma

Changes in the concentrations of proteins, hormones and vitamins in plasma and sera resulting from subjecting the fluid to a freeze-thaw cycle are well documented [83, 151]. In contrast, little is known about how the freeze-thaw process affects metal-ion speciation in plasma and sera samples.

Figure 3.11 shows the SEC chromatogram at 210 nm for fresh plasma collected into citrate, and the corresponding ICP-MS chromatograms for copper in the same fresh plasma sample and in that sample after a freeze-thaw cycle.

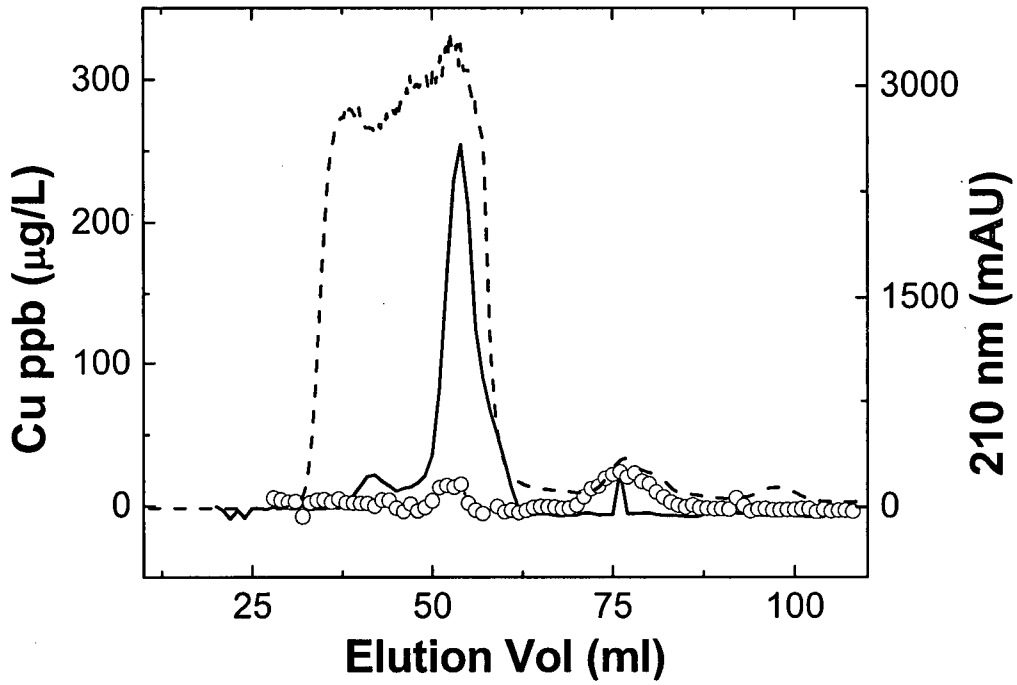

Figure 3.11 The effects of freezing on copper speciation in blood plasma collected in citrate: copper concentrations (ppb) for fresh plasma in citrate (solid line), copper concentrations (ppb) for thawed plasma in citrate (circles), plasma absorbance at 210 nm (dashed line).

In the citrate-stabilized fresh plasma sample, essentially all of the copper remains in chromatographic fractions containing plasma proteins (*i.e.*, at V_e between 35 and 60 mL). Following the freeze-thaw cycle a new and substantial Cu^{2+} peak is observed near V_e = 80 mL, the elution volume for citrate in the Bio-SEC column. A concomitant loss of Cu^{2+} from protein-containing fractions of the chromatogram is also observed, indicating that the freeze-thaw cycle has a dramatic effect on the distribution of the Cu^{2+} ion. Perturbations in the distributions of other metal ions within the elution chromatogram were also observed as a result of freeze-thawing of citrate-stabilized plasma (see Appendix B). For example, in the absence of freezing, most of the cobalt present in the sample associates with citrate (Figure 3.5). Following the freeze-thaw process, cobalt and other low abundance ions are displaced

to facilitate citrate complexation with Cu^{2+} and Zn^{2+}, which are both present in plasma at relatively high total concentration.

Unlike the citrate-stabilized samples, plasma collected in heparin-coated tubes undergoes no significant change in metal-ion distribution following freezing and thawing (Figure 3.12 and *Appendices A and B*). Thus, heparin would appear to be the more useful anticoagulant when the objective is to interrogate the metallo-proteome and metal-ion speciation in plasma or sera samples.

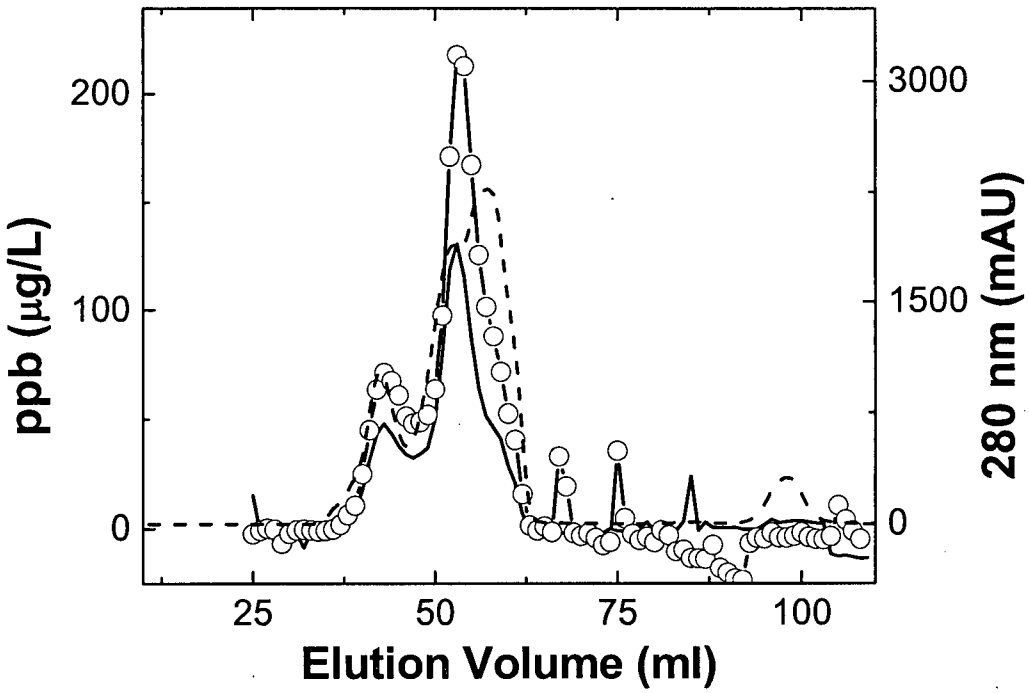

Figure 3.12 The effects of freezing on copper speciation in blood plasma collected in lithium heparin: copper concentrations (ppb) for fresh plasma in lithium heparin (solid line), copper concentrations (ppb) for thawed plasma in lithium heparin (circles), plasma absorbance at 280 nm (dashed line).

3.4 Conclusions

The establishment of methods to quantify metal-ion speciation in blood and blood plasma samples requires overcoming a number of technical challenges, including achieving an efficient nondestructive fractionation method and the specific and sensitive analytical detection of each elemental species of interest. Due to its extraordinary sensitivity and ability to discriminate between metals, ICP-MS has long been used for the detection of metals in chromatography, usually either ion exchange or size exclusion, of biological fluids [67, 78, 80, 85]. In chapter 2 of this thesis, I determined that despite its generally nondestructive nature, size-exclusion chromatography can distort metal-ion speciation away from that in the parent plasma sample, bringing into question the range of applicability of this fractionation method to the study of metals in blood.

Here, I provide preliminary data characterizing the influence of blood collection and processing of plasma samples intended for clinical studies, including quantification of biomarkers or speciation profiles of essential and non-essential metals. SEC/ICP-MS successfully detected significant changes in the distribution of a number of metals in plasma due to the influence of the chosen anticoagulant and subjection of the sample to a freeze-thaw cycle. The results therefore support at least the limited use of the technology in plasma diagnostics. My results also suggest that plasma metallo-proteomics studies are best conducted with fresh plasma samples collected into lithium heparin vacutainer tubes. However, more studies are necessary to confirm this observation and to establish the mechanism of heparin's protective effect and citrate's destabilizing effect during sample freezing.

Chapter 4

Concluding Remarks

The field of "metallomics" is concerned with the identities and concentrations of metal species in biological systems. Species of interest in metallomics include aquated trace elements and their complexes with endogenous and induced biomolecules, including organic acids, sugars, proteins, and oligonucleotides. Deciphering the metallome therefore has the potential to provide insights into the distribution of an element in a cell, fluid or tissue, the coordination environments of that element, and the concentrations of each metal-containing species present. As metal ions are utilized in a number of fundamental biological processes, and the absence or excessive presence of metals is known to be connected to a variety of disease states, elucidating the mechanisms by which metals are stored, transported, sensed and incorporated within the human biosystem should provide important insights into metal homeostasis and metal-related diseases.

The establishment of metallomics as a useful approach to studying biological function requires the development of reliable technology for fractionating and probing a metallome and its associate proteome in a manner that allows identified metals to be connected to their various complexing agents. Although very few metallomics studies have been reported, the most promising approach to studying the blood plasma metallome involves coupling size-exclusion chromatography to an ICP-MS detector [78, 80, 88, 152]. However, the ability of this approach to preserve metal-ion distributions during chromatographic fractionation and ICP-MS detection has not been investigated, bringing into question the potential for

processing artifacts. I have shown that SEC fractionation of aqueous solutions containing simple and complex metal-ion equilibria can distort that equilibria such that metal-ion speciation patterns detected by ICP-MS do not reflect speciation in the parent sample. Some general guidelines for assessing the extent of perturbation away from the desired state are provided by the chromatographic behavior of simple 1:1 chelate:metal complexes. I further show that these guidelines must ultimately be amended to include the fact that the lifetime of a given metal-ion complex within a multi-complex solution matrix is not solely dependent on the properties of the isolated complex, but also depends on the concentrations and stabilities of all complexes within the sample competing for the metal. Thus, as a metallo-protein discovery tool, LC(SEC)/ICP-MS will be most reliable at identifying metallo-proteins that bind metal(s) with high affinity.

SEC/ICP-MS may also prove to be a useful platform for interrogating the quality of plasma and sera samples, including the influence of sample processing and storage conditions. In this work, I report preliminary data that identifies significant differences in the metallomes of plasma samples collected into two different anticoagulants and either analyzed in their freshly prepared state or following freezing and subsequent thawing of each sample. In addition to supporting the development of SEC/ICP-MS for quality control of plasma samples, the work suggests that human plasma metallomic studies are best performed on fresh plasma drawn into lithium heparin vacutainer tubes.

Appendix A

Metal ion Profiles in Blood Plasma Samples Achieved with SEC/ICP-MS

Raw metal ion profiles of blood plasma samples treated in four different ways:

A.1 Fresh plasma collected in citrate – final concentration 13 mM

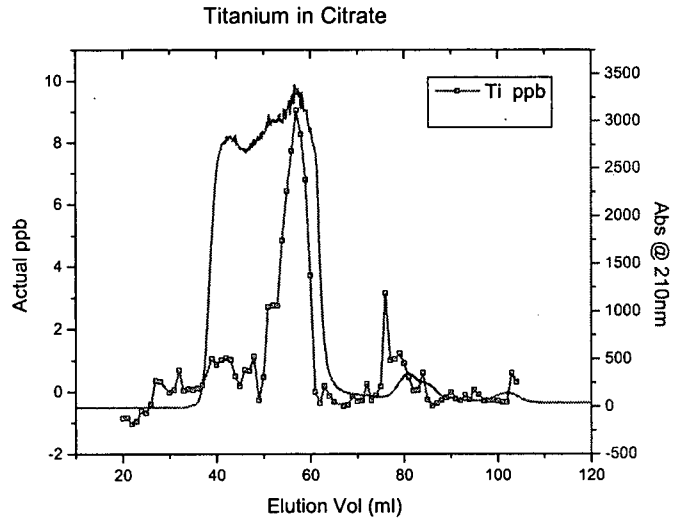

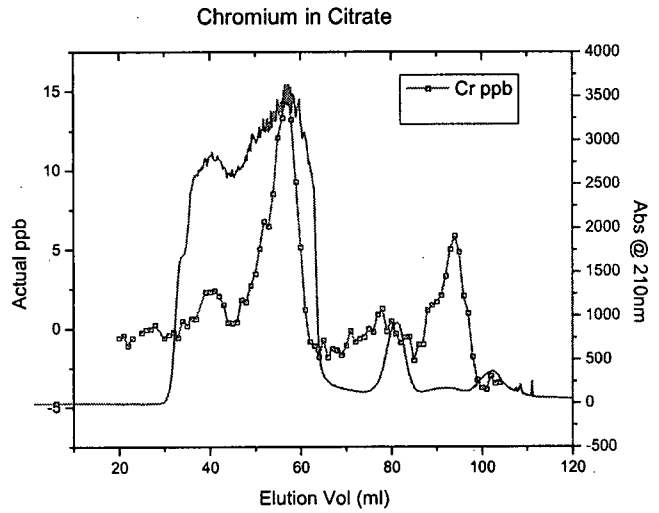

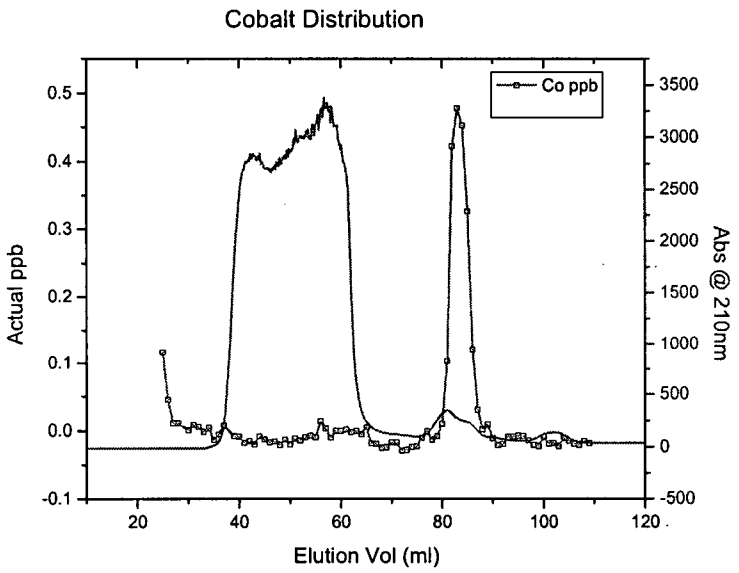
Cobalt Distribution
Co ppb
Actual ppb
Abs @ 210nm
Elution Vol (ml)
0.5
0.4
0.3
0.2
0.1
0.0
-0.1
3500
3000
2500
2000
1500
1000
500
0
-500
20
40
60
80
100
120

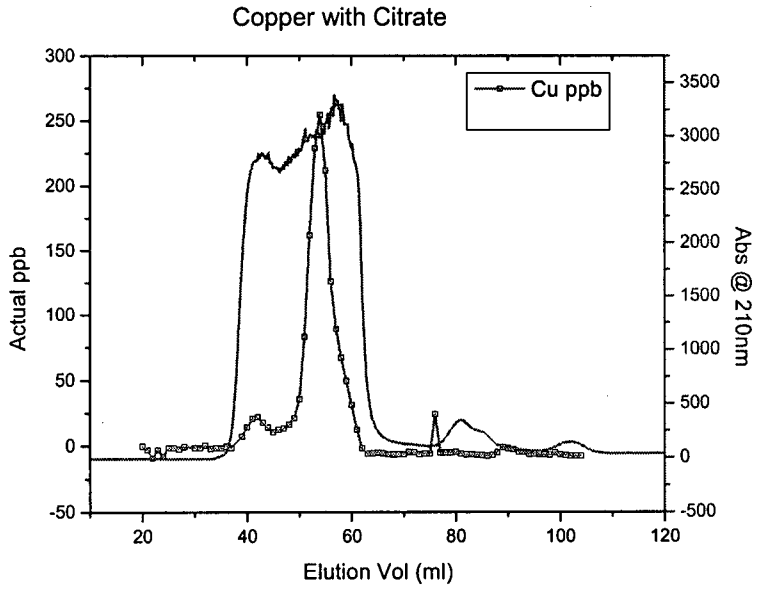
Copper with Citrate
Cu ppb
Actual ppb
Abs @ 210nm
Elution Vol (ml)
300
250
200
150
100
50
0
-50
3500
3000
2500
2000
1500
1000
500
0
-500
20
40
60
80
100
120

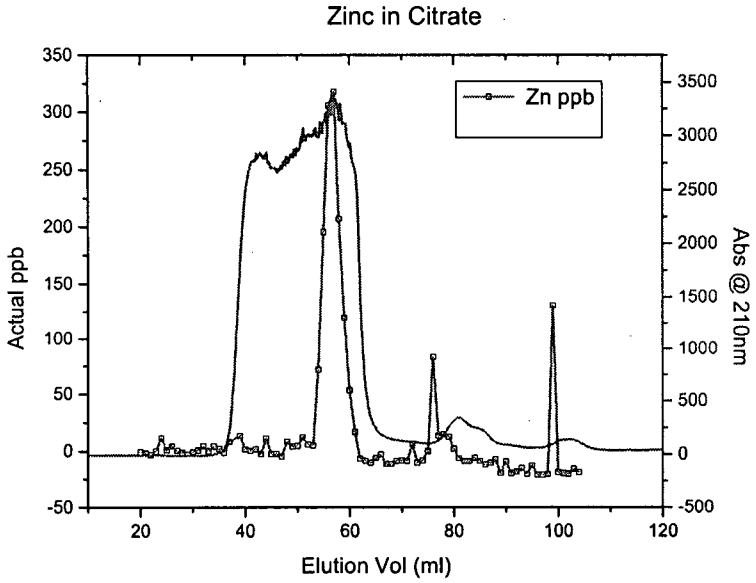
Zinc in Citrate
Zn ppb
Actual ppb
Abs @ 210nm
Elution Vol (ml)
350
300
250
200
150
100
50
0
-50
3500
3000
2500
2000
1500
1000
500
0
-500
20
40
60
80
100
120

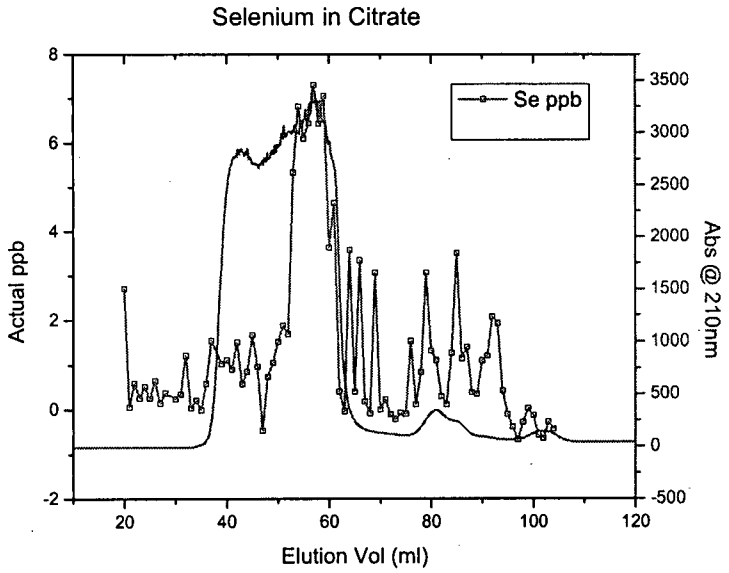
Selenium in Citrate
Se ppb
Actual ppb
Abs @ 210nm
Elution Vol (ml)
8
6
4
2
0
-2
3500
3000
2500
2000
1500
1000
500
0
-500
20
40
60
80
100
120

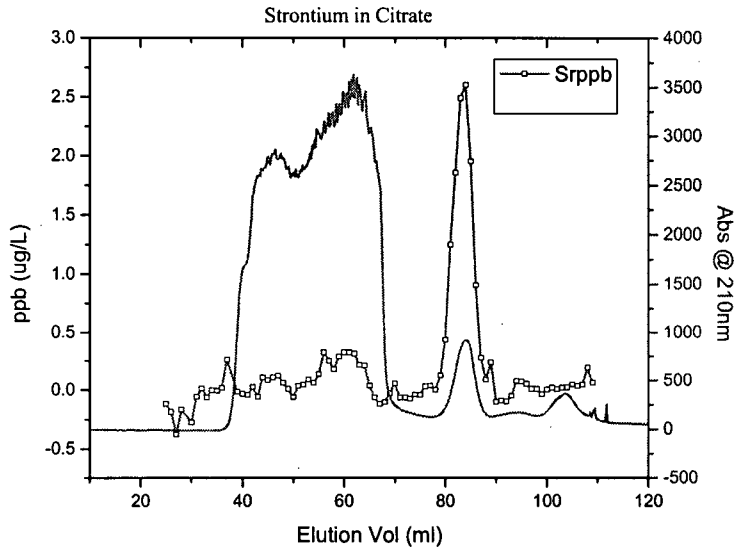

A.2 Freeze-thawed plasma collected in citrate – final concentration 13 mM

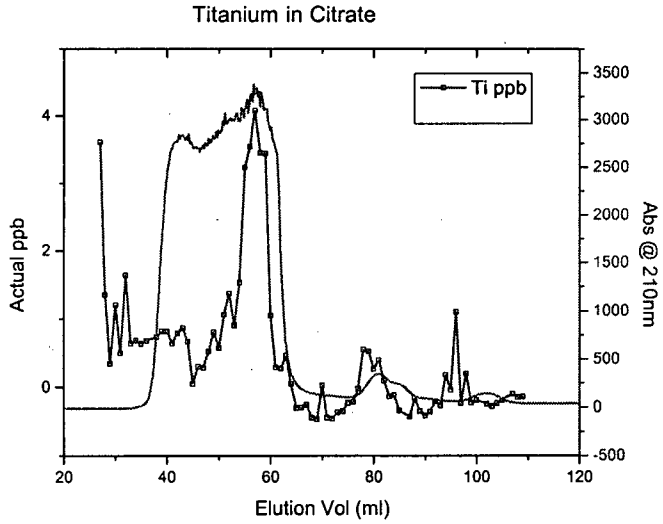

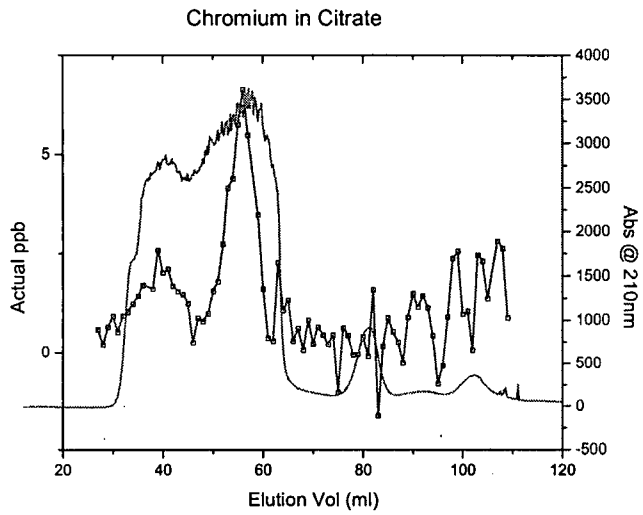
Chromium in Citrate
Actual ppb
Abs @ 210nm
Elution Vol (ml)
5
0
4000
3500
3000
2500
2000
1500
1000
500
0
-500
20
40
60
80
100
120

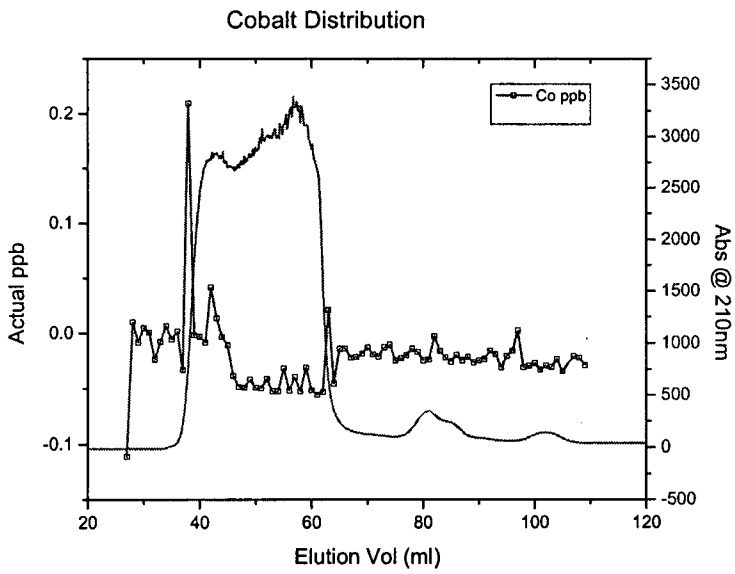
Cobalt Distribution
Co ppb
Actual ppb
Abs @ 210nm
Elution Vol (ml)
0.2
0.1
0.0
-0.1
3500
3000
2500
2000
1500
1000
500
0
-500
20
40
60
80
100
120

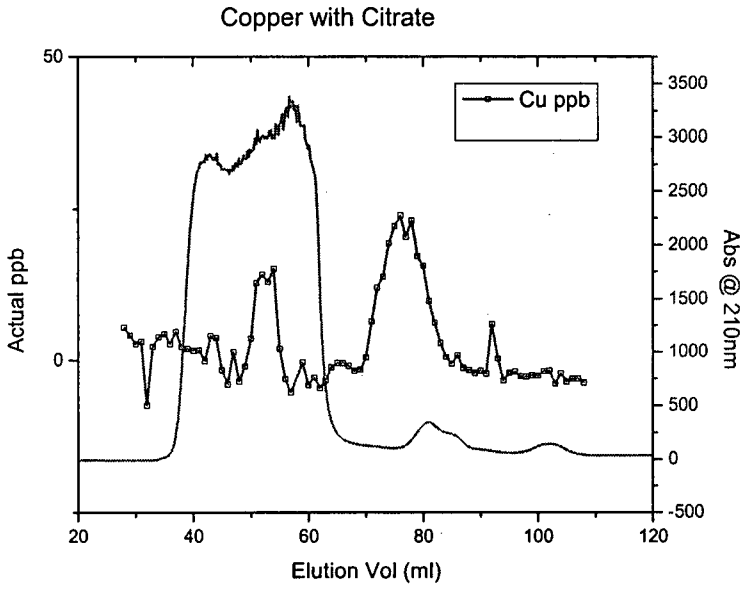
Copper with Citrate
Cu ppb
Actual ppb
Abs @ 210nm
Elution Vol (ml)
50
0
3500
3000
2500
2000
1500
1000
500
0
-500
20
40
60
80
100
120

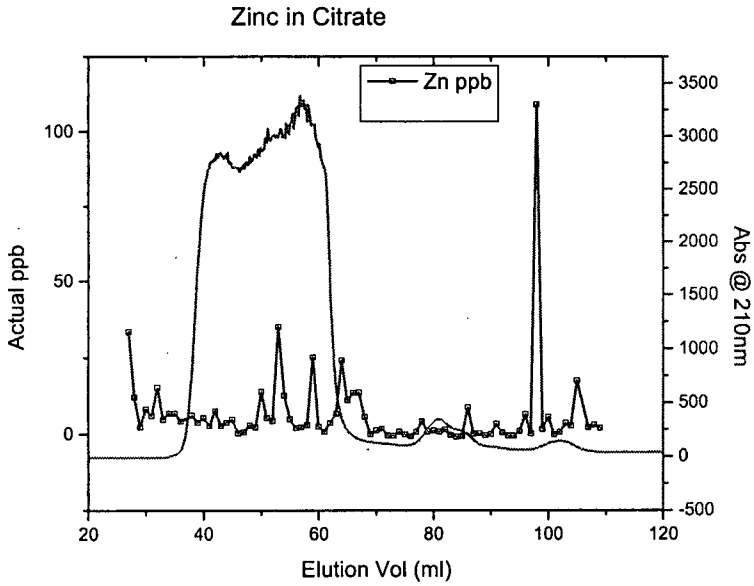
Zinc in Citrate
Zn ppb
Actual ppb
Abs @ 210nm
Elution Vol (ml)
100
50
0
3500
3000
2500
2000
1500
1000
500
0
-500
20
40
60
80
100
120

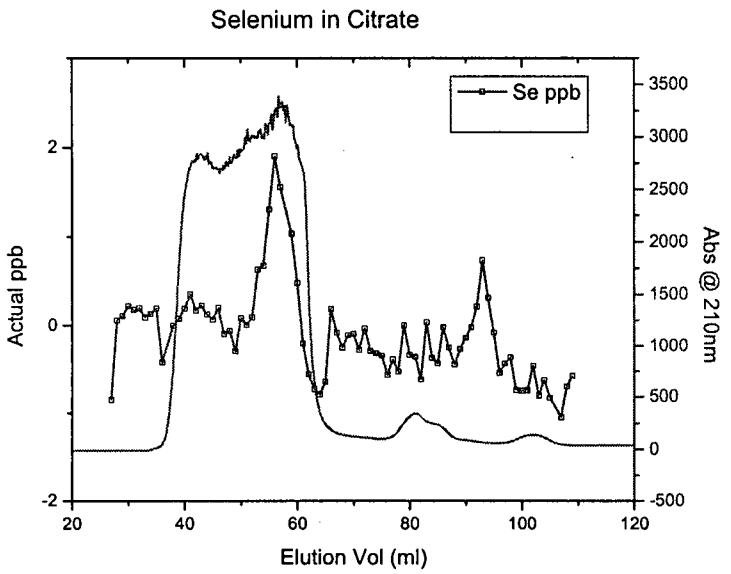
Selenium in Citrate
Se ppb
Actual ppb
Abs @ 210nm
Elution Vol (ml)
2
0
-2
3500
3000
2500
2000
1500
1000
500
0
-500
20
40
60
80
100
120

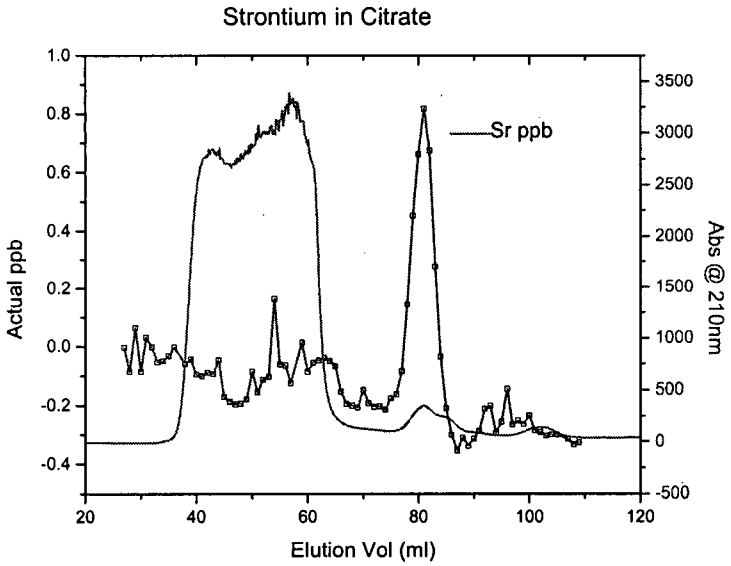
Strontium in Citrate
Sr ppb
Actual ppb
Abs @ 210nm
Elution Vol (ml)
1.0
0.8
0.6
0.4
0.2
0.0
-0.2
-0.4
3500
3000
2500
2000
1500
1000
500
0
-500
20
40
60
80
100
120

A.3 Fresh plasma collected in lithium heparin

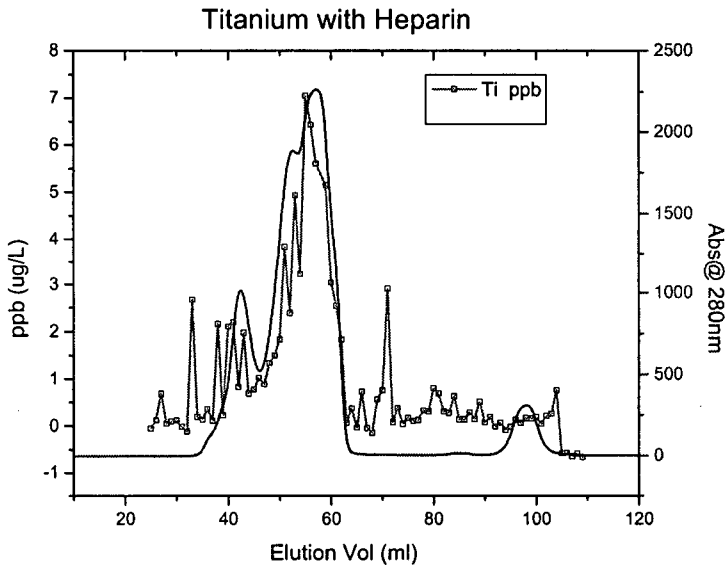

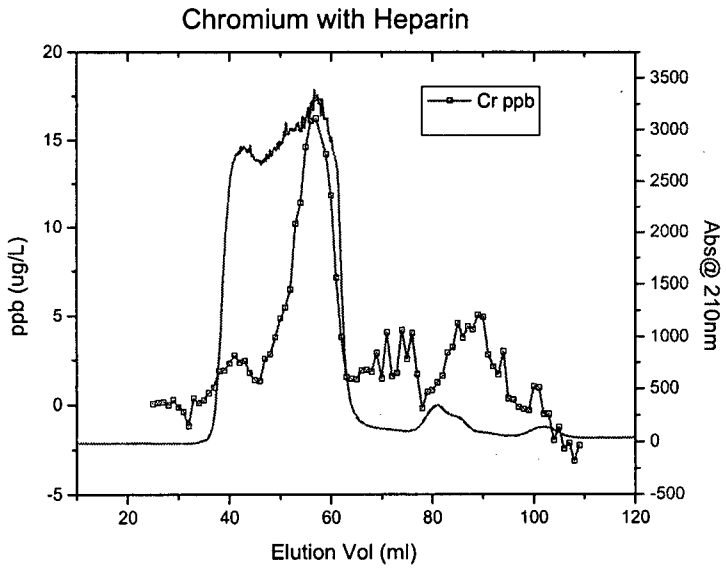

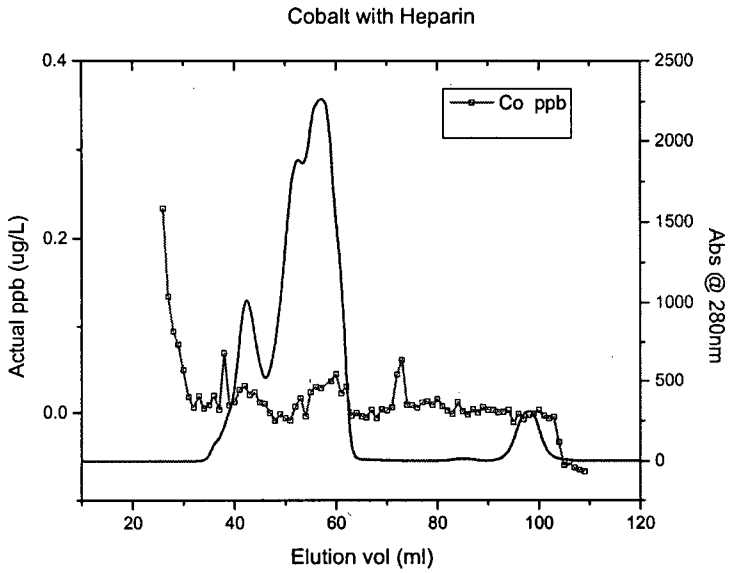
Cobalt with Heparin
Co ppb
Actual ppb (ug/L)
Abs @ 280nm
Elution vol (ml)
0.4
0.2
0.0
2500
2000
1500
1000
500
0
20
40
60
80
100
120

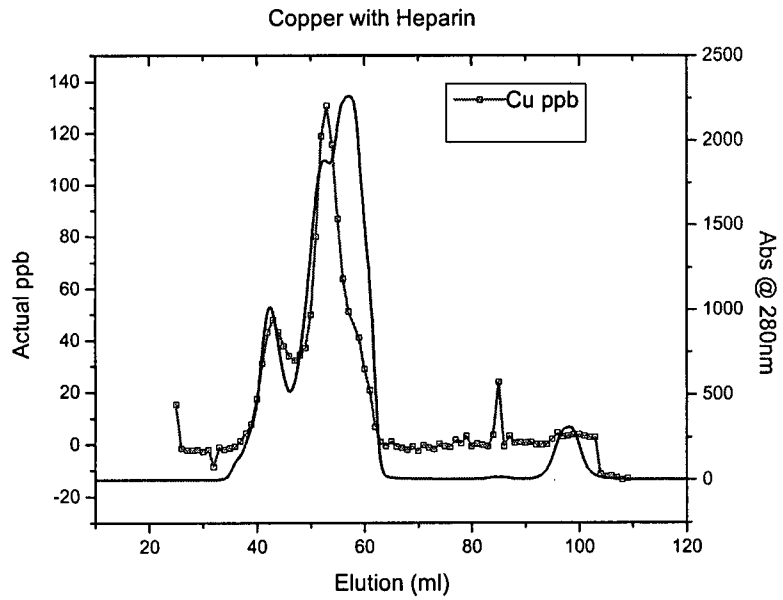
Copper with Heparin
Cu ppb
Actual ppb
Abs @ 280nm
Elution (ml)
140
120
100
80
60
40
20
0
-20
2500
2000
1500
1000
500
0
20
40
60
80
100
120

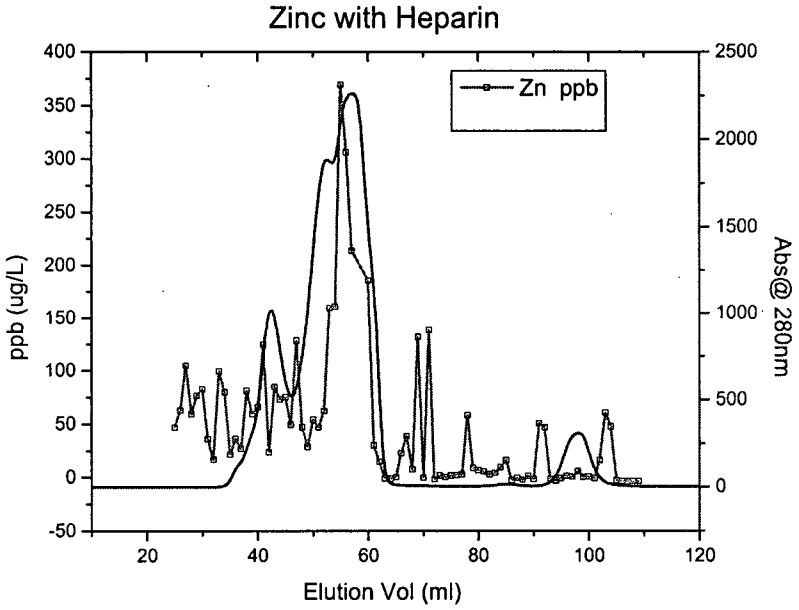
Zinc with Heparin
Zn ppb
ppb (ug/L)
Abs@ 280nm
Elution Vol (ml)
400
350
300
250
200
150
100
50
0
-50
2500
2000
1500
1000
500
0
20
40
60
80
100
120

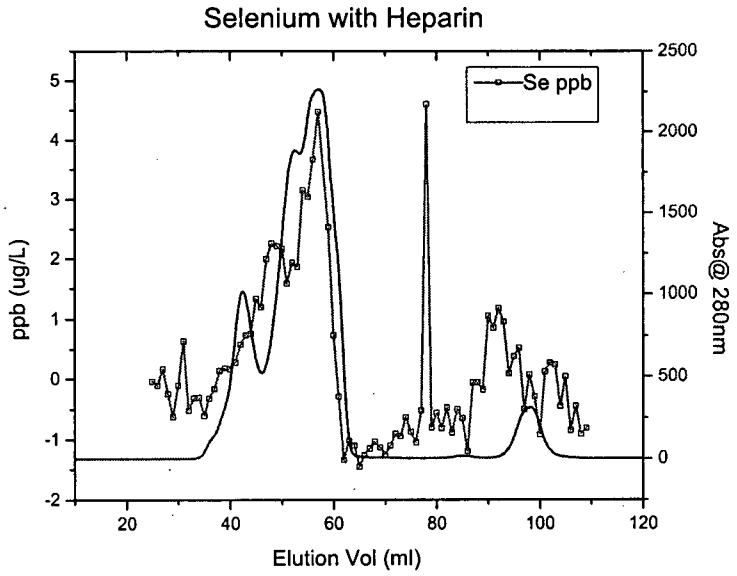
Selenium with Heparin
Se ppb
ppb (ug/L)
Abs@ 280nm
Elution Vol (ml)
5
4
3
2
1
0
-1
-2
2500
2000
1500
1000
500
0
20
40
60
80
100
120

A.4 Freeze-thawed plasma collected in lithium heparin

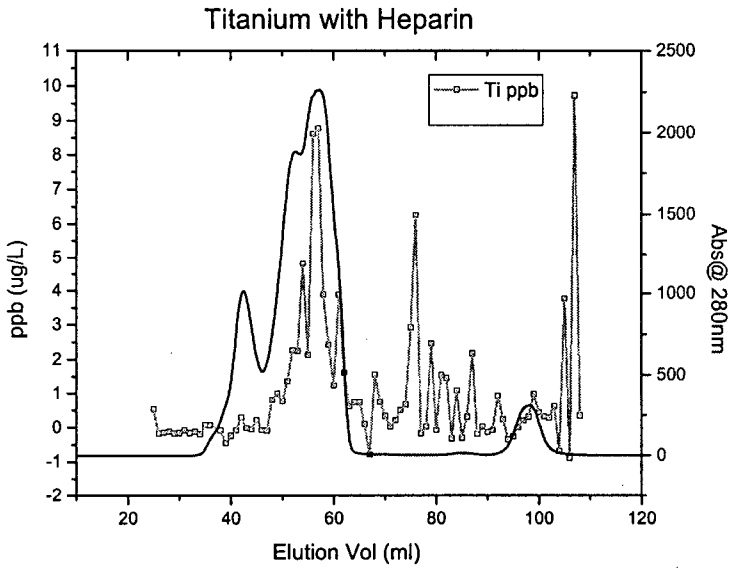

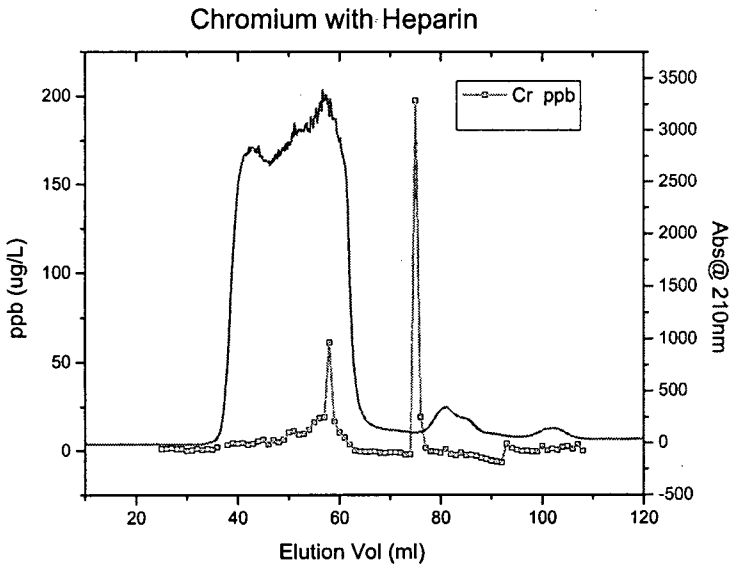

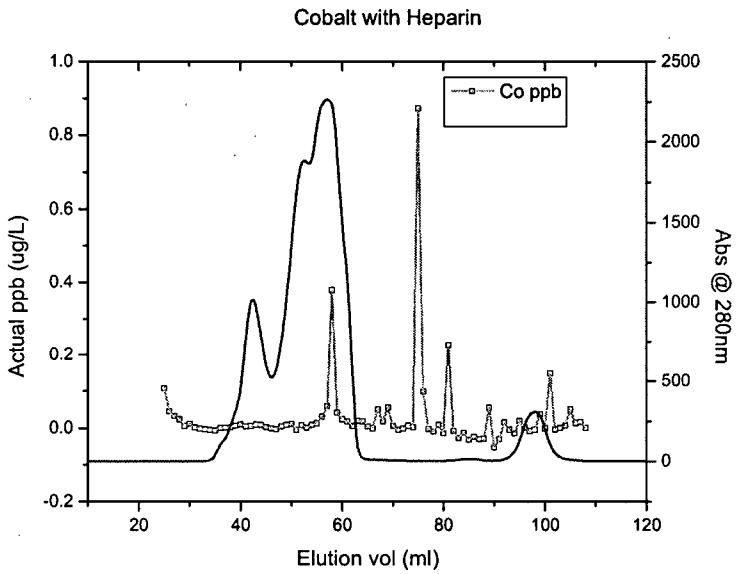
Cobalt with Heparin
Co ppb
Actual ppb (ug/L)
Abs @ 280nm
Elution vol (ml)
1.0
0.8
0.6
0.4
0.2
0.0
-0.2
2500
2000
1500
1000
500
0
20
40
60
80
100
120

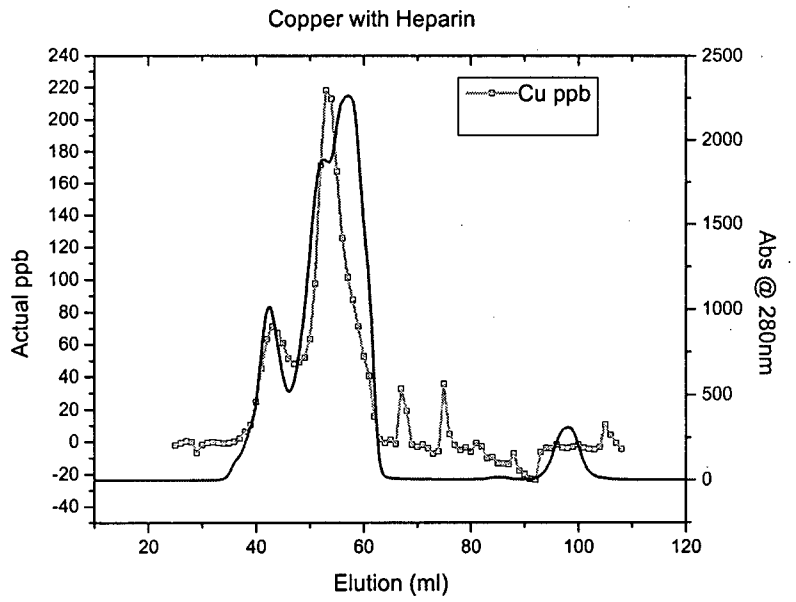
Copper with Heparin
Cu ppb
Actual ppb
Abs @ 280nm
Elution (ml)
240
220
200
180
160
140
120
100
80
60
40
20
0
-20
-40
2500
2000
1500
1000
500
0
20
40
60
80
100
120

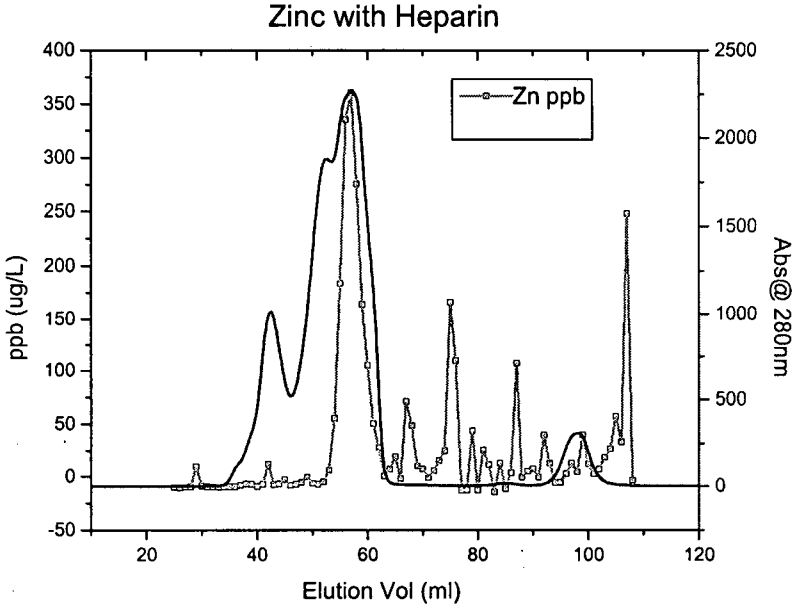
Zinc with Heparin
Zn ppb
ppb (ug/L)
Abs@ 280nm
Elution Vol (ml)
400
350
300
250
200
150
100
50
0
-50
2500
2000
1500
1000
500
0
20
40
60
80
100
120

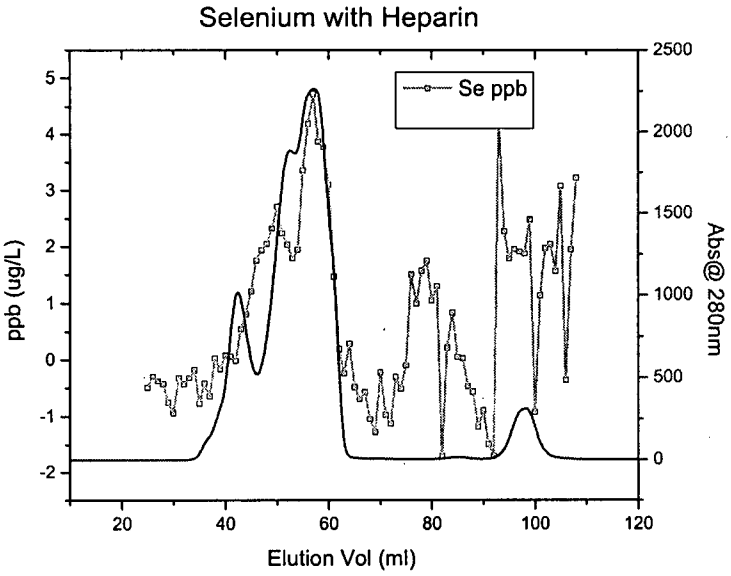
Selenium with Heparin
Se ppb
ppb (ug/L)
Abs@ 280nm
Elution Vol (ml)
5
4
3
2
1
0
-1
-2
2500
2000
1500
1000
500
0
20
40
60
80
100
120

Appendix B

Smoothed Metal ion Profiles in Blood Plasma Samples Achieved with SEC/ICP-MS

B.1 Fresh plasma collected in citrate – final citrate concentration 13 mM

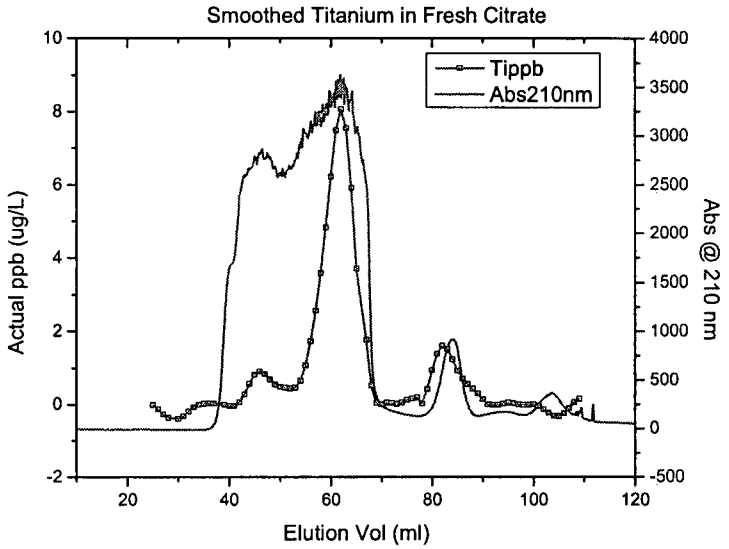

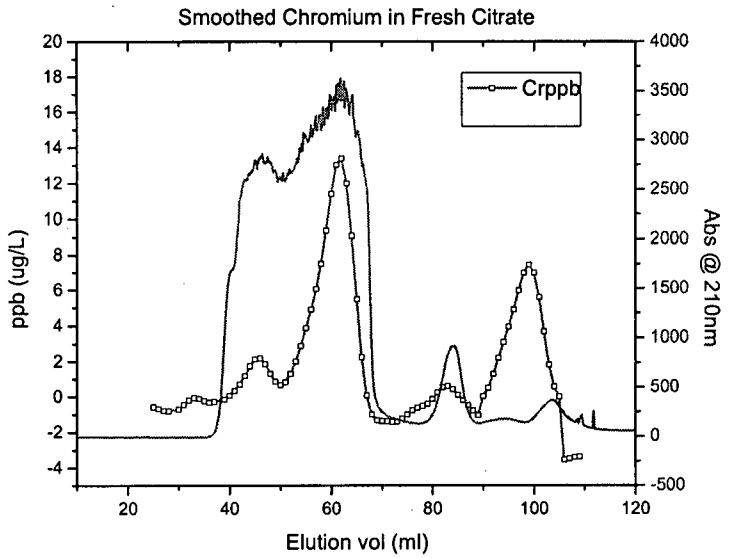

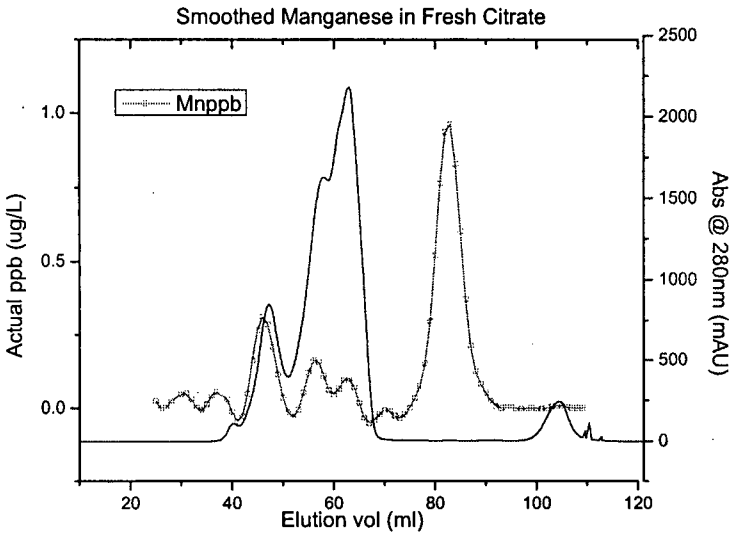
Smoothed Manganese in Fresh Citrate
Mnppb
Actual ppb (ug/L)
Abs @ 280nm (mAU)
Elution vol (ml)
1.0
0.5
0.0
2500
2000
1500
1000
500
0
20
40
60
80
100
120

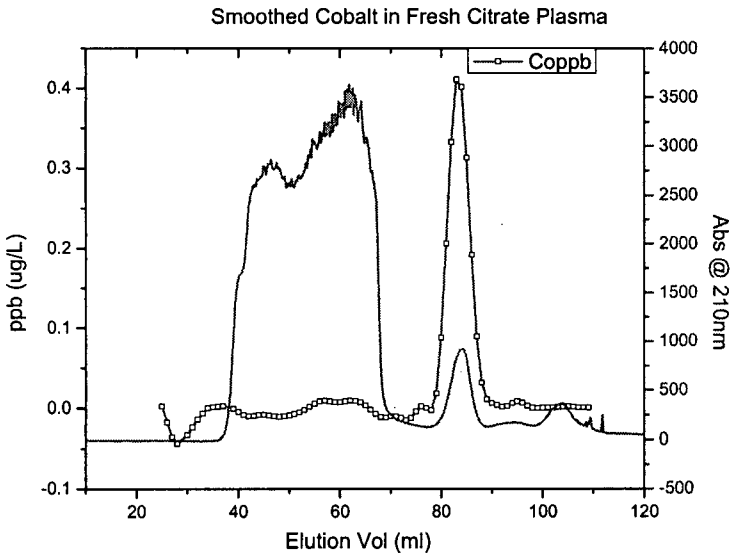
Smoothed Cobalt in Fresh Citrate Plasma
Coppb
ppb (ug/L)
Abs @ 210nm
Elution Vol (ml)
0.4
0.3
0.2
0.1
0.0
-0.1
4000
3500
3000
2500
2000
1500
1000
500
0
-500
20
40
60
80
100
120

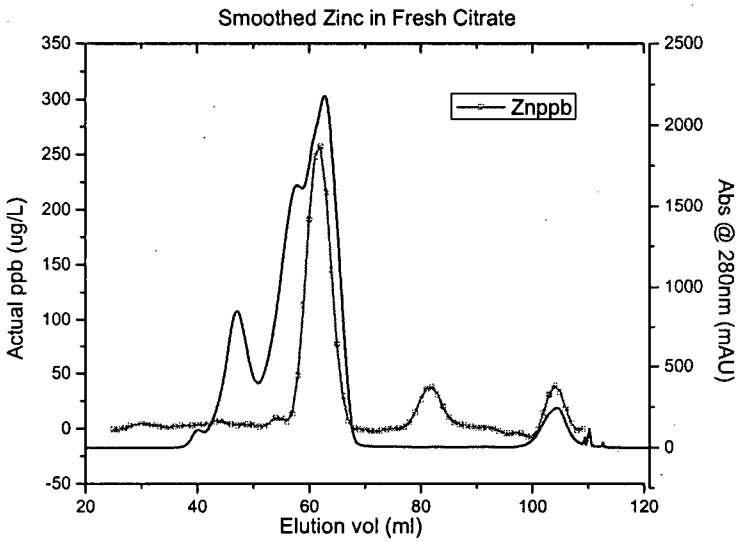
Smoothed Zinc in Fresh Citrate
Znppb
Actual ppb (ug/L)
Abs @ 280nm (mAU)
Elution vol (ml)
350
300
250
200
150
100
50
0
-50
2500
2000
1500
1000
500
0
20
40
60
80
100
120

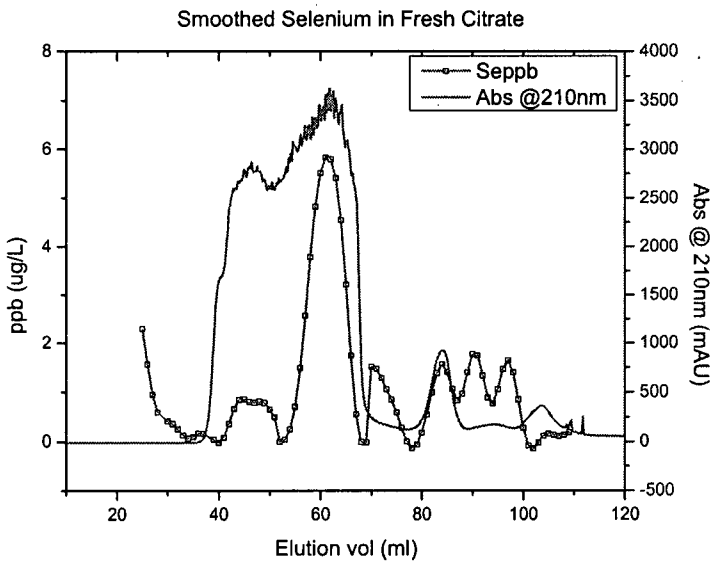
Smoothed Selenium in Fresh Citrate
Seppb
Abs @210nm
ppb (ug/L)
Abs @ 210nm (mAU)
Elution vol (ml)
8
6
4
2
0
4000
3500
3000
2500
2000
1500
1000
500
0
-500
20
40
60
80
100
120

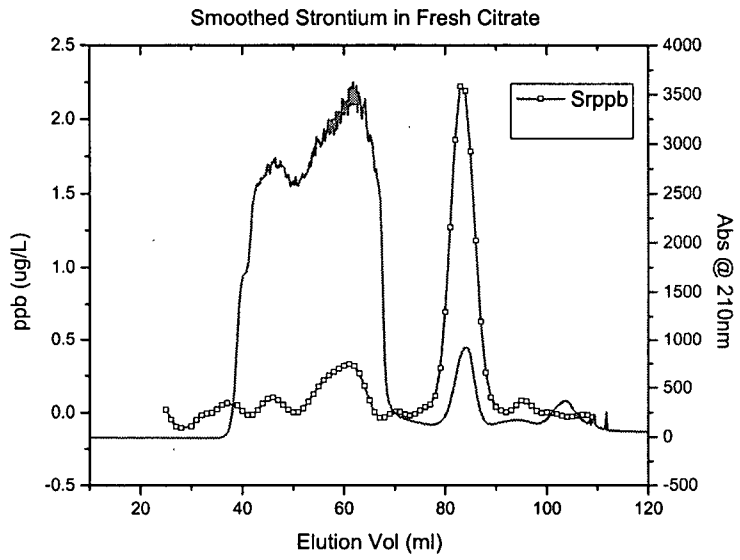

B.2 Freeze-thawed plasma collected in citrate – final citrate concentration 13 mM

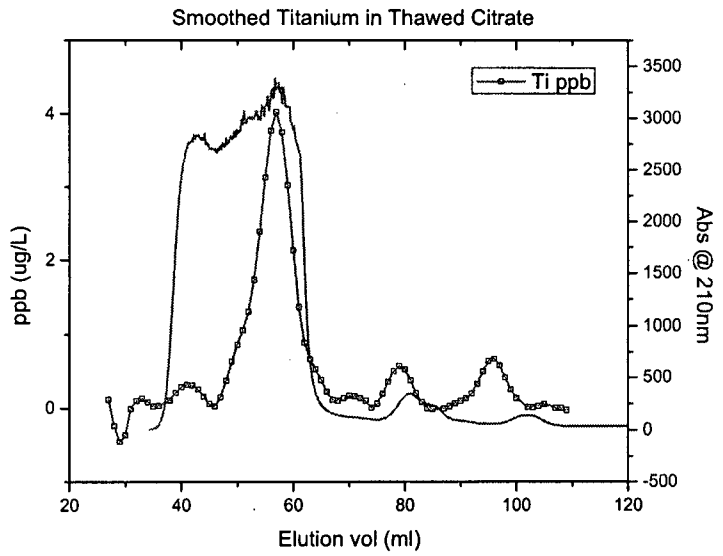

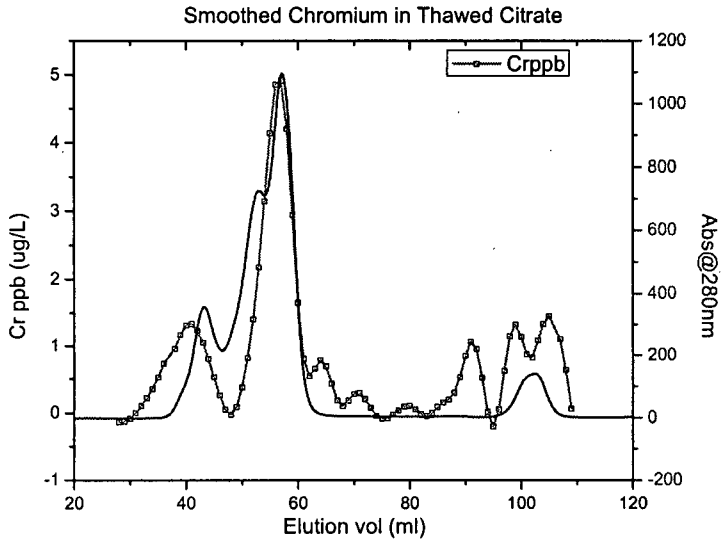
Smoothed Chromium in Thawed Citrate
Crppb
Cr ppb (ug/L)
Abs@280nm
Elution vol (ml)
5
4
3
2
1
0
-1
1200
1000
800
600
400
200
0
-200
20
40
60
80
100
120

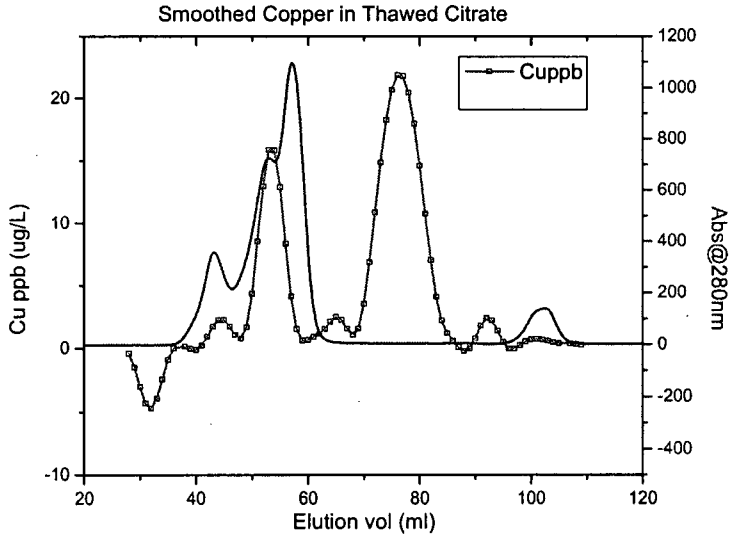
Smoothed Copper in Thawed Citrate
Cuppb
Cu ppb (ug/L)
Abs@280nm
Elution vol (ml)
20
10
0
-10
1200
1000
800
600
400
200
0
-200
-400
20
40
60
80
100
120

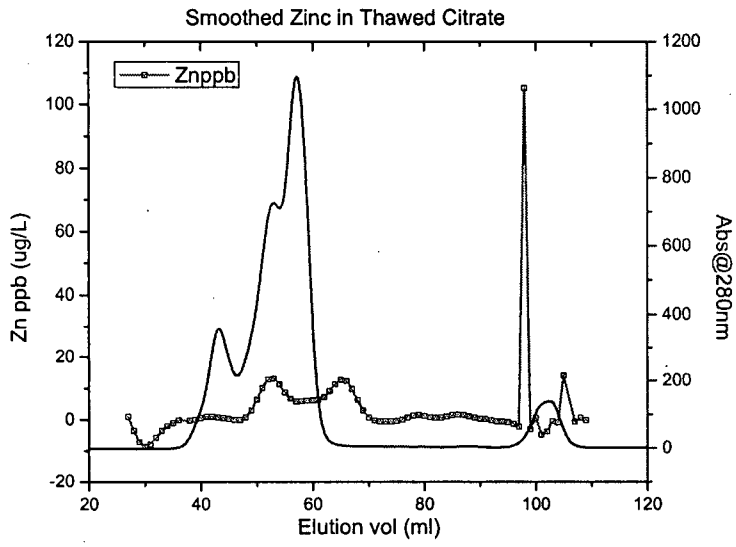
Smoothed Zinc in Thawed Citrate
Znppb
Zn ppb (ug/L)
Abs@280nm
Elution vol (ml)
120
100
80
60
40
20
0
-20
1200
1000
800
600
400
200
0
20
40
60
80
100
120

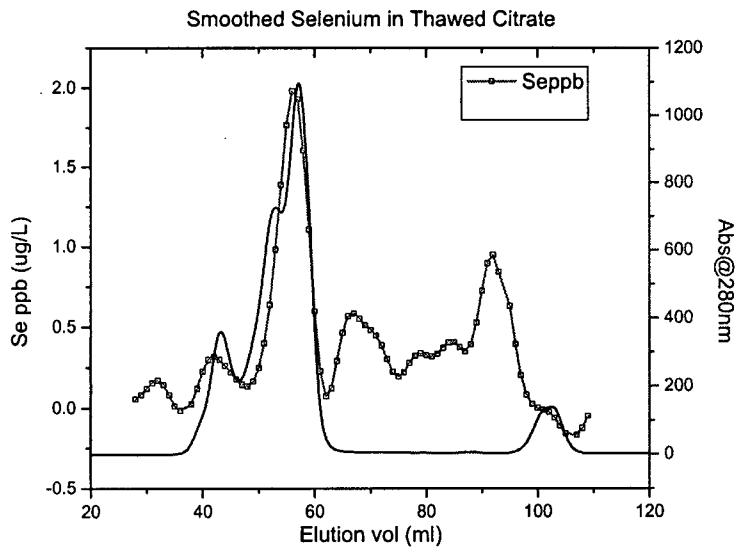
Smoothed Selenium in Thawed Citrate
Seppb
Se ppb (ug/L)
Abs@280nm
Elution vol (ml)
2.0
1.5
1.0
0.5
0.0
-0.5
1200
1000
800
600
400
200
0
20
40
60
80
100
120

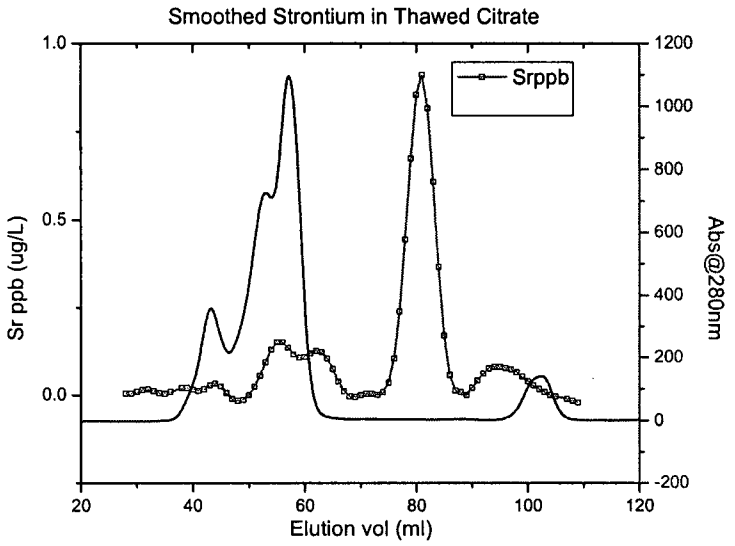

B.3 Fresh plasma collected in lithium heparin

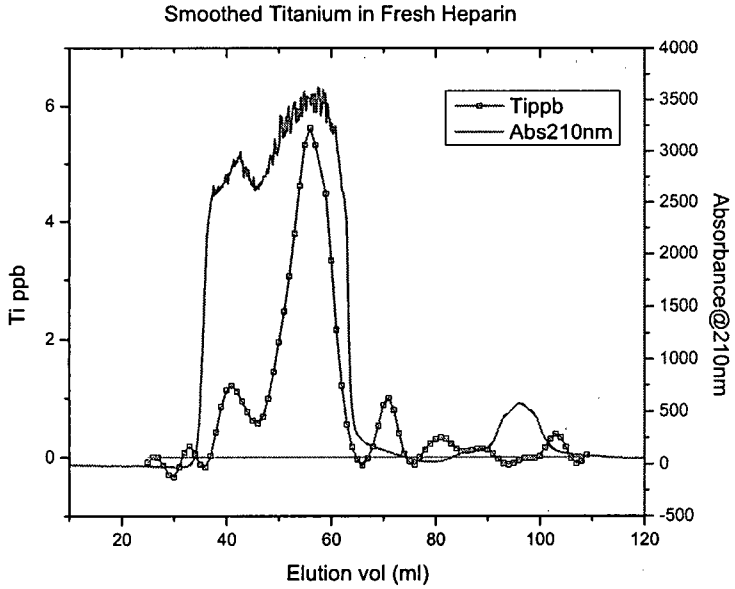

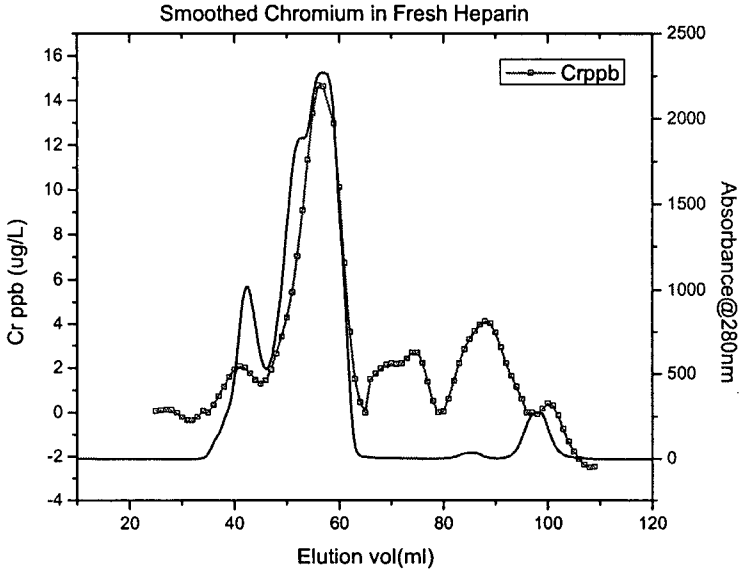
Smoothed Chromium in Fresh Heparin
Crppb
Cr ppb (ug/L)
Absorbance@280nm
Elution vol(ml)
16
14
12
10
8
6
4
2
0
-2
-4
2500
2000
1500
1000
500
0
20
40
60
80
100
120

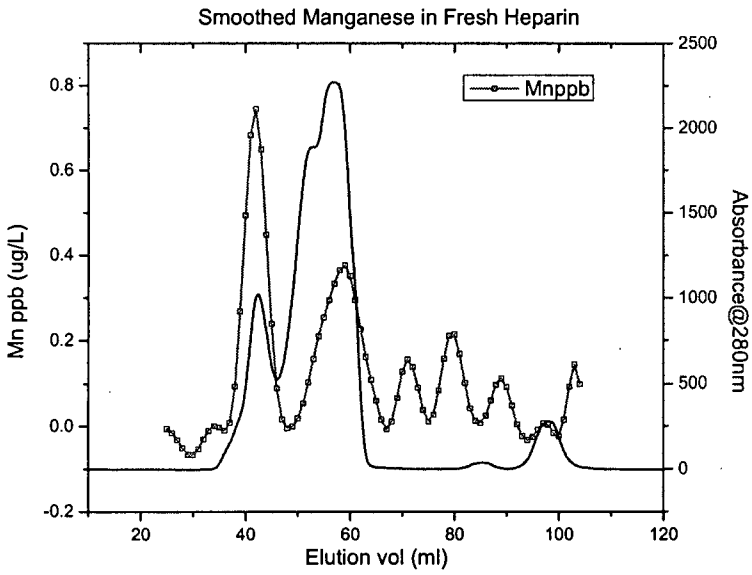
Smoothed Manganese in Fresh Heparin
Mnppb
Mn ppb (ug/L)
Absorbance@280nm
Elution vol (ml)
0.8
0.6
0.4
0.2
0.0
-0.2
2500
2000
1500
1000
500
0
20
40
60
80
100
120

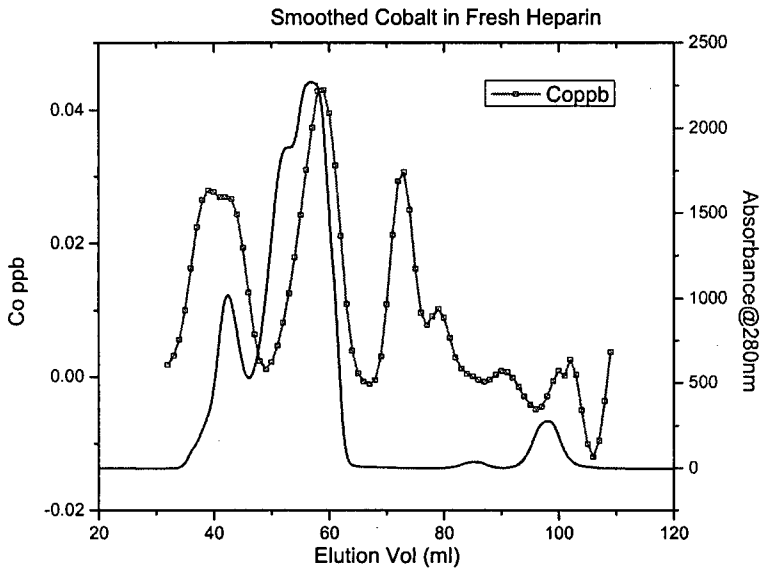
Smoothed Cobalt in Fresh Heparin
Coppb
Co ppb
Absorbance@280nm
Elution Vol (ml)
0.04
0.02
0.00
-0.02
2500
2000
1500
1000
500
0
20
40
60
80
100
120

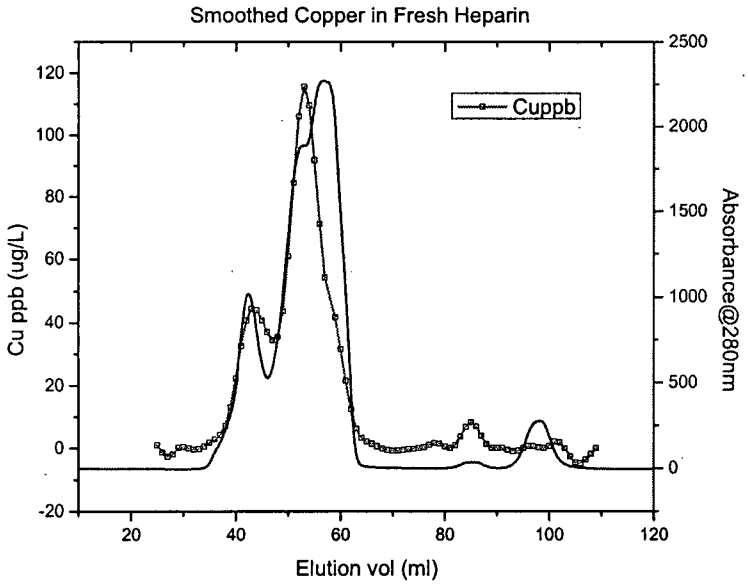
Smoothed Copper in Fresh Heparin
Cuppb
Cu ppb (ug/L)
Absorbance@280nm
Elution vol (ml)
120
100
80
60
40
20
0
-20
2500
2000
1500
1000
500
0
20
40
60
80
100
120

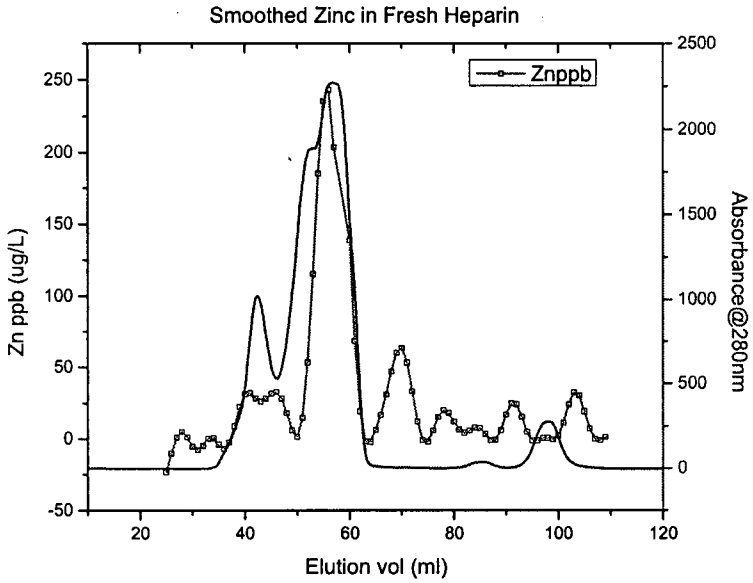
Smoothed Zinc in Fresh Heparin
Znppb
Zn ppb (ug/L)
Absorbance@280nm
Elution vol (ml)
250
200
150
100
50
0
-50
2500
2000
1500
1000
500
0
20
40
60
80
100
120

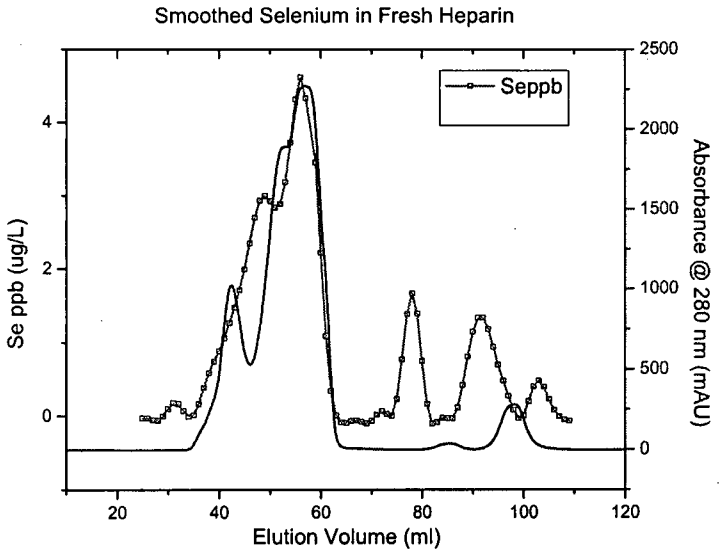
Smoothed Selenium in Fresh Heparin
Seppb
Se ppb (ug/L)
Absorbance @ 280 nm (mAU)
Elution Volume (ml)
4
2
0
2500
2000
1500
1000
500
0
20
40
60
80
100
120

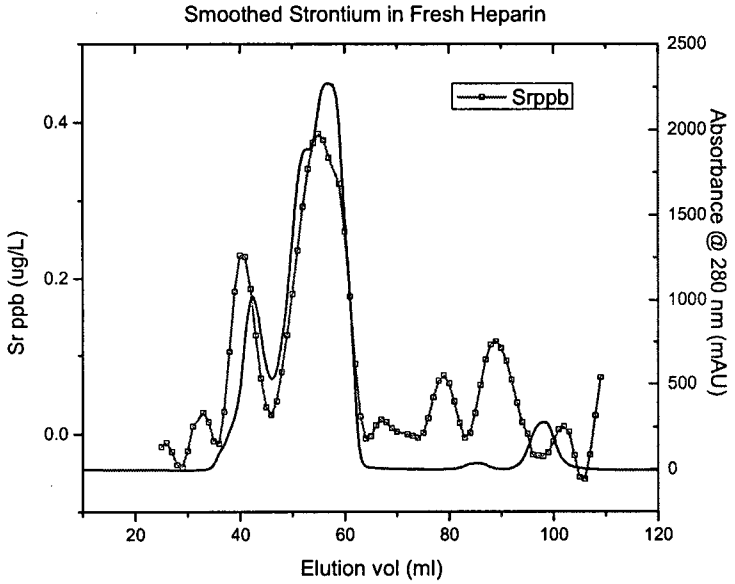

B.4 Freeze-thawed plasma collected in lithium heparin

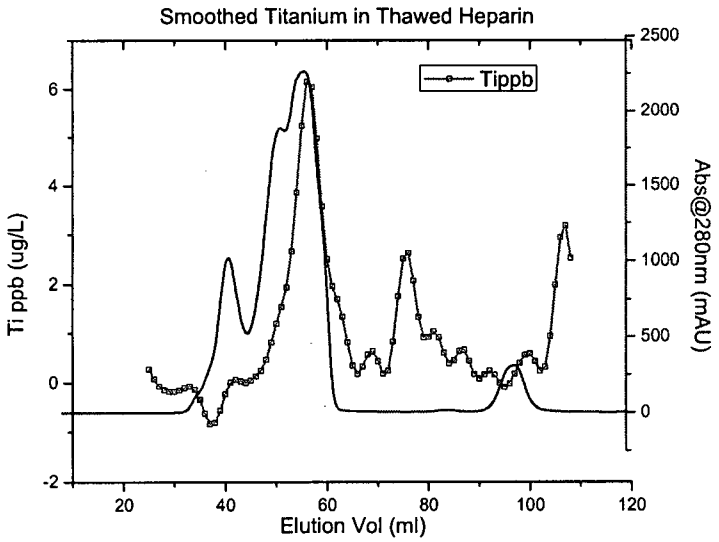

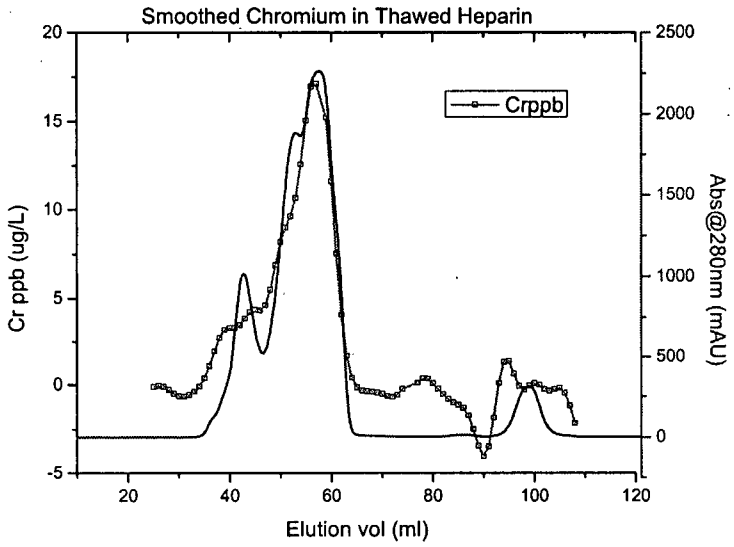
Smoothed Chromium in Thawed Heparin
Crppb
Cr ppb (ug/L)
Abs@280nm (mAU)
Elution vol (ml)
20
15
10
5
0
-5
2500
2000
1500
1000
500
0
20
40
60
80
100
120

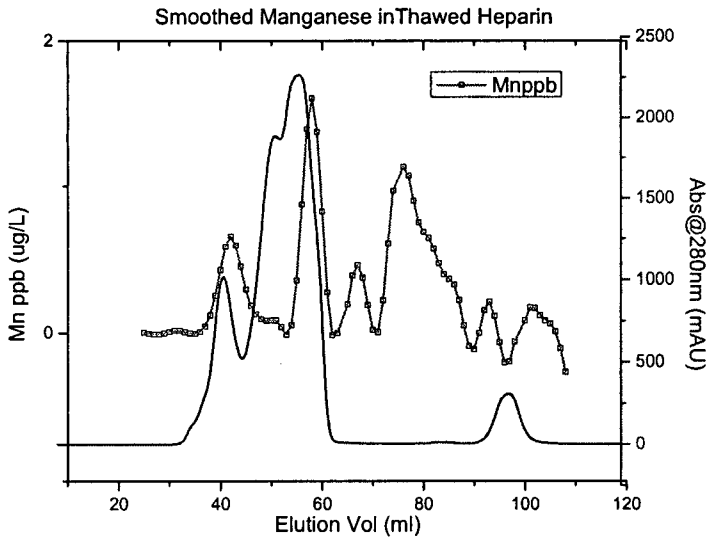
Smoothed Manganese inThawed Heparin
Mnppb
Mn ppb (ug/L)
Abs@280nm (mAU)
Elution Vol (ml)
2
0
2500
2000
1500
1000
500
0
20
40
60
80
100
120

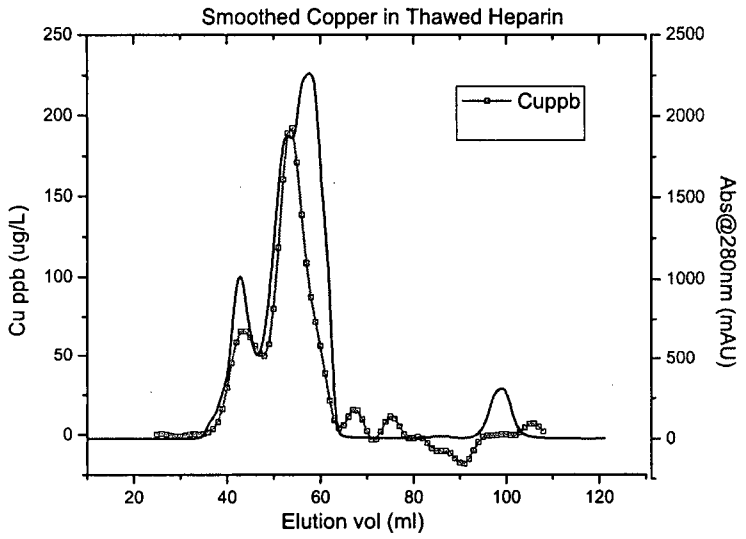
Smoothed Copper in Thawed Heparin
Cuppb
Cu ppb (ug/L)
Abs@280nm (mAU)
Elution vol (ml)
250
200
150
100
50
0
2500
2000
1500
1000
500
0
20
40
60
80
100
120

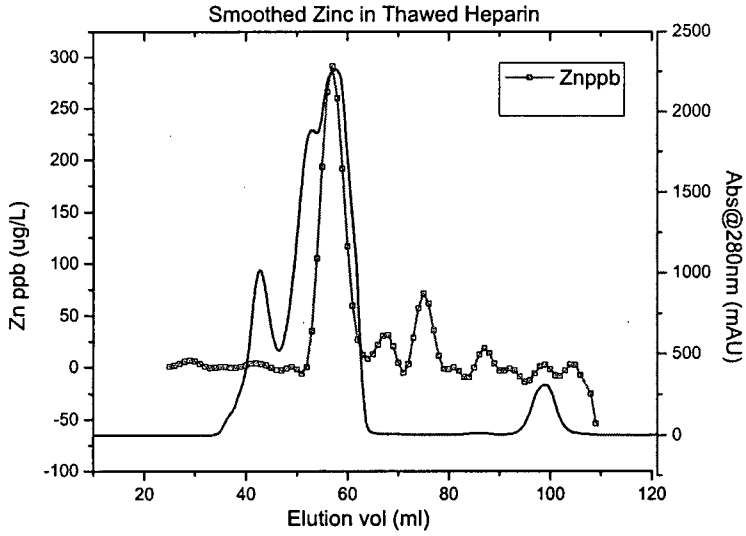
Smoothed Zinc in Thawed Heparin
Znppb
Zn ppb (ug/L)
Abs@280nm (mAU)
Elution vol (ml)
300
250
200
150
100
50
0
-50
-100
2500
2000
1500
1000
500
0
20
40
60
80
100
120

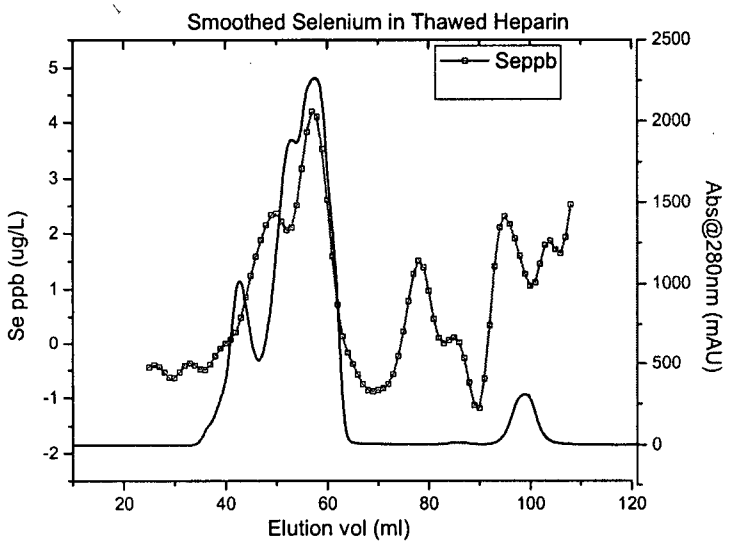

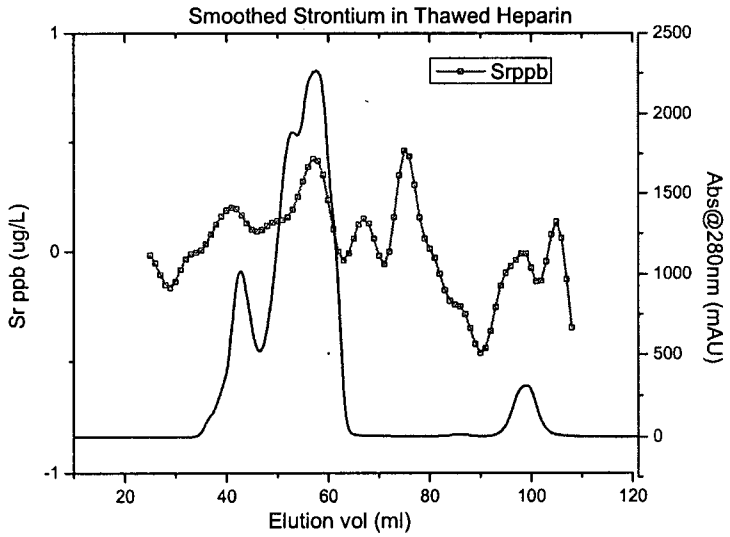

Smoothing was performed using FFT filtering with averaging of every 3 points.

Bibliography

1. Lippard, S.J. and J.M. Berg, *Principles of Bioinorganic Chemistry*, ed. A. Kelly. 1994, Mill Valley: University Science Books. 411.

2. Berlow, Burton, and Routh, *Introduction to the Chemistry of Life*. 1974, New York: Saunders College Publishing.

3. Merck, *Chapter 12. Water, Electrolyte, Mineral, And Acid-Base Metabolism, Section 2 Endocrine / Metabolic Disorders*, in *The Merck Manual of Diagnosis and Therapy*, M.H. Beers and R. Berkow, Editors. 1999-2004, Merck & Co.: Internet edition.

4. Merck, *Chapter 4. Mineral Deficiency And Toxicity , Section 1. Nutritional Disorders*, in *The Merck Manual of Diagnosis and Therapy*, M.H. Beers and R. Berkow, Editors. 1999-2004, Internet edition.

5. Lodish, H., D. Baltimore, A. Berk, S.L. Zipursky, P. Matsudaira, and J. Darnell, *Molecular Cell Biology*. 3rd ed, ed. J. Darnell. 1995, New York: Scientific American Inc. 1344.

6. Anastassopoulou, J. and T. Theophanides, *The role of metal ions in biological systems and medicine.* NATO ASI Series, Series C: Mathematical and Physical Sciences (Bioinorganic Chemistry), 1995. **459**: p. 209-18.

7. Goswami, T., A. Rolfs, and M.A. Hediger, *Iron transport: emerging roles in health and disease.* Biochemistry and Cell Biology, 2002. **80**(5): p. 679-689.

8. Rao, M., A. Tanksale, M. Ghatge, and V. Deshpande, *Molecular and Biotechnological Aspects of Microbial Proteases.* Microbiology and Molecular Biology Reviews, 1998. **62**(3): p. 597-635.

9. Prasad, A.S., *Zinc deficiency* BMJ, 2003. **326**(7386): p. 409-410.

10. Rolfs, A. and M.A. Hediger, *Metal ion transporters in mammals: structure, function and pathological implications.* Journal of Physiology (Cambridge, United Kingdom), 1999. **518**(1): p. 1-12.

11. Merck, *Chapter 1. Nutrition: General Considerations, Section 1. Nutritional Disorders*, in *The Merck Manual of Diagnosis and Therapy*, M.H. Beers and R. Berkow, Editors. 1999-2004, Internet edition.

12. Carrillo-Ponce, M.d.L., V.A. Martinez-Ordaz, V.M. Velasco-Rodriguez, A. Hernandez-Garcia, M.C.Hernandez-Serrano, and F. Sanmiguel, *Serum lead, cadmium, and zinc levels in newborns with neural tube defects from a polluted zone in Mexico.* Reproductive Toxicology, 2004. **19**: p. 149-154.

13. U.S.Department-of-Labor and O.S.a.H. Administration, *Toxic Metals*, in *Safety and Health Topics*, C. Jones and O.D.o.E. Programs, Editors. 2004: Washington.

14. Suzuki, H. and S. Ishiguro, *Thermodynamics and structures of nickel(II) chloro complexes in N,N-dimethylacetamide.* Inorganic Chemistry, 1992. **31**(20): p. 4178-4183.

15. Ozutsumi, K., Y. Abe, R.Takahashi, and S. Ishiguro, *Chloro and Bromo Complexation of the Manganese(II) Ion and Solvation Structure of the Manganese(II), Iron(II), Cobalt(II), Nickel(II), Copper(II), and Zinc(II) Ions in Hexamethylphosphoric Triamide.* Journal of Physical Chemistry, 1994. **98**(39): p. 9894-9899.

16. Pearson, R.G., *Hard and Soft Acids and Bases.* Chemistry in Britain, 1967. **3**: p. 103-107.

17. Richarz, A.-N. and P. Bratter, *Speciation analysis of trace elements in the brains of individuals with Alzheimer's disease with special emphasis on metallothioneins.* Anals of Bioanalytical Chemistry, 2002. **372**: p. 412-417.

18. Nagaoka, M.H., T. Yamazaki, and T. Maitani, *Binding patterns of vanadium ions with different valence states to human transferrin studied by HPLC/high resolution ICP-MS.* Biochemical and Biophysical Research Communications, 2002. **296**: p. 1207-1214.

19. Nelson, N., *Metal ion transporters and homeostasis.* EMBO Journal, 1999. **18**(16): p. 4361-4371.

20. Sun, H., H. Li, and P. Sadler, *Transferrin as a metal ion mediator.* Chem. Rev., 1999. **99**: p. 2817-2842.

21. Martin, R.B., J. Savory, S. Brown, R.L. Bertholf, and M.R. Wills, *Transferrin binding of Al3+ and Fe3+.* Clin Chem, 1987. **33**(3): p. 405-7.

22. Bal, W., J. Christodoulou, P.J. Sadler, and A. Tucker, *Multi-metal binding site of serum albumin.* Journal of Inorganic Biochemistry, 1998. **70**(1): p. 33-39.

23. Masuoka, J., J. Hegenauer, B.V. Dyke, and P. Saltman, *Intrinsic stoichiometric equilibrium constants for the binding of zinc(II) and copper(II) to the high affinity site of serum albumin.* Journal of Biological Chemistry, 1993. **268**(29): p. 21533-21537.

24. Sokolowska, M., A. Krezel, M. Dyba, Z. Szewczuk, and W. Bal, *Short peptides are not reliable models of thermodynamic and kinetic properties of the N-terminal metal binding site in serum albumin.* European Journal of Biochemistry, 2002. **269**: p. 1323-1331.

25. Zhang, Y. and D. Wilcox, *Thermodynamic and spectroscopic study of Cu(II) and Ni(II) binding to bovine serum albumin.* Journal of Bio-Inorganic Chemistry, 2002. **7**(3): p. 327-337.

26. Cartana, J., L. Arola, and A. Mas, *Effects of acute nickel toxicity upon plasma and liver metal homeostasis as a function of sex.* Toxicology, 1991. **69**(2): p. 133-41.

27. Harris, Z. and J. Gitlin. *Aceruloplasminemia.* in *INABIS '98 - 5th Internet World Congress on Biomedical Sciences. Invited Symposium.* 1998. McMaster University, Canada.

28. Osaki, S., D. Johnson, and E. Frieden, *The Possible Significance of the Ferrous Oxidase Activity of Ceruloplasmin in Normal Human Serum.* J Biol Chem, 1966. **241**: p. 2746-2757.

29. Harris, Z.L., Y. Takahashi, H. Miyajima, M. Serizawa, R.T.A. MacGillivray, and J.D. Gitlin, *Aceruloplasminemia: Molecular characterization of this disorder of iron metabolism.* Proceedings of the National Academy of Sciences of the United States of America ,, 1995. **92**: p. 2539-2543.

30. Strausak, D., J.F.B. Mercer, H.H. Dieter, W. Stremmel, and G. Multhaup, *Copper in disorders with neurological symptoms: Alzheimer's, Menkes, and Wilson diseases.* Brain Research Bulletin, 2001. **55**(2): p. 175-185.

31. Bush, A.I., *The metallobiology of Alzheimer's disease.* Trends in Neurosciences, 2003. **26**(4): p. 207-214.

32. Burdette, S.C. and S.J. Lippard, *Meeting of the minds: Metalloneurochemistry.* Proceedings of the National Academy of Sciences of the United States of America ,, 2003. **100**(7): p. 3605-3610.

33. Basun, H., L.G. Forssell, L. Wetterberg, and B. Winblad, *Metals and trace elements in plasma and cerebrospinal fluid in normal aging and Alzheimer's disease.* Journal of Neural Transmission: Parkinson's Disease and Dementia Section, 1991. **3**(4): p. 231-58.

34. Jones, D.C., N.T. Young, C. Pigott, S.V. Fuggle, M.C.N.M. Barnardo, Marshall, and M. Bunce, *Comprehensive hereditary hemochromatosis genotyping.* Tissue Antigens, 2002. **60**: p. 481-488.

35. Anderson, N.L., M. Polanski, R. Pieper, T. Gatlin, R.S. Tirumalai, T.P. Conrads, T.D. Veenstra, J.N. Adkins, J.G. Pounds, R. Fagan, and A. Lobley, *The Human Plasma Proteome: A Nonredundant List Developed by Combination of Four Separate Sources.* Molecular & Cellular Proteomics, 2004. **3**: p. 311-326.

36. Pieper, R., C.L. Gatlin, A.J. Makusky, P.S. Russo, C.R. Schatz, S.S. Miller, Q. Su, A.M. McGrath, M.A. Estock, P.P. Parmar, M. Zhao, S.T. Huang, J. Zhou, F. Wang, R. Esquer-Blasco, N.L. Anderson, J. Taylor, and S. Steiner, *The human serum proteome: display of nearly 3700 chromatographically separated protein spots on two-dimensional electrophoresis gels and identification of 325 distinct proteins.* Proteomics, 2003. **3**(7): p. 1345-64.

37. Aldred, S., M.M. Grant, and H.R. Griffiths, *The use of proteomics for the assessment of clinical samples in research.* Clinical Biochemistry, 2004. **37**: p. 943-952.

38. Anderson, N.L. and N.G. Anderson, *The human plasma proteome: history, character, and diagnostic prospects.* Molecular & Cellular Proteomics, 2002. **1**(11): p. 845-67.

39. Zhang, Z., R.C. Bast, Y. Yu, J. Li, L.J. Sokoll, A.J. Rai, J.M. Rosenzweig, B. Cameron, Y.Y. Wang, X.-Y. Meng, A. Berchuck, C.v. Haaften-Day, N.F. Hacker,

H.W.A.d. Bruijn, A.G.J.v.d. Zee, I.J. Jacobs, E.T. Fung, and D.W. Chan, *Three Biomarkers Identified from Serum Proteomic Analysis for the Detection of Early Stage Ovarian Cancer.* Cancer Research, 2004. **64**: p. 5882-5890.

40. Rai, A., Z. Zhang, J. Rosenzweig, I.M. Shih, T. Pham, E. Fung, L. Sokoll, and D. Chan, *Proteomic approaches to tumor marker discovery.* Arch Pathol Lab Med, 2002. **126**(12): p. 1518-26.

41. Lehrer, S., J. Roboz, H. Ding, S. Zhao, E. Diamond, J. Holland, N. Stone, M. Droller, and R. Stock, *Putative protein markers in the sera of men with prostatic neoplasms.* BJU International, 2003. **92**(3): p. 223-5.

42. Doherty, N., B. Littman, K. Reilly, A. Swindell, J. Buss, and N. Anderson, *Analysis of changes in acute-phase plasma proteins in an acute inflammatory response and in rheumatoid arthritis using two-dimensional gel electrophoresis.* Electrophoresis, 1998. **19**(2): p. 355-363.

43. Belov, M., G.A. Anderson, M.A. Wingerd, H.R. Udseth, K. Tang, D.C. Prior, K.R. Swanson, M.A. Buschbach, E.F. Strittmatter, R.J. Moore, and R.D. Smith, *An automated high performance capillary liquid chromatography-Fourier transform ion cyclotron resonance mass spectrometer for high-throughput proteomics.* Journal of the American Society for Mass Spectrometry, 2004. **15**: p. 212-232.

44. Harada, K., A. Kuniyasu, H. Nakayama, M. Nakayama, T. Matsunaga, Y. Uji, H. Sugiuchi, and H. Okabe, *Separation of human serum transferrins with different iron-binding states by high-performance liquid chromatography using a pyridinium polymer column.* Journal of Chromatography B, 2002. **767**: p. 45-51.

45. Reitsma, P.H. and G. de Koster Ch, *'Proteomics': the mapping of all human proteins.* Ned Tijdschr Geneeskd, 2003. **147**(3): p. 99-104.

46. Tissot, J., P. Schneider, R. James, R. Daigneault, and D. Hochstrasser, *High-resolution two-dimensional protein electrophoresis of pathological plasma/serum.* Applied Theoretical Electrophoresis, 1991. **2**: p. 7-12.

47. Szpunar J, L.R., *Multidimensional approaches in biochemical speciation analysis.* Anal Bioanal Chem, 2002. **373**(6): p. 404-411.

48. Stutz, H., G. Bordin, and A.R. Rodriguez, *Trends in metal-binding proteins analysis using capillary electrophoresis.* Current Topics in Analytical Chemistry, 2002. **3**: p. 157-191.

49. Adkins, J.N., S.M. Varnum, K.J. Auberry, R.J. Moore, H.A. Nicolas , R.D. Smith, D.L. Springer, and J.G. Pounds, *Toward a Human Serum Proteome: Analysis By Multidimensional Separation Coupled With Mass Spectrometry.* Molecular & Cellular Proteomics, 2002. **1**: p. 947-955.

50. Tirumalai, R.S., K.C. Chan, D.A. Prieto, H.J. Issaq, T.P. Conrads, and T.D. Veenstra, *Characterization of the low molecular weight human serum proteome.* Mol Cell Proteomics, 2003. **2**: p. 1096-1103.

51. Mantovani, G., A. Maccio, C. Madeddu, L. Mura, E. Massa, G. Gramignano, M. Lusso, V. Murgia, P. Camboni, and L. Ferreli, *Reactive oxygen species, antioxidant mechanisms and serum cytokine levels in cancer patients: impact of an antioxidant treatment.* Journal of Cellular and Molecular Medicine, 2002. **6**(4): p. 570-582.

52. Putnam, F.W., *Perspectives Past, Present and Future*, in *The plasma proteins: structure, function, and genetic control.*, F.W. Putnam, Editor. 1975, Academic Press: New York.

53. Sarkar, B., *Metal protein interactions.* Progress in food and nutrition science, 1987. **11**(3-4): p. 363-400.

54. Hill, K.E., M. Dasouki, J.A.I. Phillips, and R.F. Burk, *Human Selenoprotein P gene maps to 5q31.* Genomics, 1996. **36**: p. 550-551.

55. MacGillivray, R., E. Mendez, J. Shewale, G. Sinha, J. Lineback-Zins, and K. Brew, *The primary structure of human serum transferrin.* Journal of Biological Chemistry, 1983. **258**: p. 3543-3553.

56. Mc Mahon, R. and R. Cousins, *Mammalian zinc transporters.* Journal of Nutrition, 1998. **128**: p. 667-670.

57. Glennon, J. and B. Sarkar, *Nickel(II)-transport in human blood serum: studies of nickel(II)-binding to human albumin, native sequence peptide and ternary complex formation with L-histidine.* Biochemical journal, 1982. **203**: p. 15-23.

58. Ohyoshi, E., Y. Hamada, K. Nakata, and S. Kohata, *The interaction between human and bovine serum albumin and zinc studied by a competitive spectrophotometry.* Journal of Inorganic Biochemistry, 1999. **75**: p. 213-218.

59. *Risk Assessment: Chromium*, in *Part 3: Trace elements*. 2003. p. Expert Group on Vitamins and Minerals 2003.

60. Sarkar, B., *Albumin as the major plasma protein transporting metals.* Life Chemistry Reports, 1983. **1**(3): p. 165-207.

61. Allen, P.C., E. Hill, and A. Stokes, *Plasma proteins; analytical and preparative techniques*. 1977, London: Blackwell Scientific Publications.

62. Lindgren, A., A. Kilander, E. Bagge, and E. Nexo, *Holotranscobalamin – a sensitive marker of cobalamin malabsorption.* Eur J Clin Invest, 1999. **29**: p. 321-9.

63. Barashkov, G.K., L.I. Zaitseva, M.A. Kondakhchan, and E.A. Konstantinova, *Distribution of chemical elements in whole blood and plasma.* Biomeditsinskaya Khimiya, 2003. **49**(3): p. 297-302.

64. Cornelis, R., E. Sabbioni, and M.T. Van der Venne, *Trace element reference values in tissues from inhabitants of the european community. VII. Review of trace elements in blood, serum and urine of the Belgian population and critical evaluation of their possible use as reference values.* The science of the total environment, 1994. **158**: p. 191-226.

65. Sasaki, T., *Measurement of heavy metals in blood serum by ICP (inductively coupled plasma) radiation analysis.* ,. Kensa to Gijutsu, 1990. **18**(3): p. 219-24.

66. Okazaki, Y., *The analysis of toxic metals in blood and urine and the significance.* Sumitomo Sangyo Eisei, 1978. **14**: p. 1-8.

67. Muniz, C.S., J.L. Fernandez-Martin, J.M. Marchante-Gayon, J.I.G. Alonso, J.B. Cannata-Andia, and A. Sanz-Medel, *Reference values for trace and ultratrace elements in human serum determined by double-focusing ICP-MS.* Biological Trace Element Research, 2001. **82**(1-3): p. 259-272.

68. Kocyigit, A., S. Gur, O. Erel, and M.S. Gurel, *Associations among plasma selenium, zinc, copper, and iron concentrations and immunoregulatory cytokine levels in*

patients with cutaneous leishmaniasis. Biological Trace Element Research, 2002. **90**((1-3)): p. 47-55.

69. Neilsen, J.L., A. Abildtrup, J. Christensen, P. Watson, A. Cox, and C.W. McLeod, *Laser ablation inductively coupled plasma-mass spectrometry in combination with gel electrophoresis: a new strategy for speciation of metal binding serum proteins.* Spectrochimica Acta Part B, 1998. **53**: p. 339-345.

70. Wang, J., R.S. Houk, D. Dreessen, and D.R. Wiederin, *Speciation of trace elements in proteins in human and bovine serum by size exclusion chromatography and inductively coupled plasma-mass spectrometry with a magnetic sector mass spectrometer.* Journal of Bio-Inorganic Chemistry, 1999. **4**: p. 546-553.

71. Koyama, H., Y. Kasanuma, C. Kim, A. Ejima, C. Watanabe, H. Nakatsuka, and H. Satoh, *Distribution of selenium in human plasma detected by high performance liquid chromatography-plasma ion source mass spectrometry.* Tohoku Journal of Experimental Medicine, 1996. **178**(1): p. 17-25.

72. Harrison, I., D. Littlejohn, and G. Fell, *Distribution of selenium in human blood plasma and serum.* Analyst, 1996. **121**(2): p. 189-94.

73. Kannamkumarath, S.S., R.G. Wuilloud, and J.A. Caruso, *Studies of various elements of nutritional and toxicological interest associated with different molecular weight fractions in brazil nuts.* Journal of Agricultural and Food Chemistry, 2004. **52**: p. 5773-5780.

74. Pomazal, K., C. Prohaska, and I. Steffan, *Hydrophobic interaction chromatographic separation of proteins in human blood fractions hyphenated to atomic spectrometry as detector of essential elements.* Journal of Chromatography A, 2002. **960**: p. 143-150.

75. Pomazal, K., C. Prohaska, I. Steffan, G. Reich, and J.F.K. Huber, *Determination of Cu, Fe, Mn, and Zn in blood fractions by SEC-HPLC-ICP-AES coupling.* The Analyst, 1999. **124**(5): p. 657-63.

76. Ponce de Leon, C.A., M. Montes-Bayon, and J.A. Caruso, *Elemental speciation by chromatographic separation with inductively coupled plasma mass spectrometry detection.* Journal of Chromatography A, 2002. **974**: p. 1-21.

77. Sutton, K.L. and J.A. Caruso, *Liquid chromatography-inductively coupled plasma mass spectrometry.* Journal of Chromatography A, 1999. **856**: p. 243-258.

78. Ferrarello, C.N., M.R. Fernandez de la Campa, and A. Sanz-Medel, *Multielement trace-element speciation in metal-biomolecules by chromatography coupled with ICP-MS.* Analytical Bioanalytical Chemistry, 2002. **373**: p. 412-421.

79. Shum, S.C.K., R. Neddersen, and R.S. Houk, *Elemental speciation by liquid chromatography-inductively coupled plasma masss spectrometry with direct injection nebulization.* Analyst, 1992. **117**: p. 577-582.

80. Sanz-Medel, A., M. Montes-Bayon, and M.L.F. Sanchez, *Trace element speciation by ICP-MS in large biomolecules and its potential for proteomics.* Anals of Bioanalytical Chemistry, 2003. **377**: p. 236-247.

81. Wu, C.S., *Handbook of Size Exclusion Chromatography and Related Techniques*. 2nd Edition ed. 2004, New York: Dekker Press.

82. Lobinski, R., *Speciation-targets, analytical solutions and markets.* Spectrochimica Acta Part B, 1998. **53**: p. 177-185.

83. Reimers, T., J. McCann, R. Cowan, and P. Concannon, *Effects of storage, hemolysis, and freezing and thawing on concentrations of thyroxine, cortisol, and insulin in blood samples.* Proc Soc Exp Biol Med, 1982. **170**(4): p. 509-516.

84. Vemuri, S., C.D. Yu, and N. Roosdorp, *Effect of cryoprotectants on freezing, lyophilization, and storage of lyophilized recombinant alpha1-antitrypsin formulations.* Journal of Pharmaceutical Science & Technology, 1994. **48**: p. 241-246.

85. Garcia Alonso, J.I., M.G. Camblor, M. Montes Bayon, J.M. Marchante Gayon, and A. Sanz-Medel, *Different Quantification Analysis for the Analysis of Biological and Environmental Samples Using Inductively Coupled Plasma mass Spectrometry.* Journal of Mass Spectrometry, 1997. **32**: p. 556-564.

86. Tanner, S.T., V.I. Baranov, and D.R. Bandura, *Reaction cells and collision cells for ICP-MS: a tutorial review.* Spectrochimica Acta Part B, 2002. **57**: p. 1361-1452.

87. May, P.M., P.W. Linder, and D.R. Williams, *Computer simulation of metal-ion equilibriums in biofluids: models for the low-molecular-weight complex distribution of calcium(II), magnesium(II), manganese(II), iron(III), copper(II), zinc(II), and lead(II) ions in human blood plasma.* Journal of the Chemical Society, Dalton Transactions: Inorganic Chemistry (1972-1999), 1977. **6**: p. 588-95.

88. Adams, F.C., *Elemental speciation: Where do we come from? where do we go?* Journal of Analytical Atomic Spectrometry, 2004. **19**: p. 1090-1097.

89. Caruso, J.A. and M. Montes-Bayon, *Elemental speciation studies - new directions for trace metal analysis.* Ecotoxicology and Environmental Safety, 2003. **56**: p. 148-163.

90. Davidge, J., C.P. Thomas, and D.R. Williams, *Conditional formation constants or chemical speciation data.* Chemical Speciation and Bioavailability, 2001. **13**(4): p. 129-134.

91. Scott, B.J. and A.R. Bradwell, *Identification of the serum binding proteins for iron, zinc, cadmium, nickel, and calcium.* Clinical Chemistry, 1983. **29**(4): p. 629-633.

92. Chatterjee, A., *Behaviour of anionic arsenic compounds in microwave system with nitric acid and hydrogen peroxide — preliminary laboratory study.* Science of the Total Environment, 1999. **228**(1): p. 25-34.

93. Prohaska, C., K. Pomazal, and I. Steffan, *Determination of Ca, Mg, Fe, Cu, and Zn in blood fractions and whole blood of humans by ICP-OES.* Fresenius' Journal of Analytical Chemistry, 2000. **367**: p. 479-484.

94. Lintschinger, J., P. Schramel, A. Hatalak-Rauscher, I. Wendler, and B. Michalke, *A new method for the analysis of arsenic species in urine by using HPLC-ICP-MS.* Fresenius' Journal of Analytical Chemistry, 1998. **362**(3): p. 313.

95. Saito, H., *Haemostasis and Thrombosis*, ed. A. Bloom, et al. Vol. 1. 1994: Churchill Livingstone. 289.

96. Hoffer, L., H. Schwinn, L. Biesert, and D. Josic, *Improved virus safety and purity of a chromatographically produced factor IX concentrate by nanofiltration.* Journal of Chromatography B Biomedical Applications, 1995. **669**(2): p. 187-196.

97. Josic, D., H. Horn, P. Schulz, H. Schwinn, and L. Britsch, *Size-exclusion chromatography of plasma proteins with high molecular masses.* Journal of Chromatography A, 1998. **796**(2): p. 289-298.

98. Palumbo, A., M. d'Ischia, G. Misuraca, L. Carratu, and G. Prota, *Activation of mammalian tyrosinase by ferrous ions.* Biochim Biophys Acta, 1990. **1033**(3): p. 256-260.

99. Tainer, J.A., Elizabeth D. Getzoff, J.S. Richardson, and D.C. Richardson, *Structure and mechanism of copper, zinc superoxide dismutase.* Nature, 1983. **306**: p. 284-287.

100. Tsukihara, T., H. Aoyama, E. Yamashita, T. Tomizaki, H. Yamaguchi, K. Shinzawa-Itoh, R. Nakashima, R. Yaono, and S. Yoshikawa, *The Whole Structure of the 13-Subunit Oxidized Cytochrome c Oxidase at 2.8 Å.* Science, 1996. **272**(5265): p. 1136-1144.

101. Percival, S.S. and E.D. Harris, *Copper transport from ceruloplasmin: characterization of the cellular uptake mechanism.* American Journal of Physiology Cell Physiology, 1990. **258**(1): p. C140-C146.

102. Gacheru, S., P. Trackman, M. Shah, C. O'Gara, P. Spacciapoli, F. Greenaway, and H. Kagan, *Structural and catalytic properties of copper in lysyl oxidase.* Journal of Biological Chemistry, 1990. **265**(31): p. 19022-19027.

103. Thiele, D., *Metal-regulated transcription in eukaryotes.* Nucleic Acids Research, 1992. **20**(6): p. 1183-1191.

104. Martell and Smith, *NIST Standard Reference Database 46.* 2003. **7**.

105. Sigurskjold, B., C. Berland, and B. Svensson, *Thermodynamics of inhibitor binding to glucoamylase.* Biochemistry, 1994. **33**: p. 10191-10199.

106. Juang, R.-S. and L.-C. Lin, *Electrochemical treatment of copper from aqueous citrate solutions using a cation-selective membrane.* Separation and Purification Technology, 2001. **22-23**: p. 627-635.

107. Madinzi, A., M.E. Amane, and H. Atmani, *Synthese, caracterisation et comportement electrochimique des complexes citrates issus du cuivre II et du ligand citrate disodique.* Ann. Chim. Sci. Mat., 2000. **25**: p. 179-185.

108. Miloserdova, N.A., N.A. Dobrynina, L.S. Nikolaeva, E.A. Mezhonova, A.M. Evseev, and A.P. Mozhaev, *A study by mathematical modelling and pH-potentiometry of complex formation by copper(II) with citric acid.* Russian Journal of Inorganic Chemistry, 1992. **37**(12): p. 1418-1420.

109. Dunhill, R.H. and J.R. Pilbrow, *Electron spin resonance of copper(II) Citrate chelates.* The Journal of Chemical Physics, 1966. **45**(3): p. 1474-1481.

110. Aisen, P., A. Leibman, and H.A. Reich, *Studies on the binding of iron to transferrin and conalbumin.* J Biol Chem, 1966. **241**(8): p. 1666-71.

111. Konigsberger, L.-C., E. Konigsberger, P.M. May, and G.T. Hefter, *Complexation of iron (III) and iron (II) by citrate. Implications for iron speciation in blood plasma.* Journal of Inorganic Biochemistry, 2000. **78**: p. 175-184.

112. Schreiber, G., *Kinetic studies of protein-protein interactions.* Current Opinion in Structural Biology, 2002. **12**(1): p. 41-47.

113. Allen, S., J. Chen, M. Davies, A. Dawkes, J. Edwards, C. Roberts, J. Sefton, J. Tendler, and P. Williams, *Detection of antigen-antibody binding events with the atomic force microscope.* Biochemistry, 1997. **36**: p. 7457-7463.

114. Izrailev, S., S. Stepaniants, M. Balsera, Y. Oono, and K. Schulten, *Molecular dynamics study of unbinding of the avidin-biotin complex.* Biophysical Journal, 1997. **72**: p. 1568-1581.

115. Kowalik-Jankowska, T., M. Ruta, K. Wisniewska, and L. Lankiewicz, *Coordination abilities of the 1-16 and 1-28 fragments of beta-amyloid peptide towards copper(II) ions: a combined potentiometric and spectroscopic study.* Journal of Inorganic Biochemistry, 2003. **95**(4): p. 270-282.

116. Remelli, M., M. Luczkowski, A.M.A. Bonna, Z. Mackiewicz, C. Conato, and H. Kozlowski, *Cu(II) ion coordination to SPARC: a model study on short peptide fragments.* New Journal of Chemistry, 2003. **27**(2): p. 245-250.

117. Conato, C., W. Kamysz, H. Kozlowski, M. Luczkowski, Z. Mackiewicz, F. Mancini, P. Mlynarz, M. Remelli, D. Valensin, and G. Valensin, *Cu-II ion coordination to an unprotected pentadecapeptide containing two His residues: Competition between the terminal amino and the side-chain imidazole nitrogen donors.* European Journal of Inorganic Chemistry, 2003. **9**: p. 1694-1702.

118. Gaggelli, E., N. D'Amelio, D. Valensin, and G. Valensin, *H-1 NMR studies of copper binding by histidine-containing peptides.* Magnetic Resonance in Chemistry, 2003. **41**(10): p. 877-883.

119. Mylonas, M., J.C. Plakatouras, N. Hadjiliadis, A. Krezel, and W. Bal, *Potentiometric and spectroscopic studies of the interaction of Cu(II) ions with the hexapeptides AcThrAlaSeHisHisLysNH(2), AcThrGluAlaHisHisLysNH(2), AcThrGluSerAlaHisLysNH(2) and AcThrGluSerHisAlaLysNH(2), models of C-terminal tail of histone H2A.* Inorganica Chimica Acta, 2002. **339**: p. 60-70.

120. Orfei, M., M. Alcaro, G. Marcon, M. Chelli, M. Ginanneschi, H. Kozlowski, J. Brasun, and L. Messori, *Modeling of copper(II) sites in proteins based on histidyl and glycyl residues.* Journal of Inorganic Biochemistry, 2003. **97**(3): p. 299-307.

121. Furia, T.E., *Stability Constants (log K1) of Various Metal Chelates*, in *from Chapter 6: Sequestrants in Foods. In CRC Handbook of Food Additives 2nd Edition.* 1972.

122. Walsh, P.N., *Platelet coagulation-protein interactions.* Seminars in Thrombosis and Hemostasis, 2004. **30**(4): p. 461-471.

123. Pratt, C., H.C. Whinna, and F.C. Church, *A comparison of three heparin-binding serine proteinase inhibitors.* The Journal of Biological Chemistry, 1992. **267**(13): p. 8795-8801.

124. Dahlback, B., *Blood Coagulation.* Lancet, 2000. **355**: p. 1627-1632.

125. Colman, R., V. Marder, E. Salzman, and J. Hirsh, *Plasma coagulation factors*, in *Hemostasis and Thrombosis*, R. Colman, et al., Editors. 1994, JB Lippincott: Philadelphia. p. 3-18.

126. Van Cott, E. and M. Laposata, *Coagulation*, in *The Laboratory Test Handbook*, D. Jacobs, Editor. 2001, Lexi-Comp: Cleveland. p. 327-358.

127. Nachman, R. and R. Silverstein, *Hypercoagulable States.* Annals of Internal Medicine, 1993. **119**: p. 819-827.

128. Duncan, T.P. and H. Roberts, *Hypercoagulability in Venous and Arterial Thrombosis.* Annals of Internal Medicine, 1997. **126**(8): p. 638-644.

129. Jackson, C., *Mechanism of heparin action.* Baillieres Clinical Haematology, 1990. **3**(3): p. 483-504.

130. Hirsh, J., *Heparin.* New England Journal of Medicine, 1991. **324**: p. 1565-1574.

131. Allison, S., T. Randolph, M. Manning, K. Middleton, A. Davis, and J. Carpenter, *Effects of drying methods and additives on structure and function of actin: mechanisms of dehydration-induced damage and its inhibition.* Archives of Biochemistry and Biophysics, 1998. **358**(1): p. 171-181.

132. Iversen, L. and O. Thorlacius-Ussing, *Short-time stability of markers of coagulation and fibrinolysis in frozen plasma.* Thrombosis Research, 1996. **81**(2): p. 253-261.

133. Woodhams, B., O. Girardot, M.J. Blanco, G. Colesse, and Y. Gourmelin, *Stability of coagulation proteins in frozen plasma.* Blood Coagulation and Fribrinolysis, 2001. **12**(4): p. 229-236.

134. McNerlan, S., V. Crawford, and R. Stout, *Measurement of fibrinogen in frozen plasma.* Thrombosis Research, 1997. **88**(6): p. 481-484.

135. Smith, P., R. Krohn, G. Hermanson, A. Mallia, G. FH, M. Provenzano, E. Fujimoto, N. Goeke, B. Olson, and D. Klenk, *Measurement of protein using bicinchoninic acid.* Analytical Biochemistry, 1985. **150**: p. 76-85.

136. Voet, D., J. Voet, and C. Pratt, *Fundamentals of Biochemistry.* 1999, Toronto: John Wiley & Sons. 931.

137. Creighton, T.E., *1.3 Amino Acid Residues*, in *Proteins: Structures and Molecular Properties*. 1993, W.H. Freeman and Company: New York. p. 15.

138. Wetlaufer, D.B., *Ultraviolet spectra of proteins and amino acids.* Advanced Protein Chemistry, 1962. **17**: p. 303-390.

139. Hulmes, J.D., D. Bethea, K. Ho, S.-P. Huang, D.L. Ricci, G.J. Opiteck, and S.A. Hefta, *An Investigation of Plasma Collection, Stabilization, and Storage Procedures for Proteomic Analysis of Clinical Samples.* Clinical Proteomics, 2004. **1**(1): p. 17-32.

140. Thavasu, P., S. Longhurst, S. Joel, M. Slevin, and F. Balkwill, *Measuring cytokine levels in blood. Importance of anticoagulants, processing, and storage conditions.* Journal of Immunological Methods, 1992. **153**(1-2): p. 115-124.

141. Chan, B.Y.Y., K.A. Buckley, B.H. Durham, J.A. Gallagher, and W.D. Fraser, *Effect of Anticoagulants and Storage Temperature on the Stability of Receptor Activator for Nuclear Factor-B Ligand and Osteoprotegerin in Plasma and Serum.* Clinical Chemistry, 2003. **49**(12): p. 2083-2085.

142. Burin, M., C. Dutra-Filho, J. Brum, T. Mauricio, M. Amorim, and R. Giugliani, *Effect of collection, transport, processing and storage of blood specimens on the activity of lysosomal enzymes in plasma and leukocytes.* Brazilian Journal of Medical and Biological Research, 2000. **33**(9): p. 1003-1013.

143. Frank, E.L., M.P. Hughes, D.D. Bankson, and W.L. Roberts, *Effects of Anticoagulants and Contemporary Blood Collection Containers on Aluminum, Copper, and Zinc Results.* Clinical Chemistry, 2001. **47**(6): p. 1109-1112.

144. Buckley, K. and W. Fraser, *Receptor activator for nuclear factor kB ligand and osteoprotegerin: regulators of bone physiology and immune responses/potential therapeutic agents and biochemical markers.* Annals of Clinical Biochemistry, 2002. **39**: p. 551-556.

145. Alvarez, L., P. Peris, N. Guanabens, S. Vidal, I. Ros, and F. Pons, *Serum osteoprotegerin and its ligand in Paget's disease of bone: relationship to disease activity and effect of treatment with bisphosphonates.* Arthritis and Rheumatology, 2003. **48**: p. 824-828.

146. Cummins, P., E. Cotter, and P. Cahill, *Hemodynamic regulation of metallopeptidases within the vasculature.* Protein Peptide letters, 2004. **11**(5): p. 433-442.

147. Creighton, T.E., *9.3 Examples of Enzyme Mechanisms-Metalloproteases*, in *Proteins: Structures and Molecular Properties*. 1993, W.H. Freeman and Company: New York. p. 431-433.

148. Mason, J., H. Yancy, K. Lashley, M. Jett, and A. Day, *Comparative study of matrix metalloproteinase expression between African American and Caucasian Women.* Journal of Carcinogenesis, 2004. **3**(1): p. 15-21.

149. Ziolkowska, M., M. Kurowska, and A. Radzikowska, *High levels of osteoprotegerin and soluble receptor activator of nuclear factor kB ligand in serum of rheumatoid arthritis patients and their normalization after anti-tumor necrosis factor a treatment.* Arthritis and Rheumatology, 2002. **46**: p. 1744-1753.

150. Haynes, D., E. Barg, and T. Crotti, *Osteoprotegerin expression in synovial tissue from patients with rheumatoid arthritis, spondyloarthropathies and osteoarthritis and normal controls.* Rheumatology, 2003. **42**: p. 123-134.

151. Petrakis, N., *Banking of biological samples for disease diagnostics, with special reference to blood.* National Cancer Institute Monograph 107, 2003. **NIH publication No. 03-2713**: p. 193-208.

152. Szpunar, J., *Metallomics: a new frontier in analytical chemistry.* Anals of Bioanalytical Chemistry, 2004. **378**: p. 54-56.